Novel analytical approaches for solid dispersion characterization

Inauguraldissertation

zur

Erlangung der Würde eines Doktors der Philosophie

Vorgelegt der

Philosophisch-Naturwissenschaftlichen Fakultät

der Universität Basel

von

Sandra Jankovic

Basel, 2020

Genehmigt von der Philosophisch-Naturwissenschaftlichen

Fakultät auf Antrag von

Erstbetreuer: Profs. Dr. G. Imanidis and M. Kuentz

Zweitbetreuer: PD Dr. M. Smiesko

Externe Experte: Prof. Dr. Zamostny

Basel, den 26.05.2020

Prof. Dr. Martin Spiess

Dekan

“Behind every problem, there is an opportunity.”

Galileo Galilei

Abstract

The overall aim of the thesis was to introduce new analytical techniques to characterize solid dispersion formulations. Solid dispersion formulations are employed to enhance the dissolution behavior and apparent solubility of poorly soluble compounds. This formulation strategy uses typically an amorphous physical form of a poorly soluble drug and combines it with a carrier for stabilization. The amorphous form presents higher free energy compared to a crystalline drug form thereby yielding a higher dissolution rate and possibly more complete oral absorption as well as bioavailability. The selection of appropriate excipients is crucial to guarantee the formulation performance and stability during the shelf life of the final product. To investigate drug formulation characteristics and predict their performance, different analytical techniques are needed. Along with the classical characterization techniques, novel approaches such as fluorescence spectroscopy and diffusing wave spectroscopy are introduced in the present thesis. The chapters 1 and 2 of this thesis cover fundamental aspects of poorly soluble drugs: an overview is given on amorphous solid dispersion (ASD) manufacturing technologies and characteristics of polymers and surfactants used in ASD. Moreover, analytical tools to characterize solid dispersions are presented. Among them, special emphasis is given to novel approaches such as Diffusing Wave Spectroscopy (DWS) and Fluorescence Spectroscopy.
As for the selection of excipients, drug polymer miscibility is a crucial requisite for the performance of an ASD formulation. One of the methods to predict drug-polymer miscibility is to employ solubility parameter approach; its application in solid dispersion formulations is outlined in the Chapter 3.

The first study introduces a novel fluorescence quenching approach together with size exclusion chromatography to study drug-polymer interactions that emerge from ASDs drug release in an aqueous medium. Celecoxib was combined with different pharmaceutical polymers and the resulted solid dispersion was evaluated by the (modified) Stern-Volmer model. Drug accessibility by the quencher and its affinity to the drug were compared in physical mixtures as well as within the ASDs using different polymer types. It was possible to gain knowledge about specific drug-polymer interactions and the amount of drug embedded in the evolving drug-polymer aggregates upon formulation dispersion and drug dissolution. More research in the future will show how such *in vitro* findings translate into performance of an ASD *in vivo*.

The second study of this thesis has also a biopharmaceutical focus and investigates formulation differences from a microrheological perspective by considering further an *in vitro* absorption sink using a biphasic dissolution equipment. Indeed, biphasic dissolution testing can simulate an intestinal absorption from dispersed formulation by using an organic layer. This study employed ketoconazole, a poorly soluble drug, together with different grades of HPMCAS and formulations were produced by hot melt extrusion (HME). Diffusing wave spectroscopy highlighted microrheological differences among the different polymer grades and plasticizers in the aqueous phase. These differences were found to influence drug release and finally the uptake in the organic layer that was intended to mirror the absorption process. There is surely more research needed before final conclusions can be drawn but the obtained findings point already to an important contribution of microrheological differences that evolved upon formulation dispersion.

The third study also emphasized microrheology but with a focus on non-dispersed solid dispersions. It was aimed to investigate microstructuring during phase transitions in drug-polymer solid dispersions. This formulation microstructuring is critical for the physicochemical properties such as stability of the final dosage form. In this study, eutectic mixtures of polyethylene glycol (PEG) were investigated using two drugs: fenofibrate and flurbiprofen. Unlike fenofibrate, the drug flurbiprofen was strongly interacting with the polymer and this was also confirmed by the rheological characterization. Therefore, broadband DWS provided valuable mechanistic information on the drug-polymer interactions and macromolecular structuring during the cooling of the eutectic melts.

.

Acknowledgments

I would like to thank Prof. Dr. Imanidis for the opportunity to carry out this PhD thesis, for fruitful discussions and all his advice. I am also grateful to Prof. Dr. Kuentz for all the scientific discussions and his enthusiasm.
I would like to thank the IPT group in Muttenz, especially to Ursula and Michael for their friendship and support. I would like to thank also Dr. Aleandri for his support in using instruments and learning about fluorescence spectroscopy. I am also thankful to ls instruments for technical support as well as scientific discussions about DWS.

I am grateful to all of my friends, Federica for her support, advises and motivation during all these years, Teresa, and Antoin, who always make me laugh, Isabelle for her patience and help in learning German and exploring the Swiss culture, Anne for discussions about the value of science, Chiara, and Valentina for their support and introducing me to “italianistics”. Thanks also go to all my shared apartment friends for listening, teaching me different recipes, and for making me always laugh.

Also, I would like to thank my parents and my sister who were always there to support me.

Contents

Chapter 1

1 Introduction

1.1 Background

Drugs which exhibit poor water solubility are a major challenge to formulation scientist because they might show low oral absorption and bioavailability. For an orally administered drug to have a therapeutic effect, the drug molecule must first dissolve in the gastrointestinal (GI) fluids, pass through GI mucosa to reach the systemic circulation to finally exhibit a pharmacological interaction with the target site. When the drug is poorly soluble, drug molecules may not dissolve completely in the GI fluids so that already the absorption step becomes erratic.

Based on solubility and permeability characteristics, drugs are classified in four different classes and this schematic approach is called biopharmaceutical classification system (BCS).[1] BCS Class I is assigned to drugs with high solubility and high permeability, BCS II compounds have low solubility and high permeability, BCS III drugs exhibit high solubility and low permeability and finally, BCS IV drugs show low solubility and low permeability. (Figure 2.1).The BCS approach has not been tailored for formulation development so that the approach was modified to the developability classification system (DCS), which differentiates within the Class II between dissolution rate-limited and solubility-limited class II compounds.[2] This aspect is crucial for the determination of an appropriate formulation strategy to enhance oral bioavailability.

Numerous formulation strategies focus on the enhancement of the dissolution rate to increase oral bioavailability of BCS class II compounds.[3–5] Some formulations can generate drug supersaturation so they temporarily lead a higher apparent solubility and solid dispersions (SDs) are here a key formulation approach.[3–5] This technology combines an active pharmaceutical ingredient (API) in usually its amorphous form together with a polymer as excipient. Amorphous materials lack the long-range ordering in the solid-state that is otherwise typical for crystalline molecules. This lack of crystallinity is especially advantageous in terms of

generating apparent solubility and a high dissolution rate.[6] However, not every drug is susceptible to be transformed into its amorphous form. To assess if a drug is suitable of being developed in its amorphous solid form, the glass-forming ability (GFA) of the drug should be estimated. The GFA is commonly understood as the ease of vitrification of a liquid upon cooling.[7] This tendency to form a glass is not only relevant to form an ASD but also for the tendency of the drug to reconvert to its crystalline form. The crystallization might be fast or long depending on the storage conditions and on the physicochemical drug properties.[1] Indeed, the amorphous form presents a high free energy form with increased molecular mobility compared to their crystalline solid form.[1] The latter mobility can be differentiated based on different kinds of relaxation and these are critical for physical stability.[8] To increase the physical stability of an amorphous form in the solid-state, the drug is commonly formulated with a polymer. The presence of a polymer is generally required to obtain an appropriate level of stability of the amorphous form because it inhibits the solid-state crystallization and there is also a common biopharmaceutical functionality. Thus, polymers can maintain a certain level of drug supersaturation within the dissolution medium, which drives permeation to a higher extent of drug absorption.[9–15]

To provide stability and inhibit recrystallization of the amorphous form, a molecular mixing between the API and the carrier is required. Generally, phase separation or crystallization can be avoided by restricting the molecular mobility of an amorphous drug and polymer during the preparation and storage. A relatively high glass transition temperature (*Tg*) of the polymer increases the *Tg* of the amorphous mixture to lower the mobility of the drug molecules thereby acting as crystallization inhibitor. In addition, drug-polymer interactions enhance the stabilization of the amorphous form.[1] Drug and polymer should be homogeneously mixed at a molecular level during processing, and the miscibility between the formulation components should be maintained during storage conditions.[1] Apart from crystallization, there could be also amorphous de-mixing of drug and polymer, which in turn accelerates the crystallization step of no longer stabilized drug. Therefore, the knowledge of phase behavior of the drug and carrier system is required to understand such a phase separation. Various methods are used for the prediction of drug-polymer miscibility. Among them, Flory-Huggins interaction parameter and solubility parameter can be used for this purpose. This topic of drug-polymer miscibility is treated in more detail in the following chapter.

As mentioned, the goal of solid dispersion formulations is to increase the apparent solubility

and dissolution rate following oral administration. This intended advantage in the dissolution behavior of amorphous over crystalline form is typically a rapid dissolution and then minimized or retarded precipitation until the concentration reaches the solubility limit of the crystalline form.[16]. The proposed mechanistic view of drug dissolution from ASD includes the carrier-controlled and drug-controlled dissolution depending on the solubility of the drug in the concentrated solution of the carrier.[17] In the carrier-controlled dissolution, the drug dissolves into the polymer-rich diffusion layer at a high rate that there is an insufficient time for the particles to be released intact into the medium.[17] As a consequence, the drug is molecularly dispersed within the polymer-rich diffusion layer.[17] When the dissolution of the drug into the polymer-rich diffusion layer is rather slow, the drug is released as solid particles. Consequently, the dissolution is mainly influenced by the properties of the drug itself such as particle size or the physical form and this mechanism is described as drug-controlled dissolution.[17] Many of the carriers used might increase the apparent or thermodynamic solubility of the drug, through the formation of a soluble complex, as described for the case of cyclodextrins.[17] Indeed, it has been reported that solid dispersions might form different aggregates also with bile salts and other lipids present in the GI tract, which might help to maintain a high level of drug supersaturation *in vivo*.[18] The drug and polymer nanostructure formation occurs rapidly in aqueous media and due to their stability, they create an aqueous suspension that can enhance oral drug absorption. These drug and polymer nanoaggregates were usually observed with hydroxypropyl methylcellulose acetate succinate (HPMCAS) that is an enteric coating polymer, presenting various advantages such as an amphiphilic nature.[18,19]

Depending on the physicochemical characteristics of the API and polymer, ASDs are primarily manufactured by either the fusion method or a solvent method.[20] Hot melt extrusion (HME) is one of the commonly employed fusion methods, where the API and the polymer are heated to form a molten mixture that is subsequently cooled and solidified. The crystalline API should be melted, and the polymer should have a *Tg* that is as low as possible to promote softening at these temperatures. Another commonly applied method for solid dispersion manufacturing is spray drying, where the carrier and the drug are mixed in a volatile solvent following atomization of the solution or suspension and fast drying of the liquid with a stream of heated air.[21] Since both API and the carrier are dissolved in a common volatile solvent, this method favorites molecular mixing.[22] Independent of the manufacturing process, drug and polymer miscibility is a key aspect to consider when formulating solid dispersions.

1.2 Objectives

The general aim of this thesis is to introduce novel analytical approaches to assist in developing solid dispersion formulations. Considering the high number of low water-soluble APIs, solid dispersions represent a key technology to increase dissolution rate and therefore apparent drug solubility. In a solid dispersion, the API is mixed with an excipient either on a molecular, colloidal or particulate level. There are standard techniques to analyze the physical state of the solid form but there is an increasing interest to have further analytical options to gain a deeper understanding of drug-excipient interactions both in the undispersed formulation as well as following aqueous dispersion. Therefore, the objective of this thesis is to explore the potential of Fluorescence Spectroscopy and Diffusing Wave Spectroscopy (DWS) in analytics of oral solid dispersions.

Following an introduction to the important aspects of solid dispersion technology, there is chapter 3 dedicated to the solubility parameter approach and how it is used for drug-excipient miscibility in solid dispersions and other oral formulations. This is followed by the main objectives to introduce an approach of Fluorescence Spectroscopy as well as DWS to characterize solid dispersions. The former approach is intended to analyze celecoxib, a native fluorescent drug by quenching to achieve mechanistic drug-excipient interactions upon aqueous dispersions of the formulations (Chapter 4). A particular aim of this work is to better understand how accessible or “free” the drug is to a fluorescence quencher since the topic of free drug in supersaturating formulations is of great interest in this field of pharmaceutical technology.
Apart from this approach of fluorescence analysis, the present thesis aims to explore the potential of DWS to characterize solid dispersions.
One aim is to use DWS to study aqueous dispersions of amorphous systems to achieve a better mechanistic understanding of drug release from solid dispersions. This study is complemented with release analysis by considering an absorption sink using an organic phase and fiber optical UV probes for kinetic concentration determination, which provides a biopharmaceutical framework to the DWS analysis. (Chapter 5).

This thesis further intends to evaluate DWS for the analysis of solid dispersion microstructuring during a phase transition. Eutectic mixtures are studied as solidification occurs to simulate a melt method such as hot melt extrusion (Chapter 6). This study explores the advantages of DWS in a broad frequency band to study solidification of formulations in a non-contact way and

therefore without any mechanical disturbance as it would otherwise result from, for example, any mechanical approach of rheology. Finally, the present research should contribute to an improved understanding of solid dispersions and it should provide some guidance on how excipients can be selected for practical usage.

2 Theoretical section

2.1 Dissolution and solubility

Before a drug can be absorbed, it must first dissolve in the GI fluids, which makes this step critical from a biopharmaceutical perspective. The dissolution of a drug can be described by the Brunner Nernst/Noyes Whitney equation:[23]

$$\frac{dM}{dt} = \frac{DA}{\mathrm{h}}(Cs - Ct) \qquad \text{eq. 1}$$

Where the d*M*/d*t* is the dissolution rate, while *D* is the diffusion rate coefficient, *A* is the total surface area of the drug particles, *h* is the diffusion layer thickness, *Cs* is the aqueous solubility of the drug, and *Ct* is the concentration dissolved at time *t*. From eq. 1, it is evident that drugs presenting a low solubility *(Cs)* will have also a small concentration gradient *(Cs-Ct)* resulting in a low dissolution rate. This concentration gradient could be only increased by concentrations higher than the equilibrium solubility, which requires drug supersaturation as it can be achieved from solid dispersions. While dissolution from pure drug can be described by a simple model like eq. 1, a mathematic description of release from solid dispersion formulations is substantially more complex. Drug dissolution from solid dispersions has been described by two main mechanisms: carrier controlled and drug-controlled mechanism.[17] In the carrier-controlled dissolution mechanism, the particles dissolve into the polymer-rich diffusion layer at a sufficiently high rate so that there is no time for particles to be release intact into the dissolution medium.[17] Therefore, the drug is in this scenario dispersed molecularly into the polymer rich layer. If it is not precipitating at the given concentration, the drug would diffuse through the layer slowly as predicted by the Stokes-Einstein equation (eq.2): [17]

$$D = \frac{k_b T}{6\pi r \eta} \qquad \text{eq. 2}$$

Where k_b is Boltzmann's constant, η is the viscosity and *r* is the hydrodynamic radius of the diffusing molecule at the temperature *T*. Alternative to this mechanism of carrier-controlled dissolution, the overall release of poorly water-soluble drugs in hydrophilic carriers can have the drug release as rate-limiting step. This is for example a likely mechanism in case of eutectic melts due to the crystalline nature of the poorly water-soluble drug.[17]

Solubility and permeability are characteristic for each compound and they can be divided into the four classes of the biopharmaceutical classification system (BCS) as mentioned before.

[24](Figure 2.1). This thesis will deal with BCS Class II drugs that are of primary interest to formulators as they generally have to be formulated by special formulation technology such as solid dispersions.[2] There are other classification schemes and the Developability Classification (DSC) system is particularly suited for a formulation development purpose. This scheme has been recently refined to even more adapt to the needs of formulation scientists.[2,25,26] More of a drug disposition viewpoint takes the Biopharmaceutical Drug Disposition Classification System (BDDCS) in which drugs are classified based on their metabolism and solubility.[27] This complements the BCS systems since the oral bioavailability depends not just on drug solubility and permeability but also on active influx and efflux transport as well as intestinal and hepatic metabolism.

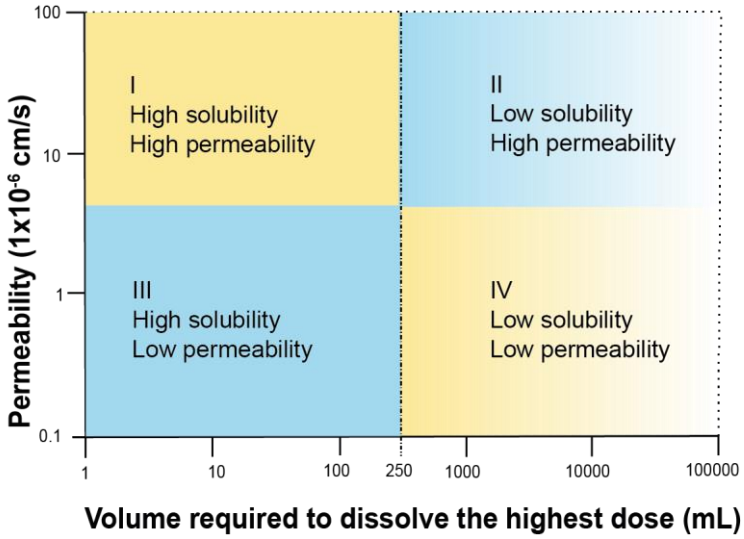

Figure 2.1: Biopharmaceutical classification system (BCS). (Adapted from Lubrizol Life Science)

Various technological approaches have been reported to increase the apparent solubility and dissolution rate of BCS class II drugs and these include particle engineering, salt formation, use of surface-active agents, lipids and/or co-solvents, and generation of solid dispersions. [3–5,28–30] As mentioned before, enhancement of apparent solubility can be obtained by changing the physical state of the API, from crystalline to an amorphous solid since the latter has as higher free energy.[31,32] The three-dimensional long-range order that exists in a crystalline material does not exist in an amorphous form, and the position of molecules is more random compared to the liquid state.[33] An amorphous material usually has different physical properties compared to the crystalline compound; it presents enhanced thermodynamic properties relative to the crystalline state and higher molecular mobility.[33] The advantage of enhanced apparent solubility comes with the disadvantage of the possibility that the amorphous form may spontaneously transform

into the crystalline state.[33] Therefore to stabilize an amorphous pure drug, a polymeric carrier or other excipients should be employed. This solid dispersion technique has gone through different generations of formulation types and this is dealt in more detail in the following section.[34]

2.2 Solid dispersion

As mentioned before, solid dispersions represent one of the main approaches to improve apparent drug solubility and dissolution rate.[1] The term solid dispersion was introduced already in 1971 by Chiou and Regelman and it was defined as the "dispersion of one or more active ingredients in a carrier at the solid-state, prepared by either the melting, the solvent or melting solvent method".[1] Chiou and Regelman were also the first to introduce a solid dispersion classification based on the physical state of the API present in the carrier. In table 2.1 the classification of different solid dispersions is presented, which considers systems with two components, drug and an excipient that is commonly a polymer.

Table 2.1 Solid dispersion classification. (Adapted from [1])

Physical state of API / Number of phases	Crystalline	Amorphous
1	Solid solution	Glass solution
2	Eutectic mixture	Glass suspension

This classification system involves the physical state of the API and the carrier. The first solid dispersions developed were eutectic mixtures. In such eutectic mixtures, API and carrier are both in a crystalline physical state.[1] The eutectic mixture consists of two components, which are completely miscible in the molten state, while they present limited miscibility in the solid form. When drug and polymer are mixed at a certain composition called the eutectic point, these two crystallize simultaneously yielding two a phase of separate crystalline components. [35–37] If the mixture is not at the eutectic point, then one component will start to crystallize and separate

until the specific mixing ratio of the eutectic point is reached. [1]

Solid solutions are comparable to the liquid solutions and consist of just one phase.[38] Solid solutions can be classified based on their miscibility, for example, continuous versus discontinuous solid solutions or according to the way the solvated molecules are distributed.[38] In the continuous solid solution, the components are miscible in all the ratios. However, this type of solid solutions has not been reported for pharmaceutical compounds.[38] Discontinuous solid solutions present a limited solubility of each component in each other, so the drug loading is a common issue for this type of solid dispersion.[1,38]

When API is in an amorphous form, solid dispersions can be divided into glass solutions and glass suspensions. A glass solution names a molecular dispersion of a drug within an amorphous carrier, yielding a homogenous single-phase system. Since the glass solution has higher viscosity compared to the liquid solution, the dispersion of an API might not be homogenous, and this needs to be improved during mixing. As amorphous carriers, there were initially low molecular excipients employed, but these days, polymers such as poly(vinylpyrrolidone) PVP and cellulose derivates are commonly used. [34,39,40]

Depending on the amount of drug in a carrier, solid solutions can be thermodynamically stable but amorphous dispersions have higher drug loading and are supersaturated within the polymer matrix. Amorphous material can exist in glassy or supercooled liquid states, separated by different glass transitions. These differing temperatures can come with two to three orders of magnitude changes in the mean relaxation time and viscosity. [1]

The mobility linked to the glass transition might be directly related to the issue of physicochemical instability.[41] However, the *Tg* alone may not directly predict the stability of several amorphous materials. In these cases, the instability was rather connected to local mobility.[41] The molecular mobility responsible for the glass transition is also called "global mobility".[41] Such global molecular motions are commonly known as α-relaxation. Glassy systems have also the mentioned local motions in which no translational degrees of freedom are given so these are typically rotational or intramolecular movements and are named β-relaxation.[41] These relaxations are also called Johari-Goldstein relaxations and they play a significant role in the physical stability of amorphous material especially below the *Tg*.[1] It has been suggested that this relaxation might be a precursor to glass transition and can influence global mobility.[41] The storage temperature of such formulations should be well below the *Tg*, to decrease such molecular mobility. Recent work particularly emphasized a *Tg(beta)* below

which all Johari-Goldstein relaxations come to a halt so that good kinetic stability can be targeted.[23,42]

The type of solid dispersion that is obtained is partly determined by global molecular mobility on the one hand and miscibility of drug and polymer on the other hand. Especially, the more concentrated systems can lead to separation of the components into a glass suspension that often has a high probability of recrystallizing.[23] Thus, increasing the drug load at a certain temperature can lead to different types of solid dispersions.

If the drug is not miscible in the polymer matrix at a given mixing ratio, rapid crystallization can occur and result in phase separation, creating drug rich and polymer-rich phases. The presence of polymer decreases the diffusion rate of the drug in the media and impedes drug crystallization from the supersaturated solution as mentioned before.[43] Interesting is the addition of a surfactant as it is often done for biopharmaceutical reasons and leads to the third generation type of solid dispersion.[34] Thus, several improvements may be achieved by such a surfactant addition such as improved drug wettability, solubility, and drug-polymer miscibility.[34] However, even if the inclusion of these excipients might increase the solubility and bioavailability, there is always a great risk for phase separation and immiscibility in the given polymer blends.[12]

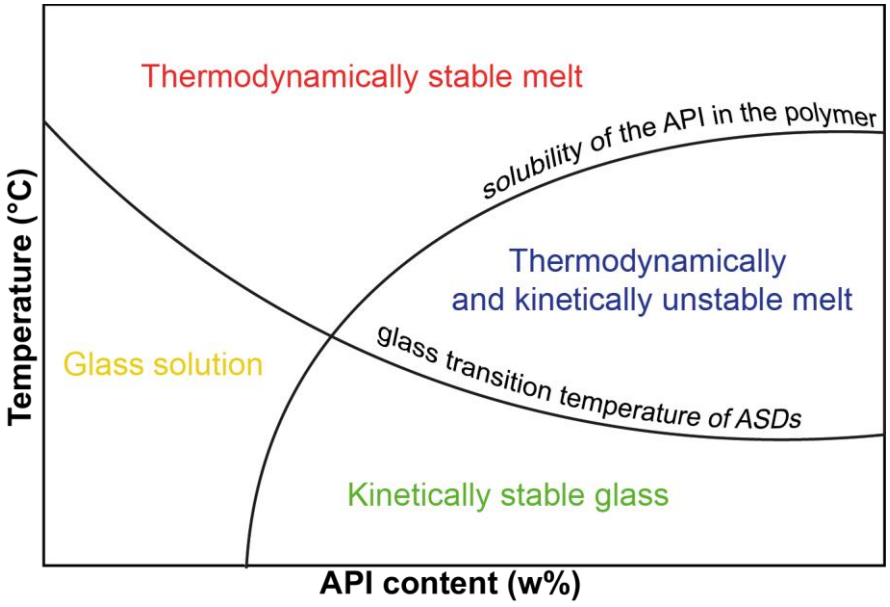

Figure 2.2 Phase diagram of the API and polymer phase behavior. (Adapted from [43,44])

While the addition of surfactant would complicate phase behavior in general, it is helpful to visualize a simplified view of phases obtained along with an increasing drug load. Such a simplified phase behavior of the API/polymer system and the temperature-dependent solubility

of the API in the polymer is presented in Figure 2.2. Four regions can be identified: a region of the thermodynamically stable melt, glass solution, kinetically stable glass and thermodynamically and kinetically unstable melt.[42] At a given temperature, an ASD is thermodynamically stable and will not crystallize when the API content is low (represented in the area of glass solution and thermodynamically stable melt).[44] For a determinate API content, the solubility line provides the temperature at which API content can be completely dissolved in the polymer, which may be determined by DSC measurements. When the amount of API is higher than its solubility in the polymer at the given temperature, the ASD is supersaturated and API recrystallization may occur (kinetically stable glass and thermodynamically and kinetically unstable melt areas in the graph). However, if the storage temperature is low enough then the glass transition temperature, the molecular mobility of the drug might be so low that the crystallization is inhibited or slowed for the pharmaceutically relevant time period.[44] These kinds of formulations are called kinetically stabilized ASDs.[44]

It is therefore important to understand drug and polymer interactions based on the features of the components to achieve adequate miscibility with the drug of interest.[45] Herein, a traditional approach to evaluate drug and polymer miscibility is to compare their solubility parameters based on the assumption that they will give a regular solution.[45–47] Also, drug and polymer interactions can stabilize the solid dispersion even in the presence of a small amount of polymer. However, drug and polymer should be mixed at a molecular level already during the processing. Assessment of the phase behavior of solid dispersions can be done by employing two complementary techniques such as powder x-ray diffraction (PXRD) and the modulated differential scanning calorimetry (mDSC), as outlined in a recent research article.[43] A detailed discussion about miscibility within the ASDs is presented in the following section.

2.2.1 Excipients for solid dispersions

Historically, excipients employed for solid dispersions might be classified in the following groups: [20,23]

1. Polyglycols: polyethylene glycoles (PEG) and polyethylene polypropylene glycol copolymers
2. Polyvinylpyrrolidone polymers: PVP, polyvinylalcohols (PVA), crospovidones (PVP-CL), polyvinylpovidone/polyvinyl acetate (PVP-VA) copolymers, polyvinyl acetate phthalate (PVAP)
3. Cellulosic derivates: hydroxypropylcellulose (HPC), hydroxypropylmethylcellulose (HPMC), carboxymethylethylcellulose (CMEC), cellulose acetate phthalate (CAP), hydroxypropylmethylcellulose phthalate (HPMCP) and hydroxypropylmethylcellulose acetate succinate (HPMC-AS)
4. Acrylates and methacrylate copolymers

Based on the type of excipients, ASDs can be classified into different generations: low molecular weight, highly water-soluble carriers, such as urea, short-chain carboxylic acids (citric/succinic acid) and sugars (sucrose, mannitol, and trehalose), polymeric carriers such as PVP, PEG, cellulose derivates and surfactant-polymer based systems.[23] A schematic representation of the different generations of solid dispersions is illustrated in Figure 2.3.

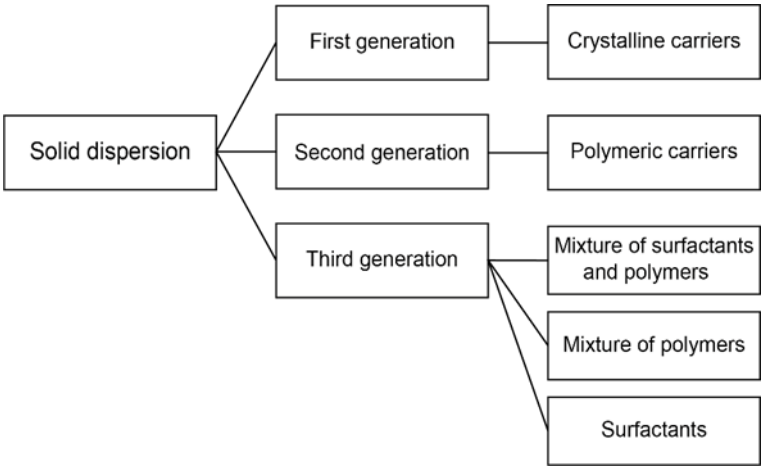

Figure 2.3. Solid dispersion classification based on complexity. (Adapted from[31])

The first generation of solid dispersion employs mostly crystalline carriers of low-molecular weight or semicrystalline carriers such as PEG or poloxamer. In PEG-based solid dispersions, the crystalline drug is usually dispersed as micronized crystalline particles or present in its

amorphous form.[48] Improvement of drug absorption is in these cases mostly due to improved wettability of drug and faster dissolution rate compared to a conventional solid dosage form.[48]. Once other polymers than PEGs are used as vehicle, a second generation of solid dispersions is obtained. This solid dispersion generation uses mostly amorphous vehicles with good solubilization properties so that drug can be incorporated in a non-crystalline form. Such polymeric carriers have been the most successful in solid dispersion formulations because they can provide amorphous drug dispersions. Polymeric carriers can be classified in synthetic and natural product-based polymers. Within the first category, polyvinylpyrrolidone (PVP), polyethylenglycole (PEG), and polymethacrylates are, for example, included; whereas natural product-based carriers are mainly starches and celluloses with further semi-synthetic derivatives than constitute again a separate category of polymeric excipients.

The selection of polymer for any amorphous solid dispersion requires first well-established oral acceptability and hence a suitable regulatory status. The polymer is further chosen for its ability to stabilize drug in the polymeric matrix as well as to promote and sustain supersaturation upon aqueous dispersion. The physical-chemical characteristics and the role of the amorphous carrier in the formulation of ASDs have been outlined in the review article by Van Duong et al. [49] and presented in Table 2.2. The selection of an amorphous carrier will impact on the physicochemical characteristics and the dissolution performance of the final ASDs. As an example, it has been widely reported that molecular weight has a strong effect on the dissolution rate. Thus, the dissolution rate generally decreases as the molecular weight of the carrier increases and there is typically a lower drug solubility of the carrier as well as a longer process of swelling with higher viscosity in the diffusion boundary layer. All of these factors contribute to a comparatively slower release with polymer selection of higher molecular weight.[49] Also, the carrier content contributes to the dissolution rate; indeed, decreasing carrier content is associated with the decrease in the dissolution rate because the drug is more concentrated and hence less stabilized in the amorphous aggregates.[49] Chemical aspects of the polymer are relevant for molecular interactions so each carrier might exert a specific influence on the dissolution rate and may exhibit particular capability to maintain supersaturation of the drug.[49] A good example of chemical modifications can be found in the group of cellulose polymers. Among them, hydroxypropyl methylcellulose acetate succinate (HPMCAS) is a particular derivate of cellulose, which is known as enteric coating polymer and presents interesting moieties of acetyl and succinoyl groups.[50] The key feature of this polymer is its capacity to dissolve at different pH due to the amount of the given acetyl and succinoyl groups. Enteric polymers employed for a pH-controlled drug release from ASDs may present especially for

drug bases an advantage. A high release of protonated base can lead to excessive supersaturation of drug upon transfer into the duodenum that exhibits a higher pH thereby leading to high risk of drug precipitation.[50] The correlation between the drug release and the substituents in HPMCAS has been investigated. Thus, the proportion of the acetyl to succinoyl substitution is highest in AS-LF which is soluble at lower pH (5.5), where the HF grade has a lowest proportion of the acetyl to succinoyl substitution and it dissolves at higher pH (6.5).[50] The ratio of succinoyl to acetyl groups was shown to play an important role in the inhibition of drug recrystallization.[51] During the dissolution process, it has been reported that numerous polymer-drug aggregates can form, which function as a drug reservoir. They provide a free drug concentration, which is sustained by replacing the amount of drug absorbed.[16,32–35]

Recently, it has been demonstrated that if the carrier has surface activity or even self-emulsifying properties, the drug release may be further improved, which led to the development of the third generation of solid dispersions.[20,56] In these systems, the polymeric carrier is either itself surface-active or a surfactant is added.[31] The presence of a surfactant in the solid dispersion formulation increases wettability, dispersion, and solubilization of the drug in aqueous media [53,57] Polyethoxylated surfactants such as Gelucire, Tween and Labrasol have shown improved dissolution and enhanced oral availability when included in the ASDs. [58,59]

Lipid-based excipients are used as well, which are ingredients derived from vegetable oils, fatty acids or waxes. Vegetable oils include triacylglycerols (fatty acid esters of glycerol), phospholipids and lipophilic vitamins.[60] They are used to produce a wide variety of ingredients by various processes and the physical properties of these lipids depend on the unsaturation in fatty acids, the fatty acid chain length, and free hydroxyl groups or fatty acid content. Therefore, these ingredients can be either liquid or solid, and they often present different polymorphic forms. These excipients may further differ in their hydrophilic lipophilic balance (HLB) value and different colloids can form in aqueous dispersion such as micelles with the more hydrophilic lipid-based surfactants.[61] Sodium lauryl sulfate and block copolymers of ethylene oxide and propylene oxide have been also employed to increase the dissolution rate and the solubility of different active ingredients.[23]

Among the lipid-based surfactants, Gelucires have been often employed for their solubilizing properties.[62,63] The Gelucire family are polyethylene glycol (PEG) glycerides composed of mono-, di- and triglycerides and mono- and diesters of PEG that have started to be employed

in ASDs formulations.[62,64–66] The presence of the PEG provides some water miscibility to the lipid bases thereby removing the necessity of incorporating surfactants or related molecules to allow drug release to occur over a relevant time scale. The lipid chain length plays here a role for sustained drug release. On this basis, there has been a growing interest in the use of Gelucire 50/13 as a vehicle for controlled release dosage forms. The mechanism of the controlled release might be because Gelucire 50/13 swells in water and forms a diffusion barrier to drug release.[67] The functionality of lipids in the formulation of poorly soluble drugs is linked to their excipient tendency to self-assemble in an aqueous environment. When lipids are included in ASDs, the mechanism of the dissolution process is more complex.[53,57] Surfactants provide better powder wetting, enhance the formation of nanoaggregates and improve drug solubility due to inclusion into micelles.[57] Formulations at high surfactant concentrations spontaneously form a fine dispersion or emulsion upon contact with water, therefore favoring higher drug dissolution. Especially the formation of colloidal dispersions can facilitate increased solubilization and absorption of poorly soluble drugs.[53] While these are biopharmaceutical advantages of using lipids in ASDs, any excipient has particular physicochemical properties that can be important for the performance of the given solid dispersion and Table 2.2. provides here an overview.

Table 2.2 Important parameters of the carrier in ASDs formulation (adapted from [49])

Property of the polymer	Importance in the SD formulation
Molecular weight	Strongly affects the viscosity and drug dissolution. In general drug dissolution decreases with increase the molecular weight.
Tg	Relates to the molecular mobility and hence the crystallization tendency and stability of ASDs.
Solubility parameter	Predicts drug-carrier miscibility; components with similar solubility parameter are likely to be miscible.
Ionization constant	Determines the solubility, ionization state, drug-polymer interaction and carrier conformation in water.
Hydrophobicity	Impacts the drug-carrier hydrophobic interaction, drug dissolution, conformation and the crystallization inhibitory effect of the carrier.
Aqueous solubility	Influences the dissolution rate of the whole system, the solubilization and supersaturation maintenance capacity.
Solvent solubility	Solubility of the carrier in the organic solvents is necessary for ASDs preparation.
Thermal solubility	Important for processing drug carrier system via heat-based methods: the carrier should not decompose at the processing temperature.
Thermoplasticity	Carrier softening tendency upon heating relates to the deformability upon extrusion.
Melt viscosity	Melt viscosity of a carrier largely depends on the temperature and shear stress that governs the deformability and processability during HME.
Functional groups	Dictate the possibility of drug-carrier molecular interactions such as hydrogen bonding, which influence physical state, dissolution behavior, supersaturation and stability of the amorphous drug.
Conformation	Relates to the drug-carrier interaction, Tg stabilization effect and supersaturation maintenance of the carrier.

2.2.2 Solid dispersion manufacturing technologies

The processing technologies are classified into two main classes, which are the following: solvent-based or fusion-based methods. A schematic classification with subgroups of the different technologies for solid dispersion manufacturing is the following:[1]

a) Solvent-based technologies where drug and excipients are first solubilized in a solvent prior to a solidification

-Spray drying (rapid removal of the solvent in a controlled temperature and pressure

environment)
-Fluid bed granulation/layering/film coating: removal of the solvent using various conventional pharmaceutical equipment
-Coprecipitation: solvent-controlled precipitation technologies such as microprecipitated bulk powder (MBP)
-Supercritical fluid-based technologies
-Cryogenic processing
-Electrospinning
-Rotating jet spinning
b) Fusion-based technologies where the drug and the excipient are mixed and heated
-Melt granulation
-Hot melt extrusion
-KinetiSol
-Deposition of molten material on a carrier by fluid bed process

There is also the possibility to prepare amorphous systems by mechanical energy, i.e. co-milling with excipients. This has in the past barely have relevance to manufacturing of solid dispersions but there is growing interest in this approach because of co-amorphous systems that are preferably prepared by this manufacturing method.[68] Therefore, mechanical energy appears to become a third class of amorphization methods apart from solvent-based and heat-based methods.

The selection of the preparation method depends on the physical properties of the API such as thermal stability, melting point, and solubility in organic solvents.[23] The solvent method involves the preparation of a solution of drug and polymer in a common solvent, followed by evaporation of the volatile solvent to yield a solid dispersion. This technique favors a molecular level mixing between the components, which increases the chance of yielding a stable ASD. Volatile solvents are usually evaporated at a low temperature, preventing thermal decomposition of the drug and/or polymer. Solvent evaporation might present challenges with respect to potential phase separation. An aspect can be therefore how fast the solvent is removed. While on a small scale there is often rotary evaporation employed, a later scale-up method is usually spray drying for which the drying conditions may become critical for the homogeneity and hence the quality of the solid dispersion.
Selecting the right solvent in which both drug and polymer are soluble might be challenging.

In this regard, solubility parameters can be helpful to screen solvent candidates regarding drug and excipient affinity to a common solvent, but it is still possible that there is finally no sufficient solubilization identified in a common pharmaceutical solvent.

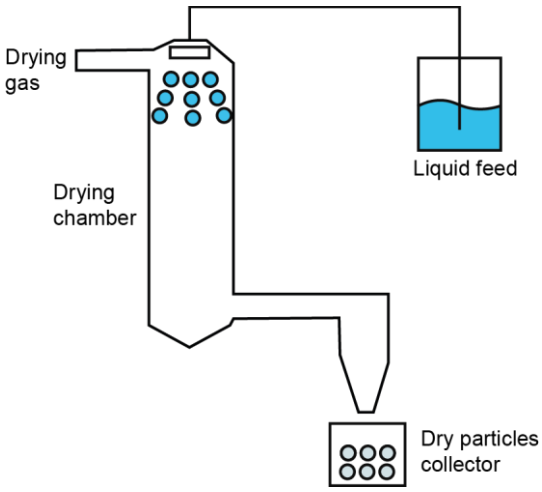

Figure 2.4. Schematic illustration of spray drying technology. (Adapted from [69])

Spray drying is the most commonly employed solvent method, which consists of four stages: the atomization of the liquid, mixing of the liquid with the drying gas, evaporation of the liquid and separation of the particles from the gas.[70] A schematic representation of spray drying technology is in Figure 2.4. The solution of API and carrier is introduced in a heated chamber *via* a pump system with controlled droplet size, and spray rate, followed by fast evaporation of the solvent and collection and separation of the remaining solid particles, which form an ASD. API and the carrier must be dissolved or suspended in a common solvent, which in most cases is organic. Numerous solvents and solvents mixtures with varying polarity can be employed; also, this technique has the advantage of being easily scaled up for manufacturing and control of the final particle size.[23] With spray drying, it is possible to obtain ASDs with superior physical stability using established manufacturing equipment. It allows rapid removal of the solvent, fast solidification, equipment available from lab to full-scale commercial products, low-temperature processing suitable for highly volatile solvents and continuous processing.[23] However, the final physical state of the API depends on the chemical nature of the substance and it might be amorphous, crystalline mixtures, crystals with induced imperfections or metastable crystal forms. The solid form depends mainly on a drug's inherent glass-forming ability and less on the preparation method.[71] In this context, the glass-forming ability of sixteen poorly soluble drugs with varying molecular structures and physicochemical properties have

been investigated.[72] The results confirmed that only half of the APIs could be amorphized completely by spray drying.[72,73]

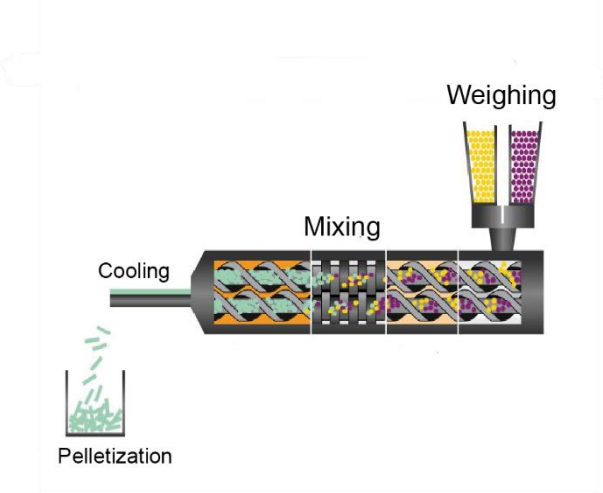

Figure 2.5. Hot melt extrusion technology. (Adapted from www.thermofisher.com)

In the class of the heat-based manufacturing method, HME has become increasingly important in recent years. As presented in Figure 2.5, a physical mixture of drug and polymer is introduced into the extruder at high temperatures, which melts or softens the mass to facilitate mixing. The material is then continuously extruded, cooled and chopped into small pieces for further down-stream processing to, for example, a powder or pellets. The main advantages compared to other methods is that it is solvent-free, it can run continuously, scale-up is straight forward and the footprint of HME in a manufacturing facility is rather low.[74] At process temperatures, the crystalline API should be melted and stable at these high temperatures, and the polymer should have a sufficiently low *Tg* to obtain softening at these temperatures. Besides, processing parameters such as feed rate, shear force, temperature, die geometry, barrel design, and screw speed are key aspects in the process design of the final product.[75]

The selection of a suitable polymer for HME is important for stabilizing ASDs, as well as for the processing characteristics. Therefore, the selected polymer enhances formulation characteristics but also enables the process itself. Small molecules can be further added as excipients to the physical mixture to lower the viscosity of the molten material or to decrease the processing temperature.[1] In some cases, the drug itself might provide better processing characteristics and may act, for example, a plasticizer for the polymer.[76,77]

An important factor in the solid dispersion formulation is the mixing process, which is relevant

for different manufacturing processes as well as for the final drug product stability. As outlined in the next paragraphs, miscibility is studied using *in silico* as well as experimental tools. However, the manufacturing process likely influences the practical mixing capacity and phase behavior kinetics of solid dispersions. Previous research outlines that heat is an important energy input for drug and excipient mixing. Heat pre-treatment of the solution before spray drying can result in higher kinetic miscibility. Amorphization of the copolymer by spray drying before using it as an excipient for hot melt extrusion can represent a benefit. It was reported that spray drying might produce more stable solid dispersions due to the molecular mixing of the drug and the polymer in a common solvent.[78,79] On the other hand, a recent research article outlined that HME allows higher drug loading. These considerations show that based on the given drug and polymer matrix, there is not a completely free choice of the manufacturing technique, but the given physicochemical mixture properties are likely to favor one over the other technique. If there is a strategic preference for one manufacturing technique, then these processes should be already considered in the selection of the formulation apart from aspects of stability and biopharmaceutical performance.[79]

2.3 Selected aspects of ASDs formulation

2.3.1 Drug-polymer miscibility

Drug and polymer miscibility is one of the key aspects to consider for adequate excipient selection in ASDs. Not just during the manufacturing, but also during the shelf life of the product, drug and polymer miscibility should be maintained in a single phase to present the advantages associate with the amorphous physical form of the drug. Phase changes might occur due to water absorption during storage and they are likely to occur during dissolution.[14] Water increases the molecular mobility of the system and decreases the *Tg*, which might lead to phase separation if only kinetic miscibility of the components was given. It is important to assess if miscibility between the polymer and the drug will be achieved during processing, for example, hot-melt extrusion, spray drying, or freeze-drying. Experimentally, this is commonly done with Differential Scanning Calorimetry (DSC). A single *Tg* will be detected in the case of a miscible homogenous solid dispersion. This temperature will be observed between the values of the individual *Tg* values of the single components. However, one limitation of this approach is that the phase separation should be larger than on a level of 30 nm domains when using DSC for detecting the *Tg*. Indeed, when the phase separation is on such a microscopic scale, the conventional analytical techniques such as DSC powder X-ray diffraction (PXRD) are typically

not able to detect it.

For this purpose, further analytical tools such as atomic force microscopy are attractive to study early signs of phase separation.[80] Moreover, confocal Raman imaging shows promising results when analyzing the excipient distribution within solid dispersions.[81] It was shown that a distinctive single *Tg* by DSC is not always an indication of a homogenous ASD and therefore cannot provide all the necessary information for physical stability.[81] As a result, the physical stability of ASD and processing conditions demonstrated a better correlation when using Raman microscopy as an additional tool.[81]

Besides the experimental approaches, numerous other methods can predict polymer and drug miscibility. The two main theoretical approaches for drug and polymer miscibility are based on the Flory-Huggins (F-H) theory and that of the solubility parameter.[1] Flory-Huggins theory is based on lattice approach and addresses particularly the situation of polymers to estimation of free energy of mixing of polymer-solvent or polymeric mixtures. The obtained parameter, $\chi_{d\text{-}p}$ is known as the F-H interaction parameter. This can be estimated from different experimental as well as theoretical approaches, including the solubility parameter prediction and the melting point depression approach.[82] The determination of drug solubility within the polymer matrix is commonly done employing the melting point depression method. Polymer-induced melting point depression can be used to experimentally determine the drug-polymer miscibility, just by DSC: various physical mixtures of a drug and polymer are heated at a different rate and the end of the melting point endotherm is determined as the intersection between the dissolution endotherm and the baseline after dissolution.[1,82] The F-H theory is a classical theory for polymer-solvent system to provide the Gibbs free energy of mixing. A small molecule such as a drug can be considered equivalent to the solvent in the polymeric mixtures, and therefore can be described by the F-H theory.[83] Apart from the F-H theory approach to drug-polymer miscibility, the use of solubility parameters is extensively reported in the literature to aid in the development of solid dispersions. A recent review article highlights the application of solubility parameters to assist with bio-enabling formulations such as lipid-based formulation, mesoporous silica, and solid dispersions.[84] The solubility parameter approach is based on the concept of 'like dissolves like', meaning that compounds with similar properties will more likely be miscible.[85] Historically various approaches have been developed in this field, but the main are the Hildebrand total solubility parameter or consideration of partial solubility parameters as Hansen Solubility Parameters (HSP). When considering the total solubility

parameter, cohesive energy density is the central aspect. It represents the sum of different energies per volume arising from drug and polymer interactions, including Van der Waals and polar interactions as well as hydrogen bonding. The final value for the solubility parameter is obtained from the square root of the cohesive energy density CED (eq. 3). [1]

$$\delta_t = (CED)^{\frac{1}{2}} = \left(\frac{\Delta E_v}{V_m}\right)^{1/2} \quad \text{eq.3}$$

where the ΔE_v is the energy of vaporization and V_m the molar volume. *CED* is defined as the cohesive energy per unit volume. The Hansen solubility parameter can be calculated from partial contributions to cohesive energy density (eq. 4) [1]:

$$\delta^2 = \delta_d^2 + \delta_p^2 + \delta_h^2 \quad \text{eq. 4}$$

Where $\delta_d, \delta_p, \delta_h$ are the dispersive, polar and hydrogen bonding respectively. HSP considers the dispersion, polar interaction, and hydrogen bond contribution for a given molecule. The main application is still in the solubility assessment in different solvents.[86,87] However, it has also been applied to predict drug and excipient miscibility for ASDs. A recent research article compares the Hildebrand and Hansen solubility parameter prediction to the experimental set up of data for polymers.[88] Using 75 different polymers, it has been reported that both Hansen and Hildebrand solubility parameter have similar predictive accuracy (circa 70%).[88]

Miscibility prediction based on the Hildebrand approach was employed for ASDs by Greenhalgh et al.[89] This approach considers the difference in solubility parameters between the drug and the polymer. It was observed that for a difference between 1.6 to 7.0 MPa, the system was completely miscible; on the contrary, when this difference was between 10.8 and 18.0 MPa, the systems were immiscible. Partially immiscible systems in the liquid state were found to have a value between 7.4 and 15.9 MPa.[89]

Similar results have been reported also with HSP. Solubility parameter differences below 7 predict a miscible system as in the case of, for example, Soluplus or arabic gum with lacidipine.[90] Based on the HSP, these two carriers have been selected as the most effective nucleation and crystal growth inhibitors.[91] HSP is also reliable in the prediction of a co-crystal formation.[92] The established cut off was 8.5 MPa, but this, however, did not bring real advantages.[92] The solubility parameter prediction was not reliable in the case of some drug-polymer interactions, for example when pronounced acid and basic interactions were present.[28]

Thus, the main drawbacks of the solubility parameter prediction have been evaluated by Thurpin et al.[93] This article highlighted the theoretical limitations in employing the solubility parameter approach; in particular when a neglected entropic contribution was highly relevant for the experimental system. The same authors propose new *in silico* methods that consider all parts of the free energy of mixing and predicted then more accurately drug-polymer miscibility.[93] New prediction methods are employed for the calculation of solubility parameters based on pure chemical structure. Among them, screening charge densities of molecular surfaces (the so-called σ-profiles) have also been used by the conductor like screening model for real solvents (COSMO-RS) and can be employed in a quantitative structure-property relationship (QSPR) to predict solubility parameters.[94] Another study suggested using partial solvation parameters instead of the Hansen solubility parameter since the novel concepts have several advantages, in particular, the distinction between hydrogen bond acceptors and donors.[82] The different methods to predict drug-excipient miscibility may show in the future even further advancements. Interesting is here, for example, the use of machine learning algorithms if sufficient data are available to train algorithms. In a recent research article, a machine learning approach was used for the prediction of the physical stability of solid dispersions. The prediction success is 82% for ASD stability. Also, modeling and experimental data were compared and they confirmed the results.[95]

2.3.2 Drug supersaturation

As mentioned before, ASDs benefit from a higher apparent solubility and therefore higher dissolution rate due to the relatively higher energy of the amorphous form. Higher concentration in solution compared to the intrinsic solubility of a compound is called supersaturation. The ability to achieve supersaturation is key to generate a high concentration gradient in the GI lumen to drive absorption and an ideal ASD formulation should maintain such supersaturation during the dissolution process.

The theory of the behavior of supersaturating formulations has called this ability to supersaturate a “spring” effect, while the capacity to sustain such high concentrations was named a “parachute”.[16] Upon water dispersion, the high-energy amorphous compound quickly dissolves and thereby reaches supersaturated concentrations and the extent of this spring effect is depending on the compound properties. Also depending on the compound are the kinetics of crystallization that may bring the compound to a less soluble but more stable crystalline form. Some excipients, such as polymeric carriers used in ASD, might retard or inhibit the rate and

the extent of precipitation of dissolved compound, leading to a further increase in absorption due to this "parachute" effect.[16] (Figure 2.6)

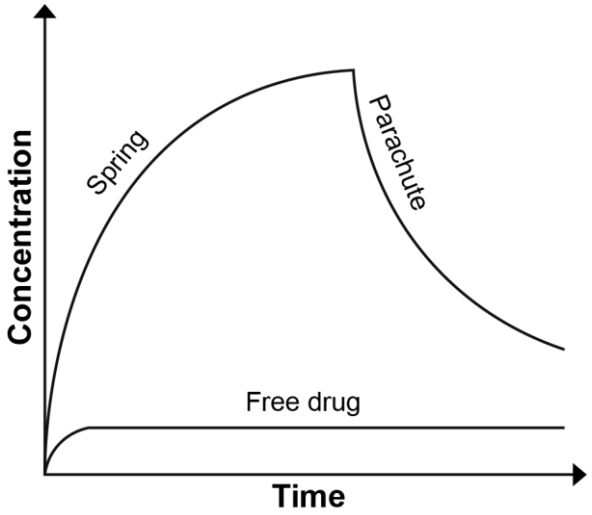

Figure 2.6. Representation of the "spring" and "parachute" effect. (Adapted from [16])

Of all the formulation factors considered, selection of the carrier and the drug loading are the most important. The presence of the carrier inhibits the crystallization of the API already in the solid form and prevents that crystallization occurs that would diminish generation of initial drug supersaturation and hence the "spring effect". Polymers maintain supersaturation of the API during the dissolution by different mechanisms. Molecular interactions of drug and polymer can interfere with nuclei formation and the formation of drug-polymer aggregates has been reported.[50,96] Polymers can also retard crystallization by growth inhibition and hereby the adsorption on surfaces and local generation of high viscosity are mechanisms that can account for this.[97] Recent studies have outlined that increasing hydrophobicity of the polymer, for example adding hydrophobic moieties improves the stability and the supersaturation of the API in the solid dispersion.[98] Such introduced hydrophobicity facilitates direct dispersive interactions of drug and polymer that can form a basis of the "parachute effect" of a formulation. It is helpful to recall that dissolution of an ASD can be kinetically mediated primarily by either the drug or polymer.[17] Upon contact with an aqueous environment, solid dispersions yield a polymer-rich and a drug rich diffusion layer.[17] In the case of carrier-mediated dissolution, the drug diffuses fast into the diffusion layer while in the case of a drug-driven dissolution mechanism, drug particles migrate from the ASD to the dissolution medium. No formation of a polymer-rich diffusion layer is then observed in this scenario.[17]

The interactions of drug and excipients can be complex especially in the intestinal environment

that further includes endogenous compounds such as bile salts and phospholipids. Therefore, interactions are more difficult to understand and predict due to the complex phase separation that is often involved. Previous studies have reported that upon contact with an aqueous solution simulating the gastrointestinal media, ASDs rapidly disperse and provide numerous drug-polymer aggregates.[18,19,99–102]

Therefore, a more complex system evolves when an amorphous formulation dissolves and disperses into a wide range of species ranging from the free or solvated drug, bile salt micelles, free or solvated polymer, polymer colloids, amorphous drug and polymer aggregates and large amorphous and drug particles.[18,103] Formation of nanoaggregates provides a more complex view to explain the sustained supersaturation of solid dispersions because the drug may form nanoaggregates that act as a reservoir that continuously replace the supersaturated free drug in solution.[18,19]

The free drug concentration that is the true supersaturation driving the absorption is due to the release from these particles and colloids in an aqueous environment. The aqueous dispersion of a lipophilic drug alone can exhibit complex phase behavior, leading to a drug rich and water-rich phase. This phenomenon is called liquid-liquid phase separation (LLPS).[104,105] Such generation of a LLPS is expected to occur regularly when ASDs disperse in GI fluids. This phenomenon is observed when the drug concentration exceeds the amorphous drug solubility in the aqueous environment, provoking the formation of mentioned two different phases, a drug rich and a water-rich phase. In the water-rich phase, the amorphous solubility of the compound is present, while the drug rich phase includes a water-saturated amorphous compound but as nanodroplets. The presence of these represents the drug reservoir, which provides drug to the water-rich phase until the amount of the drug in the drug rich phase have been depleted. To gain a deeper understanding of the drug distribution in the drug rich or water-rich phase, fluorescence spectroscopy was employed. One peak was present when the drug was distributed in the drug rich phase, while two peaks were observed when the drug was partitioning in the drug rich phase.[106] Such work suggests that fluorescence spectroscopy can provide valuable insights into the mechanism of drug dissolution.[107] Indeed, it appeared that drug loading represented the main reason for the limiting dissolution mechanism; at low drug loading, dissolution is mainly polymer-controlled, while at higher drug loading it becomes mainly drug-controlled.[107] This example highlights the importance of novel analytical approaches not just to guide the selection of excipients and drug loads but also to achieve an improved mechanistic understanding of

ASDs.

2.4 Physical characterization of solid dispersions

Many challenges might arise during the formulation of ASDs. New emerging characterization techniques can yield valuable insights into the characteristics of ASDs, both quantitatively and quantitatively. These techniques might be employed to investigate the physicochemical properties at different stages of formulation development. Recent review articles outlined the most important techniques used for the ASD characterization.[6,108,109] Among the available techniques, thermal analysis techniques and spectroscopic techniques are the most abundantly employed techniques for solid-state characterization.

Among the thermal characterization methods, differential scanning calorimetry (DSC) or modulated- temperature differential scanning calorimetry (mDSC) are most often employed to determine the solid-state of the drug and drug-polymer interactions within the formulation. In the solid dispersion, if the drug is in its amorphous form, no endothermic peak will be present. Also, a shift of the *Tg* in case of drug-polymer interactions might be observed.[110] Moreover, melting point depression is one of the most common experimental methods to assess drug-polymer miscibility as mentioned before.

Apart from thermal methods, drug-polymer miscibility can be assessed also by spectroscopic techniques. Fourier Transform Infrared (FT-IR) Spectroscopy is employed to study specific interactions between the polymer and the drug functional groups.[110] FT-IR and Raman microscopy can even provide direct visualization of the distribution of the different excipients as well as the physical form of the components.[43,111,112] These two vibrational spectroscopic imaging techniques differ in spatial resolution: indeed this resolution is reported to be around 10 µm for FT-IR microscopy and 1 µm for Raman microscopy.[111] Moreover, Terahertz Raman Imaging has been used to detect different polymorphic forms and to monitor API crystallization during the dissolution process and also to characterize the physical form of excipient including their spatial distribution.[111] Solid-State Nuclear Magnetic Resonance (ssNMR) is another method to determine the physical form of the components and to assess drug-polymer interactions and miscibility. The main advantage of this technique is the detection of phase separated domains with a size below the detection limit of DSC. The miscibility and the drug-polymer interaction are estimated from the spin-lattice relaxation times (^1H T_1).[113,114] When phase separation is present, protons in each phase will have their relaxation times. When a

single-phase system is present, spin diffusion averages individual relaxations resulting in a uniform average relaxation time, different from the relaxation time of pure components.[113,114] Interesting is further solid-state fluorescence spectroscopy that has been applied to study properties of the API within dry powder inhaler (DPI) formulations.[111] This is one of several versions to apply fluorescence spectroscopy and there is much potential to make use of it in the pharmaceutical analysis of amorphous systems. Thus, fluorescence spectroscopy was, for example, employed to demonstrate a phase separation with the formation of drug-rich domains.[115] The immiscibility was detected at a length scale of less than 10 nm, and this technique offered early detection of such lack of homogeneity even though the DSC results showed miscibility based on a single *Tg*.[115,116] Fluorescence spectroscopy was employed further to study phase separation which occurred in the aqueous phase during the ASD dissolution under non-sink conditions.[116] This LLPS phenomenon occurs when the amorphous solubility is exceeded and water-saturated colloidal amorphous drug aggregates form in solution. For this fluorescence analytics, an environmentally sensitive probe, i.e. Nile red, was used to detect the amount of amorphous aggregates that evolved from the various ASDs.[117]

Another promising analytical field for solid dispersion analysis is rheology. Rheological properties of amorphous solid dispersion determine the processability, the mixing and may have on a microscopic level also a biopharmaceutical relevance. Thus, polymer elasticity, viscosity, and viscoelasticity properties are considered for the development of ASDs. Recently, rheological techniques have been employed to study the ASD microstructure as a function of processing methods, drug distribution, and its physical form.[114] Indeed, crystalline particles or aggregates of API present an increased elastic response compared to the amorphous physical form.[114] Rheological measurements also outlined that the incorporation of API resulted in a plasticizing effect in the system.[114] Among the analytical techniques used for characterizing rheological properties of solid dispersions, dynamic mechanical analysis (DMA) and thermomechanical analysis (TMA) are the most employed. DMA measures the strain in the oscillator rheology versus the frequency or the temperature.[43] Recently, a new light scattering tool called Diffusing Wave Spectroscopy (DWS) started to be employed for microrheological characterizations of pharmaceutical systems.[118]

Finally, there are certainly further techniques to be named in the framework of solid dispersion analysis. Other techniques to assess drug-polymer miscibility are not limited but include dielectric relaxation spectroscopy (DRS), atomic force microscopy (AFM),[119] positron annihilation lifetime spectroscopy (PALS),[120] fluorescence resonance energy transfer

(FRET).[43] The following section provides more details on the emerging analytical methods that were relevant in the framework of the current thesis.

2.4.1 Emerging analytical tools

2.4.1.1 Fluorescence Spectroscopy

The last two decades have seen a growing trend towards fluorescence spectroscopy applications in biological sciences. Fluorescence occurs when an orbital electron of an atom or molecule relaxes to its ground state by emitting a photon from an excited singlet state.[121] In the excited singlet state, the electron in the orbital is paired to the second electron in the ground state orbital.[121] Therefore, the return to the ground state is possible and occurs rapidly with the emission of a photon. The emission rates of fluorescence are typically 10^{-8} s so that the typical fluorescence lifetime is circa 10 ns. Typically, aromatic molecules exhibit fluorescence and they are called fluorophores.[121] A schematic absorption and emission spectra for a fluorescent molecule is presented in Figure 2.7. It points to the aspect that the emission spectra occur at lower energies and therefore longer wavelengths. The energy of emission is usually less than the energy of absorption.

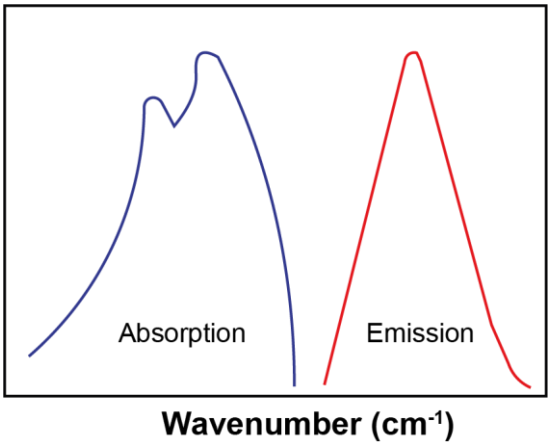

Figure 2.7. Absorption and fluorescence emission spectra. (Adapted from[121])

The fluorescence spectroscopy measurements can provide information on a broad range of molecular processes, such as the interaction of fluorescent molecules with the solvent medium, rotation diffusion of molecules, conformational changes and binding interactions.[121] Organic molecules such as drugs exhibit autofluorescence and are defined as an intrinsic fluorophore.[121] Extrinsic fluorophores such as dyes (for example Prodan) are added to the sample which does not exhibit natural fluorescence.[121]

An interesting way to get information about fluorescence lifetime and excited state deactivation is by introducing quenchers (e.g. acceptor molecules) and by observing the fluorescence intensity as a function of their concentration. From the consideration of the excited state population, it is possible to obtain the so-called Stern Volmer equation that describes fluorescence quenching. The fluorescence intensity in absence and presence of quencher F_0/F are here plotted versus the quencher concentration.[121] The plot of F_0/F versus [KI] should be linearly dependent upon the concentration of quencher and it yields an intercept of one on the y-axis and a slope equal to the Stern-Volmer quenching constant K_D (1/M × s) when the quenching process is dynamic. Analysis of the linearity or deviation from linearity in the Stern Volmer approach is of interest to learn about a given system and in particular about the accessibility of the fluorescent molecule by the quencher.[121]

Applications of fluorescence spectroscopy in pharmaceutical sciences have been limited up to now and interestingly, the Stern Volmer approach has to the best of our knowledge not yet been used to study ASDs. Other fluorescence spectroscopy methods have been applied to study the local environment of the ASD, concerning the miscibility, phase separation and ASD dissolution performance.[122–125]. Indomethacin and itraconazole two native fluorescence molecules, have an excitation band within the typical confocal microscope lasers and therefore allow to study drug distribution within the matrix.[124] A good correlation between the phase separation and reduced physical stability was found, suggesting once again that miscibility is an important factor for ASDs.[124] Fluorescence optical and fluorescence confocal microscopy allows discerning between the drug and the polymer regions in the ASD when adding fluorophores to the formulation. Hydrophobic dyes such as Prodan can partition into drug rich domains within the formulation, while hydrophilic molecules partition into polymer-rich domains.[116,126,127] Indeed, changes in the fluorescence spectrum of the drug or the fluorescent probe such as pyrene have been correlated to changes in the local environment and therefore an indication of the phase separation.[122] Distribution of different excipient within the ASD has been analyzed also using fluorescent probes such as pyrene.[115,123] Fluorescence-based techniques have been also employed to compare two different manufacturing techniques such as spin-coated ASDs and film casting; within the spatial resolution of 300 nm, smaller domains in the first techniques were observed and resolved.[126]

Various studies have assessed the efficacy of fluorescence spectroscopy in studying the mechanism of drug release from ASDs.[115,122] With this purpose, pyrene was employed as a model compound to study the mechanism of dissolution from ASDs. The ratio of emission

between the third peak and the first peak has been considered as a parameter to assess changes in the local environment of the probe. The association of the pyrene with the carrier yields a different emission spectrum compared to the spectrum of free solute in solution.[115,122] The use of fluorescence spectroscopy in drug release analysis supports the previously outlined different mechanisms of amorphous drug dissolution.[107] Indeed, drug loading represents the main reason for alternative dissolution mechanisms; at low drug loading, dissolution is mainly polymer-controlled, while at higher drug loading, it is mainly drug-controlled.[107] Drug dissolution is faster than the phase separation in an aqueous environment at low drug loading, whereas carrier phase separation due to the water absorption is leading to a decreased drug dissolution rate.[107] Fluorescence spectroscopy was also applied to study excipient interaction upon water dispersion.[123] When the dissolution behavior of itraconazole in presence of surfactant was assessed different spectra were obtained when pyrene was associated with micellar or non-micellar solutions, which provided valuable mechanistic insights.[123] The same model compound was used to study the entrapment between the polymer and surfactant.[128] Finally, fluorescence spectroscopy techniques were used to gain a deeper understanding of the drug distribution in the drug-rich or water-rich phase in liquid-liquid phase separation (LLPS).[91,96,97]. One peak was present when the drug was primarily in the drug-rich phase, while two peaks were observed when the drug was partitioning in between drug-rich phase and water-rich phase.[106]

This brief overview of fluorescence application in pharmaceutical analysis of ASDs suggests that there have been many recent advancements but there are also further analytical opportunities that remain to be explored; one of these is the use of fluorescence quenching analysis according to the Stern Volmer approach.

2.4.1.2 Diffusing Wave Spectroscopy (DWS)

Diffusing Wave Spectroscopy (DWS) is a relatively new analytical technique that explores the diffusive behavior of light in a strongly scattering media and characterizes the temporal fluctuation of multiply scattered light to the motion of scattering particles.[129] Therefore, this technique can be employed to study particle motion in concentrated fluids such as colloids, microemulsion and other systems that present strong scattering.[130–132] Compared to other light scattering techniques such as particle sizing, the main advantage is that DWS extends the application from dilute samples to more concentrated and even milky systems that are strongly scattering light.[130–132]

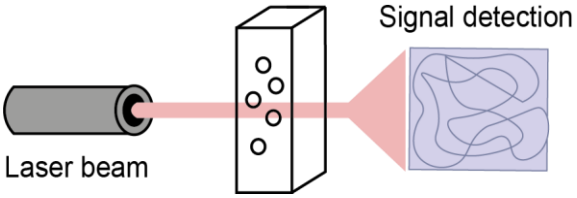

Figure 2.8. Schematic illustration of the DWS. (Adapted from www.lsinstruments.com)

Multiple scattering can be thought of as a succession of several single scattering events, which randomizes the photon path over a photon mean free path length l^*.[129] The principle of DWS illustrated in a simplified scheme Figure 2.8 as follows: coherent light waves (e.g. an incident coherent laser beam such as from an Ar^+-ion laser operating in the single frequency mode at a wavelength of 514 nm) travel through a sample along the various random scattering paths described by a photon random walk, and set up a highly irregular intensity pattern that is called "speckle".[133,134] The speckle is a result of the interference of many waves from many paths of various lengths at the detector. The time of photons passing through the scattering path is much shorter than the time t_0 which takes a colloidal particle to move a distance of the order of the optical wavelength $\lambda_0 = 2\pi/k_0$ ($t_0 = 1/Dk_0$).[133,134] An illustration of the principle of DWS is outlined in Figure 2.8. The time-dependent phase shift $\varphi_{(t)}$ of the scattered optical field due to the motion of scattering particles accumulate along the paths and give rise to the speckle. The time scale does not depend on the angle of observation, but it depends on the geometry of the scattering cell which controls the typical path length and distribution.[133]

DWS is well suited to study interparticle correlation in colloidal suspensions at very high volume fractions and with extraordinary sensitivity to a small displacement of scatters.[129]
The photon mean free path l^* is the length over which photon transport is randomized in a

multiple scattering medium. Knowing *l** is important because it is an indication of the turbidity of the system and affects the length and time scales probed by DWS.[129] The average intensity in the fluctuated light is characterized by the normalized intensity autocorrelation function (eq.5)[129]:

$$g_{(2)}(t)=\langle I(t_0)I(t_0+t)\rangle/\langle I\rangle^2 \qquad \text{eq. 5}$$

where the quantity $\langle I\rangle$ is the average intensity, while *t* represents the lag time. Using the Siegert relation (eq.6), the intensity correlation function and the field autocorrelation are related:

$$g_{(2)}(t)=1+\beta|g_{(1)}(t)|^2 \qquad \text{eq. 6}$$

where β is an instrumental factor given by the collection optics. Once the field correlation function and *l** have been measured, the mean square displacement (MSD, $\langle \Delta r^2(t)\rangle$) of a sample can be calculated employing (eq.7):[135,136]

$$g_{(2)}(t)\text{-}1 \propto \left|\int_0^\infty P(s)exp\left[-\frac{1}{3}k^2 < \Delta r^2(t) > \frac{s}{l^*}\right]\ ds\right|^2 \qquad \text{eq. 7}$$

where $k = 2\pi n/\lambda$ is the optical wavenumber including *n* as the refractive index of the medium and λ is the laser wavelength. *P(s)* represents the distribution of the photon trajectories of length *s* in the sample of thickness *L*, while *l** is the transport mean free path which characterizes the typical step length of the photon random walk.

DWS has extended the use of light scattering to numerous fields, especially in the physics and chemistry of colloids and other complex fluids.[133] The reason is that DWS presents unique rheological measurement capabilities: it employs small sample volume, short acquisition time, non-contact analytics, and good sensitivity. The local rheology is analyzed and the probe can be used to map its spatial heterogeneity and extended range of frequencies over numerous decades of time scales.[129] DWS experiments have been, for example, employed to study gelation phenomena, including physically and chemically cross-linked polymers.[137] Narita et al. studied the sol-gel transition of a solution of poly(vinyl alcohol) cross-linked by borax in water.[137] These polymer networks exhibit gel-like characteristics elasticity at time scales shorter than the lifetime of the network bridge, but show sol-like fluidity at longer time scales.[137]

Microrheological characterizations have been performed not only on polymers but also on various other biological samples. For example, a study of the hydrogel network formation of a peptide and the resulted kinetics have been investigated by DWS.[138] The resulted gelation

kinetics was slow, allowing to study the assembly and the network formation including the critical gel point.[138] A similar approach was pursued by Schultz et al., who investigated the kinetics of the gelation, including the gelation point and the relaxation time for PEG-Heparin Hydrogels.[139]

To date, several studies demonstrated the utility of DWS in the characterization of cell rheology.[140,141] Indeed, due to the high sensitivity, DWS can detect micro displacement of the tracer particles, generating the measurement of the viscoelastic moduli that are more precise and undisturbed compared to the mechanical rheology. [140,141] In this context, Palmer et al. employed DWS to study rheological properties of a biopolymer network formed by filamentous actin (F-actin).[142] F-actin is considered one of the key constituents in the mechanical integrity of eukaryotic cells because it contributes to the cell rigidity. Palmer et al. found that at small frequencies, the actin filament network is characterized as viscoelastic gels because it presents rheological characteristics of a gel, such as a much larger elastic modulus than the loss modulus. [142] On the other hand at high frequencies, F actin networks are liquid-like: the loss modulus dominates the elastic modulus and the network loses its solid-like properties.[142] In the same context, high-frequency rheological measurements were employed to study the cytoskeleton dynamic of living cells.[143] The complex network of the cytoskeleton in cells displays the viscoelastic behavior, where the elastic and viscous responses are frequency dependent. When comparing the cytoskeleton response under drug treatment, the viscoelastic properties differed in the presence of a benign or malign tumor.[143]

The application of microrheology in the field of food science has increased over the last decades. For example, particle- tracking microrheology was used to study the structural dynamics of caseinate-stabilized emulsions containing xanthan and the gelation of casein proteins, as well as glucan polysaccharides.[144,145] Various authors have employed DWS to study short and long-range interactions of β-globulin-stabilized emulsion or the flocculation stability of dextran in the presence of sucrose, the impact of chitosan on microrheological properties of soybean isolate protein-stabilized curcumin, or the caseinate-stabilized emulsions containing xanthan.[146–149] Also, the temperature effect on caseinate emulsion has been studied by DWS. [150] Interactions between high-methoxyl pectin (HMP) and soybean-soluble polysaccharide (SSPS) with sodium caseinate-stabilized emulsions were studied by DWS.[151] It showed the stabilization effect of SSPS in acidified sodium caseinate emulsions; indeed the acid-induced aggregation of the oil droplet was completely inhibited by the 0.2% of SSPS.[151]

Few studies have investigated the use of DWS in the pharmaceutical field.[118,152,153] Among these, DWS has been employed as a process analytical tool for pharmaceutical emulsion manufacturing; indeed, rheological behavior using the intensity correlation function provided qualitative information on emulsion analytics.[118] These data together with a static measurement of the transport mean free path (l^*) correlated very well the evolution of droplet size distribution occurring during manufacturing.[118]

The use of DWS has not yet been investigated upon water dispersion or during the manufacturing of ASD. The importance of rheological properties in the pharmaceutical field has been already outlined in previous studies; for example, high molecular weight polymers influence the viscosity of the diffusion boundary layer around the ASD aggregates, controlling the diffusion of the drug released. Low molecular polymer employed for ASD formulation, will dissolve rapidly, resulting in the release of the drug as a single entity.[154] Viscosity of the dissolution media increases with the food intake, influencing the drug dissolution kinetics.[154,155] Current *in vitro* models for food effect prediction often makes use of pharmacopeias compendial media, considering parameters such as pH, bile salts and lipolytic enzymes as well as phospholipid amount. The viscosity of the media might change during dissolution and permeation processes. There is a study that revealed the applicability of the *in vitro* model to predict the food viscosity effect.[156] Novel *in vitro* predictive dissolution testing considers the influence of the viscosity on the kinetics of drug dissolution. The viscosity influences the hydrodynamic environment and therefore the dissolution rate.[157]

Not just the viscosity of the media but also more generally the rheological properties of pharmaceutical materials such as polymer are central to the field of formulation development. This is particularly important for melt processing, such as hot-melt extrusion and melt granulation. Molecular weight and melt viscosity of the polymer during the processing are key parameters for HME process. Recent studies investigated the influence of a drug's solid-state on the melt viscosity and the influence of the drug concentration, temperature and shear rate on polymer crystallization using rheological tests.[158,159] Given the importance of microrheology in dosage form manufacture and biopharmaceutical considerations, there is much potential to employ DWS in pharmaceutics and a particular analytical opportunity is a use in the characterization of ASDs.

3 Application of the solubility parameter concept to assist with oral delivery of poorly water-soluble drugs - a PEARRL review

Summary

Objectives: Solubility parameters have been used for decades in various scientific fields including pharmaceutics. It is, however, still a field of active research both on a conceptual and experimental level. This work addresses the need to review solubility parameter applications in pharmaceutics of poorly water-soluble drugs.

Summary: An overview of the different experimental and calculation methods to determine solubility parameters is provided, which covers from classical to modern approaches. In the pharmaceutical field, solubility parameters are primarily used to guide organic solvent selection, co-crystals and salt screening, lipid-based delivery, solid dispersions, and nano- or microparticulate drug delivery systems. Solubility parameters have been applied for a quantitative assessment of mixtures or they are simply used to rank excipients for a given drug.

Conclusions: Especially partial solubility parameters hold great promise for aiding the development of poorly soluble drug delivery systems. This is particularly true in early stage development, where compound availability and resources are limited. The experimental determination of solubility parameters has its merits despite being rather labour-intensive because further data can be used to continuously improve *in silico* predictions. Such improvements will ensure that solubility parameters will also in the future guide scientists in finding suitable drug formulations.

Jankovic, S., Tsakiridou, G., Ditzinger, F., Koehl, N. J., Price, D. J., Ilie, A. R., ... & Griffin, B. (2019). Application of the solubility parameter concept to assist with oral delivery of poorly water-soluble drugs–a PEARRL review. *Journal of Pharmacy and Pharmacology*, *71*(4), 441-463.

3.1 Introduction

Solubility parameters have received much attention and numerous applications have been reported in diverse scientific fields.[160] Pharmaceutics has been a prime discipline for applying solubility parameters to formulation design. Previous studies have, for example, reported the use of solubility parameters to predict suitable solvents for solutes; select polymer blends, and to describe surface and adhesion phenomena.[160] It would be interesting to have an overview of such pharmaceutical applications with a particular emphasis on the development of poorly soluble drug formulations.

Development of new formulations requires the use of different tools to predict and analyse the physiochemical properties and interactions of dosage form components.[161,162] For prediction of material properties and their interactions, for example, solubility parameters are routinely used with high levels of success.[161] Historically, this strategy has been employed in drug development for the selection of solvents for coating. Since then, further applications, as well as more robust thermodynamic methods for solubility parameter calculations have also been reported. Specifically, such thermodynamic methods can be used for study and prediction of the physical and chemical properties of compounds together with their effects on mixtures and dosage forms.[161]

The definition of solubility parameter was first coined by Hildebrand and Scott in 1950.[160] An important theoretical development was then proposed later in 1967 with introduction of the so-called Hansen Solubility Parameter (HSP).[160] This concept divides the total solubility parameter (δ_t) in to three different contributions: polar, non-polar and hydrogen bonding and it is therefore more versatile than the original one-dimensional solubility parameter defined by Hildebrand which does not account these specific contributions.[161]

Solubility parameters can be derived experimentally from heat of vaporisation, internal pressures, surface tensions and other material characteristics as outlined by Hildebrand and Scott.[163] Since then, a number of researchers have reported new methods to predict more accurately solubility parameter values, considering for example purely acidic or basis compounds[164] for a specific process technique.[165] More recent predictions of solubility parameters rely on molecular dynamics simulations or on the Conductor-like Screening model (COSMO) and these computational methods have been compared by Diaz *et al.*[166] Important in this context is the research of Panayiotou and co-workers who contributed to the theoretical concept of solubility parameter and proposed a modern quantitative structure-property

relationship.[167] Noteworthy is further the recent article by Louwerse *et al.* that broadly summarized limitations of the solubility parameter concept and proposed theoretical improvments.[168]

Previously, different authors[161,169,170] have shown the practical importance of solubility parameters, but a general overview of their applications in the pharmaceutical field is missing. This article addresses the particular need to review the use of solubility parameters in pharmaceutics with respect to formulation of poorly soluble drugs. The latter oral delivery systems are central to the PEARRL research consortium that is about both, the design of such formulations as well as new tools for their biopharmaceutical assessment.

3.2 Theory and experimental aspects of the solubility parameter concept

3.2.1 Introduction to the solubility parameter concept

The principle of "like dissolves like" is a well-known term within chemical and pharmaceutical sciences, which can be more generally described as "like seeks like". The usefulness of such approaches depends of course on the ability to assign a numerical value to molecular similarity or dissimilarity. Such a quantitative number is provided by the solubility parameter, which is a rather simple but very powerful approach.

For a better understanding of the solubility parameter concept, it is helpful to discuss its historical origins that are linked to the theory of non-ideal solutions. For such solutions, the activity of a solute, α_2 is the product of the concentration X_2 (mole fraction) and the activity coefficient, γ_2 (Equation 1):

$$\alpha_2 = X_2\gamma_2 \quad (1)$$

It is a central task of thermodynamic theories to predict γ_2 and a classical approach is that by Scatchard,[171] and by Hildebrand and Wood:[172]

$$\ln(\gamma_2) = (w_{22} + w_{11} - 2w_{12})\frac{V_2\varphi_1^2}{RT} \quad (2)$$

where V_2 is the volume of the solute and φ_1 is the volume fraction of the solvent and R, T are the gas constant and temperature, respectively (Equation 2). The term w_{11} denotes the energy needed to remove solute molecules from the bulk, while w_{22} equals to the idealised removal of solvent molecules to generate a cavity in the solvent for the molecule to dissolve. Such an idealised transfer of the molecule would lead to gained insertion energy in the solvent or release

of solvation energy of -2w_{12}. It was an important idea to approximate the interaction term w_{12} by the square root of the product of w_{11} and w_{22} so that the following equation is obtained:

$$\ln(\gamma_2) = [(w_{11})^{0.5} - (w_{22})^{0.5}]^2 \frac{V_2 \varphi_1^2}{RT} \quad (3)$$

The advantage of having only pure component properties of the solvent and solute in Equation 3 is that they can be listed for the different chemicals without the need to additionally determine a specific interaction parameter like w_{12}. Hildebrand and Scott[163] coined the notion of the solubility parameter, δ_x that is here given for the solute as follows (Equation 4):

$$\delta_2 = (w_{22})^{0.5} \quad (4)$$

The solubility parameter is the square root of energy per volume and it is often named as square root of cohesive energy density. Units can also be expressed in $MPa^{0.5}$ and hence can also be viewed as an internal pressure.

Equation 3 and 4 show that in the absence of difference in the solubility parameters, the activity coefficient γ_2 becomes unity so that ideal solubility is reached and activity and concentration are equal. Regular solution theory does not consider more complex non-ideal solutions that may lead to an activity coefficient of smaller than unity. Even though regular solution theory is limited in scope, it marked the birth of the solubility parameter concept that is more broadly applicable.

The solubility parameter, for example, can be applied to any mixing process. According to Hildebrand and Scott, the enthalpy of a mixing process is proportional to the square difference in solubility parameters for the mixture components, δ_1 and δ_2 (Equation 5):[163]

$$\Delta H_M = \varphi_1 \varphi_2 V_M (\delta_1 - \delta_2)^2 \quad (5)$$

where φ_1 and φ_2 are the volume fractions of the mixing components that can be for example a drug and polymer.

Apart from mixing enthalpy, a solubility parameter can be linked to any thermal property or to any other molecular interaction parameter. A latter example is the well-known Flory chi parameter χ_{12} that can be expressed in terms of Equation 6 for mixtures that involve a polymer:[160,173]

$$\chi_{12} = \frac{V(\delta_1 - \delta_2)^2}{RT} + \beta \quad (6)$$

where β is an entropy correction term and V is the molar volume of, a solvent or drug in mixture

with a polymer. It seems that β may not be required for essentially non-polar systems but in other cases, such an empirical correction of β may be needed to avoid under prediction of χ_{12}.[160,173] These examples show that particular care is needed when the solubility parameter is used for quantitative conversion to other physicochemical properties or parameters.

The solubility parameter approach is comparatively simple but the art lies in correct application for each given system. The total solubility parameter is for example primarily useful to describe apolar components, whereas Hansen introduced the more versatile concept of partial solubility parameters.[85,160] As previously mentioned, the basic idea in this approach is to split the total cohesion energy (E_{tot}) into different parts that originate from separate molecular interactions. The dispersive energy (E_d) stems from atomic non-polar forces i.e. dispersive Van der Waals interactions, whereas forces between molecules of permanent dipoles constitute a polar energy contribution (E_p). Due to the specific nature of hydrogen bonding, this energy contribution is considered separately (E_h). These partial cohesion energies E_d, E_p, and E_h are divided by molar volume to result in the corresponding total and partial solubility parameters according to Equation 7 and 8:[160]

$$\frac{E_{tot}}{V} = \frac{E_d}{V} + \frac{E_p}{V} + \frac{E_h}{V} \quad (7)$$

$$\delta^2 = \delta_d^2 + \delta_p^2 + \delta_h^2 \quad (8)$$

Equation 8 shows that a three dimensional (3-D) version of the solubility parameter is obtained by consideration of the different partial contributions to cohesive energy density. Figure 1 depicts a series of solvents in this space of dispersive, polar, and hydrogen bonding contribution to the HSP. The invention of partial solubility parameters has certainly advanced the original cohesive energy density approach and opened the field to diverse potential applications wherever molecular interactions of the type "like seeks like" play a critical role. We will in the following part first describe the different ways to obtain total or partial solubility parameters and will then discuss the different applications in the pharmaceutical field. Finally, gaps and current trends will be discussed.

3.3 Experimental and *in silico* determination of solubility parameters

3.3.1 Introduction to solubility parameter determination

Solubility parameters can be evaluated directly by vaporisation of solvents (or sublimation of

solids) as described in the original definition. This, however, is only feasible for materials that can be either vaporised or sublimated (in case of solids), which is often not possible. Many pharmaceutically relevant materials such as coating polymers, polymers for amorphous solid dispersions, drug compounds, or surfactants, require other methods. Therefore, indirect methods have been widely used in the literature for determination of solubility parameters, which are based upon relationships between diverse physicochemical properties and cohesion energy. Solubility parameters can be deduced from measurements of other substance properties than vaporisation. Some of the different methods to obtain a solubility parameter are schematically depicted in Figure 2 and for further reference see the comprehensive review on this topic by Barton.[174] Values for solubility parameters determined using these various methods may vary based upon method setup and/or material. This section describes the methods that have or could be used to characterise pharmaceutical compounds.

3.3.2 Classical determination of solubility parameter

3.3.2.1 Classical approach via latent heat of evaporation

As mentioned earlier, the (total) solubility parameter, was introduced by Hildebrand and Scott, and was defined as the root of the cohesive energy density (*CED*). The cohesive energy density was in turn defined as the energy needed to break all attractive interactions in one mole of a solvent divided by the molar volume according to Equation 9:

$$\delta_t = (CED)^{\frac{1}{2}} = \left(\frac{\Delta E_v}{V_m}\right)^{1/2} \quad (9)$$

where ΔE_v is the latent energy of evaporation and V_m is the molar volume of the solvent. This molar cohesive energy can be further expressed as:

$$\Delta E_v = \Delta H_v - RT \quad (10)$$

Equation 10 can be expressed in terms of latent heat of vaporisation ΔH_v (in case of solvents) the universal gas constant R and the absolute temperature T. ΔH_v can be obtained from calorimetric or vapour-pressure data to finally determine δ_t.

Hansen expanded the total solubility parameter into three components, δ_d, δ_p, δ_h as discussed for Equation 8. This means for nonpolar molecules that δ_p and δ_h are zero and hence δ_t equals δ_d. For polar molecules, the situation is more difficult and calculation methods were developed to assess the partial solubility parameters based on accessible physical properties.

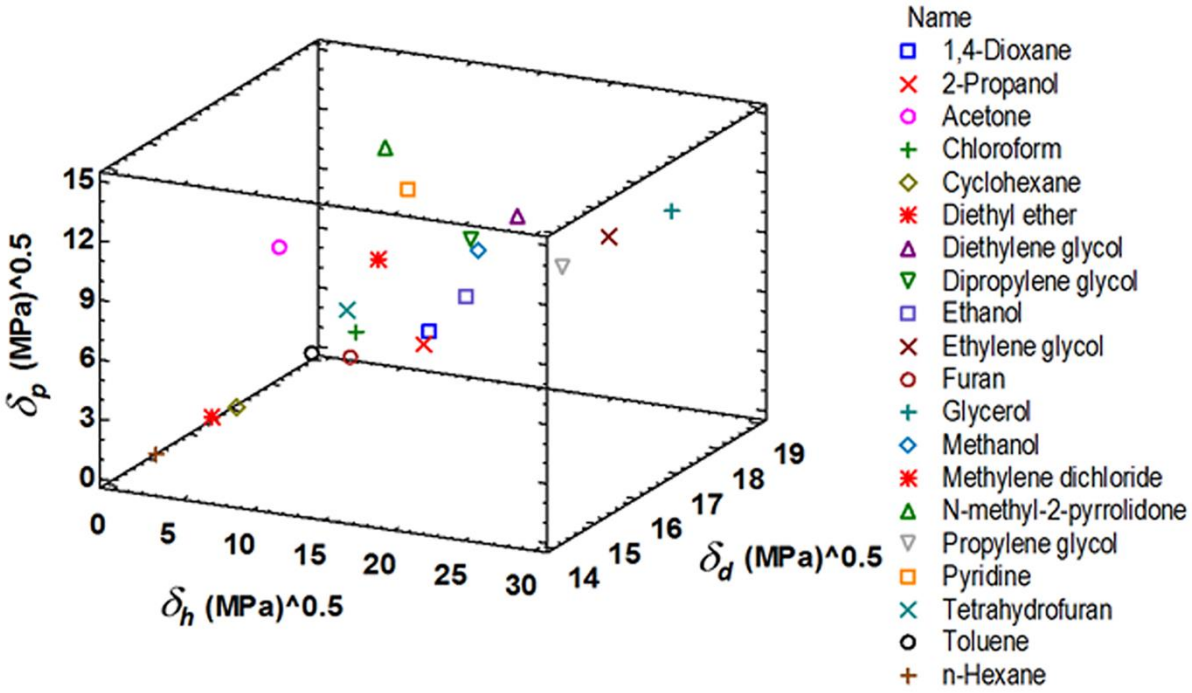

Figure 1. Common solvents are displayed according to their Hansen solubility parameter (HSP) with dispersive (dd), polar (dp) and hydrogenbonding (dh) contribution. Other excipients or also drugs can be represented in this Hansen space and a close proximity of substances suggeststheir miscibility (for colour codes please refer to the online version of the article)

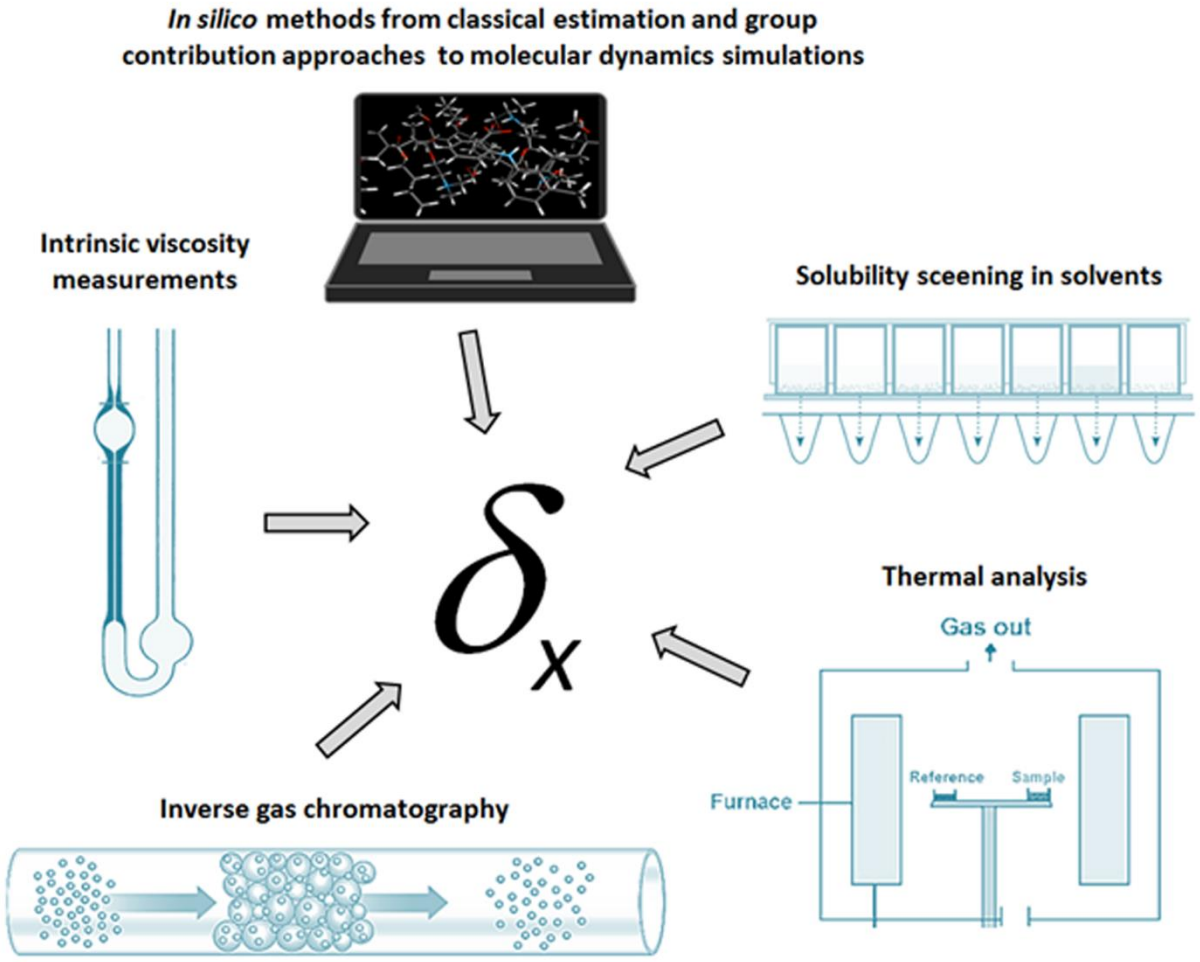

Figure 2. Different methods to obtain one or three dimensional solubility parameter (δ_x).

3.3.2.2 Calculation of the non-polar dispersion solubility parameter

The energy of evaporation can be divided into a polar and nonpolar part by using the homomorph approach.[175–177] The homomorph of a polar molecule is a nonpolar molecule with nearly the same size and shape as that of the polar molecule of interest. The dispersion energy part of evaporation of a polar molecule is therefore approached by the energy of evaporation of the homomorph at the same reduced temperature, T_r. The reduced temperature T_r is defined as:

$$T_r = \frac{T}{T_c} \tag{11}$$

Equation 11 includes the absolute temperature T and the critical temperature T_c, which can be estimated based upon the Lydersen group contributions.[160] Corrections to this approach are required for molecules containing atoms which are significantly greater than carbon, e.g. chlorine, bromine, sulphur, but not for oxygen and nitrogen.[160] For instance, when the

evaporation energy of the nonpolar carbon tetrachloride is compared with the nonpolar homomorph 2,2 dimethyl propane, a difference of 1580 cal/mol (6610 Joule/mol) is found. This difference is divided by four to obtain a correction factor for a chlorine atom in a molecule.[178] Dividing by the molar volume and then taking the square root (see Equation 9) gives the dispersion solubility parameter.[160]

3.3.2.3 Calculation of the polar solubility parameter

The polar parameter of a polar molecule was originally calculated by Hansen and Skaarup[178] using the Böttcher equation and expressed in cal/cm³ (Equation 12):

$$\delta_p^2 = \frac{12108}{V_m^2}\frac{\epsilon-1}{2\epsilon+n_D^2}(n_D^2+2)\mu^2 \quad (12)$$

where μ is the dipole moment, in Debye, V_m the molar volume in cm³/mole, n_D the refractive index using the sodium *D* line and ε the dielectric constant. Later a more simplified equation was used by Hansen and Beerbower[179] according to Equation 13 in $(MPa)^{1/2}$:

$$\delta_p = \frac{37.4\mu}{V_m{}^{1/2}} \quad (13)$$

3.3.2.4 Calculation of the hydrogen bond solubility parameter

Hansen and Skaarup[178] used data from infrared spectroscopy to assign an energy of evaporation of 5000 cal/mol for the OH···O hydrogen bond, hence for a solvent containing hydroxyl groups, the hydrogen solubility parameter can be calculated utilizing Equation 14:

$$\delta_h = \sqrt{\frac{5000N}{V_m}} \quad (14)$$

where *N* is the number of alcohol groups in the solvent molecule. More often, δ_h is calculated by subtracting the dispersion and polar contributions from the total solubility parameter according to Equation 15:[160,180]

$$(\delta_h)^2 = (\delta_t)^2 - \left(\delta_p\right)^2 - (\delta_d)^2 \quad (15)$$

Since hydrogen bonding has a profound effect on solubility, attempts have been undertaken to further expand the hydrogen bond solubility parameter. A hydrogen bond comprises a hydrogen bond donor and a hydrogen bond acceptor and molecules can therefore be classified as[174] i) proton donor e.g. trichloromethane, ii) proton acceptor, e.g. ketones, aldehydes, esters, ethers, tertiary amines, aromatic hydrocarbons, alkenes iii) proton donor/acceptor, e.g. alcohols, carboxylic acids, water, primary and secondary amines, and iv) proton non-donor/non-acceptor, e.g. alkanes, carbon disulphide and tetrachloromethane. From a qualitative point of view,

miscibility can be predicted if hydrogen bonds are formed upon mixing, while demixing occurs when hydrogen bonds are destroyed (e.g. water mixed with alkanes).

An extension of the hydrogen bond solubility parameter to account for hydrogen bond donor and acceptor properties has been suggested by Small[181] and others (Sorenson *et al.*[182]), using Equation 16:

$$\delta_h^2 = 2\delta_a\delta_b \quad (16)$$

where δ_a is the acidic solubility parameter (the donor proton of the hydrogen bond, which is the electron acceptor in the Lewis acid framework) and δ_b is the basic solubility parameter (Lewis base, electron donor). Beerbower and Martin[179] developed the concept to estimate the solubility of naphthalene, benzoic acid, *p*-hydroxybenzoic acid and methyl *p*-hydroxybenzoate in different solvents.[183] However, improvement in accurate miscibility prediction was limited (e.g. benzoic acid: 63% acceptable –i.e. less than 30% error *versus* observed - predictions using four parameters versus 60% acceptable predictions with the three Hansen solubility parameters).

3.3.3 Determination of partial solubility parameters using solvent solubility data

Determination of solubility parameters for drug substances and polymers typically cannot be accomplished through the measurement of the energy of evaporation (because of their non-volatility and due to the fact that evaporation frequently is accompanied by degradation) and therefore only indirect methods can be used. Solubility determination of a solid in a series of selected solvents, which cover the solubility design space in terms of δ_d, δ_p and δ_h, is a frequently used technique to achieve this goal.[160,184–190]

Typically, 10-40 solvents are used for the solubility measurements, which can be conducted as e.g. a classical shake-flask approach where the thermodynamic solubility is determined or only kinetic solubility values are estimated by continuously adding small drug amounts to solvents with optical detection of residual drug. Generally, the solvents are selected such that the compound of interest has good solubility in at least half of the solvents screened. The solubility parameters can then be calculated with multiple regression analysis based on mole fractions solubilised in the various solvents[185,186] or with more modern computer software that uses an iterative method for improving drug solubility parameter estimates in a Cartesian coordinate system (Figure 1) of δ_d, δ_p, δ_h.. The distances between the sample reference point to point representations are calculated for solvents. Then the iterative method adjusts the partial

solubility parameters such that the distance between compatible and incompatible solvents are minimized and maximized, respectively. This iterative minimization/maximization process can then determine a more reliable solubility parameter as recently done by Howell and co-workers.[191]

Table 1. Overview of experimentally determined HSP for pharmaceutical polymers

Polymer	δ_d **(MPa)$^{1/2}$**	δ_p **(MPa)$^{1/2}$**	δ_h **(MPa)$^{1/2}$**	**Reference**	**Remarks**
HPMC 2906, F4M	18.2	16.5	15.5	[192]	34 solvents
HPMC 2208, K4M	18.0	15.3	19.4	[192]	34 solvents
HPMC 2910 E4M	17.4	14.9	19.3	[192]	34 solvents
HPMC 2910 E15	18.8	9.4	11.8	[193]	29 solvents, calculation using HSPiP software[194]
HPMC 2910 E5	18.7	9.8	11.6	[193]	29 solvents, calculation using HSPiP software[194]
Methylcellulose A4M	18.0	15.3	19.4	[192]	17 solvents
HPC, Klucel H – Dow data	17.2	9.8	13.5	[192]	
HPC, Klucel H, Solubility data from Exxon – Dow calculation	17.6	10.2	15.4	[192]	
HPMCAS 716 (L grade)	17.7	11.87	10.19	Dow technical information	Not mentioned
HPMCAS 912 (M-grade)	16.73	12.37	10.33	Dow technical information	Not mentioned
HPMCAS 126 (H grade)	18.09	12.76	9.67	Dow technical information	Not mentioned
HPMCAS MG / Aqoat MG	16.2	10.9	9.0	[195]	Jansen analysis using HSPiP software of the solubility data of 110 solvents [194]
HPMCAS L grade	18.9	12.4	9.0	[193]	29 solvents, calculation using HSPiP software [194]
HPMC phthalate HP 50	20.4	10.2	11.7	[193]	
PVP K30	18.3	12.9	11.4	[193]	

Drug substances as well as polymers can be used as samples. For example, HPMC and HPMCAS are frequently used polymers in stabilised amorphous solid dispersions and with the

"like dissolves like" approach the solubility parameter seems as a feasible way to provide a first guess on the active pharmaceutical ingredient (API) miscibility in these systems. An overview of experimentally determined HSP using the solvent method is provided in Table 1. For HPMCAS, the values were consistent between three independent determinations (see references given in Table 1). For HPMC, a difference was noted for the polarity and hydrogen bonding parameters between Janssen and Archer.[192] This may be attributed both to i) substantial difference in molecular weight ii) the usage of a limited number of solvents, e.g. 10 and iii) the usage of water as solvent by Archer,[192] which is generally not recommended due to the complexity of the solvent.[160]

Solubility parameters obtained *via* the solvent approach have also been reported for characterization of drug molecules and solid excipients such as, preservatives.[183–185,190,196,197] These studies use about 10-25 different solvents in order to obtain an accurate determination of the partial solubility parameters, which seems to be reasonable given the number of unknowns in the regression analysis. Verheven and co-workers[185] investigated five chemically related molecules and reported that the method was sufficient enough to capture the differences between molecules. Barra *et al.*[184] reported a similar finding by investigating a number of free acids and their associated sodium salts and finally, as well as those results published by Kitak and co-workers[190] could find differences between two ibuprofen salts and the free acid. The method is therefore generally perceived as sufficiently precise to determine accurate partial solubility parameters by solubility screening in a number of organic solvents or mixtures of these.

3.3.4 Determination of partial solubility parameters using intrinsic viscosity measurements

The use of viscosity measurements is a frequently used technique to determine the solubility parameter for polymers.[160,195,206,198–205] In this approach, the intrinsic viscosity of the polymer of interest is determined in a number of solvents.[160,198,199] Intrinsic viscosity, $[\eta]$, is given by:

$$[\eta] = \lim_{c \to 0} \left(\frac{\eta_s - \eta_0}{\eta_0 \, c} \right) \quad (17)$$

Equation 17 can be expressed in terms of the solution viscosity (η_s) or, the solvent viscosity (η_0) where c is the solution concentration. The conformation of a polymer in solution is dependent on its interactions with the solvent. In so-called "good solvents" with many interactions, the polymers can swell to some extent, which increases of solutions viscosity. By contrast, in

solvents with limited interactions (i.e. a "poor solvent") the polymer will reduce the contact area to the solvent by shrinking. An interesting approach is to normalize intrinsic viscosities for a polymer in a solvent that provides the highest viscosity value. These normalised data can be used to determine the HSP according to the equations below 18-20:[199]

$$\delta_{D2} = \sum(\delta_{Di} \times [\eta]_i)/\Sigma[\eta]_i \quad (18)$$

$$\delta_{P2} = \sum(\delta_{Pi} \times [\eta]_i)/\Sigma[\eta]_i \quad (19)$$

$$\delta_{H2} = \sum(\delta_{Hi} \times [\eta]_i)/\Sigma[\eta]_i \quad (20)$$

where the subscript 2 indicates the polymer and '*i*' the solvents. The intrinsic viscosity of the *i*-th solvent is described by the parameter $[\eta]_i$. The solvents that are most compatible have the highest intrinsic viscosities and are closest to the geometric centre of a sphere in the Hansen space that encloses good solvents.[160] The separating distance from the centre of the sphere to a last still compatible solvent provides the interaction sphere radius R_0 and is defined according to Equation 21:

$$R_0^2 = 4\left(\delta_{di} - \delta_{dp}\right)^2 + \left(\delta_{pi} - \delta_{pp}\right)^2 + \left(\delta_{hi} - \delta_{hp}\right)^2 \quad (21)$$

where δ_{di}, δ_{pi}, δ_{hi} are partial solubility parameters of the last still compatible solvent, whereas δ_{dp}, δ_{pp}, δ_{hp} denote the partial solubility parameters of the sample polymer. Analogues to Equation 21, is possible to calculate the distance between the sample polymer and any solvent, which is called "solubility parameter distance", R_a. This distance parameter is of more general use and is not restricted to viscosimetry to determine solubility parameters.

An alternative method to determine the partial solubility parameters *via* intrinsic viscosity was developed by Mieczkowski.[207,208] In this method, the values of the volume fraction of a solvent (φ_s) were determined for three mixtures of solvents at which the maximum intrinsic viscosity was found. These fractions were then inserted into to Equation 22:

$$\sum_{i=1}^{3} p_i(a_i - b_i) - [\varphi_s \sum_{i=1}^{3}(a_i - b_i)^2 + \sum_{i=1}^{3} b_i(a_i - b_i)] = 0 \quad (22)$$

where p_i is the component of the solubility parameter of the polymer, a_i is the component of the first solvent and b_i is the component of the second solvent. Using this method, the HSPs for PEO (polyethylene oxide) 2000 were determined as δ_d: 17.3 ± 2 $MPa^{1/2}$, δ_p: 3.0 ± 1 $MPa^{1/2}$ and δ_h: 9.4 ± 0.5 $MPa^{1/2}$.

Furthermore, Bustamante *et al.*[202] also employed viscosity to determine the partial solubility parameter of HPMC with 28-30% methoxy and 7-12% hydroxypropyl content and an approximate molecular weight of 86 kDa (equivalent to Dow E4M). The experimental results

were fitted according to following regression model (Equation 23):

$$ln[\eta] = C_0 + C_1\delta_{1d} + C_2\delta_{1d}^2 + C_3\delta_{1p} + C_4\delta_{1p}^2 + C_5\delta_{1h} + C_6\delta_{1h}^2 \quad (23)$$

Whereas the subscripts 1 refers to solvent and the subscript 2 in the following Equations 24-26 to the polymer:

$$\delta_{2d} = -\left(\frac{C_1}{2C_2}\right) \quad (24)$$

$$\delta_{2p} = -\left(\frac{C_3}{2C_4}\right) \quad (25)$$

$$\delta_{2d} = -\left(\frac{C_5}{2C_6}\right) \quad (26)$$

An extended regression model was used to allow the determination of the Lewis acid (δ_a) and base (δ_b) solubility parameters according to Equation 27:

$$ln[\eta] = C_0 + C_1\delta_{1d} + C_2\delta_{1d}^2 + C_3\delta_{1p} + C_4\delta_{1p}^2 + C_5\delta_{1a} + C_6\delta_{1b} + C_7\delta_{1a}\delta_{1b} \quad (27)$$

Solubility parameters of HPMC for dispersion, polarity and hydrogen bonding were reported to be 14 $MPa^{1/2}$, 16.8 $MPa^{1/2}$and, 31 $MPa^{1/2}$, respectively. As can be seen in Table 1, the data obtained by Bustamante[202] for δ_d and δ_p were in line with the values obtain by Archer[192] while there was a substantial difference for the δ_h solubility parameter. This difference may be attributed to the use of different Hansen solubility parameters for water. Bustamante used 15.5 $MPa^{1/2}$, 15.95 $MPa^{1/2}$ and 42.34 $MPa^{1/2}$, while Archer used 19.5 $MPa^{1/2}$, 17.8 $MPa^{1/2}$ and 17.6 $MPa^{1/2}$ for dispersion, polar and hydrogen bonding respectively. Additionally, Madsen and co-workers[203] employed viscosity to determine the solubility parameter for the pharmaceutical polymers, PLGA and polycaprolactone (PCL). The authors demonstrated that the solubility parameter could be correlated with protein release from the two polymer systems. This example underpins again, how broadly the solubility parameter approach can be applied.

3.3.5 Determination of partial solubility parameters of liquids using inverse gas chromatography

The HSP for pharmaceutical liquids are difficult to determine experimentally using "solubility" methods. Additionally, many pharmaceutical substances including, for example, polymers, polysorbates, ethoxylated oils and vitamin E TPGS are complex mixtures without defined chemical structure and hence are difficult to approach theoretically. In such cases, the determination of the HSP by inverse gas chromatography, is a valuable option. Inverse gas chromatography has been applied to investigate the solubility parameters of polymers,[195,209–212] surfactants,[213,214], epoxidised soybean oil,[215] triglycerides[216] and liquid crystal systems.[217–219]

For measurement of solids, it is recommended for the samples to contain some amorphous fraction, so that the probe gases can enter the bulk. Otherwise, only surface interactions could skew the results for estimated solubility parameters.

Using the inverse gas chromatography method, the material of interest is the stationary phase and is placed into a column. It is then characterised using diverse volatile probes (i.e. volatile solvents with known HSPs). The HSP of the material can then be calculated based on the retention data of the solvent probes.[214] First, the retention times of the solvent probes are converted to specific retention volumes (V_g). These are then used to calculate the Flory-Huggins interaction parameter between the solvent and the sample using the following equation(Equation 28):[220–222]

$$\chi_{1,2}^{\infty} = ln\left(\frac{273.15}{M_1.V_g^{\circ}.P_1^{\circ}}.R\right) - \frac{P_1^{\circ}}{R.T}\left(B_{11} - V_1^{\circ}\right) + ln\left(\frac{\rho_1}{\rho_2}\right) - \left(1 - \frac{V_1^{\circ}}{V_2^{\circ}}\right) \quad (28)$$

where $\chi_{1,2}^{\infty}$ is the Flory-Huggins interaction parameter between the material of interest and the solvent probe, M_1 is the molecular mass, P_1° is the vapour pressure of the solvent probe at the measurement temperature calculated using the Antoine equation, V_1° is the molar volume of the probe, V_2° is the molar volume of the examined material, B_{11} is the second virial coefficient of the solvent probe calculated according to Voelkel and Fall,[223] ρ_1 and ρ_2 are the densities of the solvent probe and material, respectively. The total solubility parameter is then calculated using Equation 29:[210,213,224,225]

$$\frac{\delta_1^2}{RT} - \frac{\chi_{1,2}^{\infty}}{V_i} = \frac{2\delta_2}{RT}\delta_1 - \left(\frac{\delta_2^2}{RT} + \frac{\chi_S^{\infty}}{V_i}\right) \quad (29)$$

where δ_1 is the total solubility parameter of the consecutive test solutes and δ_2 the total solubility parameter of the material of interest, χ_S^{∞} is the entropic part of the Flory-Huggins interaction constant and is usually estimated in the range 0.2-0.4 or 0.6.[212] By plotting the left hand side of the equation versus δ_1, a straight line is obtained of which the slope and intercept are used to calculate δ_2.

Voelkel and Janas[226] extended this original concept, introduced by Price and Shillcock[217] to obtain partial solubility parameters from the linear relationships for solvent groups (*n*-alkanes for δ_{2d}, polar solvents for δ_{2p} and hydrogen bonding solvents for δ_{2h}, while *S* is indicated as the value for the slope) according to Equations 30-32:

$$\delta_{2d} = \frac{S_{n-alkanes}}{2} RT \quad (30)$$

$$\delta_{2p} = \frac{(S_{polars} - S_{n-alkanes})}{2} RT \quad (31)$$

$$\delta_{2h} = \frac{(S_{h-bonds} - S_{n-alkanes})}{2} RT \quad (32)$$

Using this approach Adamska and Voelkel[212] determined the HSPs of di-*n*-butyladipat (Cetiol), caprylocaproyl macrogol-8 glycerides (Labrasol, Gattefosse) and polysorbate 80 (Tween 80) using inverse gas chromatography. Packing of columns with semi-solids and liquid compounds often require special preparation and here, the excipients were dissolved in a suitable solvent to coat on a solid support by slow solvent evaporation. By comparison, an alternative method with fewer assumptions has been used for some of the same excipients investigated by Adamska and Voelkel[214] as described in Table 2. The method used has some parallels with the solubility approach described above. In this method the three partial parameters were iteratively and systematically changed to give the best fit between predicted and experimental values for the interaction parameter, $\chi_{1,2}^{\infty}$, for all the solvent probes tested, hence no solvent probe families were needed. The predicted interaction constant was calculated according to Equation 33:

$$\chi_{1,2}^{\infty} = C_1 + V_m \cdot C_2 \cdot \left[4(\delta_{1d} - \delta_{2d})^2 + \left(\delta_{1p} - \delta_{2p}\right)^2 + (\delta_{1h} - \delta_{2h})^2\right] \quad (33)$$

where C_1 and C_2 are constants and V_m is the molar volume of the solvent probe. This approach is adopted in the software package "Hansen Solubility Parameters in Practice", HSPiP.[194] This software is helpful as it provides tools for many processes such as determining HSP from solubility data and, estimating HSP from the chemical structure as well as databases, which include HSP values for many polymers and excipients. The values obtained for polysorbate 80 and caprylocaproyl macrogol-8 glycerides (Labrasol, Gattefosse) were somewhat different than the ones obtained by Adamska and Voelkel.[214] This is possibly due to the use of different sample preparation methods and column packing material, which influences the retention volume determination. However, it should be also noted that it may be problematic to determine a solubility parameter for surfactants and other amphiphilic substances (e.g. some copolymers) by the use of only a single set of partial solubility parameters. Superstructures such as liquid-crystalline phases are typically formed and probe gas molecules can interact with different microdomains, which is an issue of sample heterogeneity.

Table 2. Hansen solubility parameters obtained for materials using inverse phase gas chromatography compared using different data treatment.

Material	δ_d **(MPa)$^{1/2}$**	δ_p **(MPa)$^{1/2}$**	δ_h **(MPa)$^{1/2}$**	**Remark**	**Reference**
Cetiol	16.5	1.4	4.8	Inverse gas chromatography	[214]
Labrasol	18.0	0.8	3.2		
Tween 80	19.3	0.9	2.8		
PEG 2000 (at 85°C)	19.4	1.6	1.2		[212]
Labrasol	18.3	5.8	7.2	Inverse gas chromatography followed by iterative calculation using HSPiP	Internal Janssen data
PEG 400	19.7	8.3	8.8		
Tween 80	19	5.3	5.6		
Olive oil	16.9	0.6	4.2		

Klar and Urbanetz[195] investigated the solubility parameter for hypromellose acetate succinate (granular type M HPMCAS) by turbidimetric titration, inverse gas chromatography and seven different calculation methods. The total solubility parameter determined by turbidity was 24.7 ± 3.2 MPa$^{1/2}$ for moderately hydrogen bonded solvents and 24.4 ± 0.3 MPa$^{1/2}$ when determined by inverse gas chromatography. Furthermore, the partial HSPs that were determined by inverse gas chromatography and obtained data (17.69 , 12.06 and 11.7 MPa$^{1/2}$ for dispersion, polar and hydrogen bonding respectively) showed good accordance with the value generated by the calculation methods, especially those calculated *via* the Hoy and Te Nijenhuis method, using experimentally determined molecular volumes,[195] as well as the Janssen and Dow values determined from solubility data, see Table 1.

In summary, even though the practice and the theory to determine solubility parameters by inverse gas chromatography has a long tradition, there are new theoretical and practical developments.[216,227]. For future applications, it is interesting to evaluate different calculations methods for inverse gas chromatography. The use of the Flory-Huggins interaction parameters is quite abundant but the theory was developed initially for polymers so that small molecules may be better described by, for example, by the Bragg-Williams interaction parameters.[213]

3.3.6 Other experimental methods to determine solubility parameter

Besides the typical methods described in the section above, a number of other analytical

techniques have been reported in the literature used to determine the solubility parameter. These include swelling,[228–233] turbidity,[195,233–236] ultraviolet spectroscopy, and differential scanning calorimetry (DSC) as well as differential scanning microcalorimetry (µDSC).[237]

Gee described[238] the swelling of rubber in various liquids to derive its solubility parameter, an approach which has also been applied in more recent studies. For example, Eroğlu *et al.*[232] and Çavuş *et al.*[228] measured the weight of a polymer before and after addition of different solvent systems with known solubility parameters by gravimetry and then defined the solubility at the point where optimal swelling was observed. Furthermore, Çavuş *et al.*[228] also investigated the swelling of PVC and found good correlations to the theoretical calculation of the solubility parameter based upon the van Krevelen- Hoftyzer and Hoy methods.[228] The simplicity of the method is highly attractive but the swelling must be of course detectable.

For turbidimetric titration, a polymer (or another relevant excipient) is dissolved in an appropriate solvent. A second solvent that is miscible with the first solvent but acts as anti-solvent for the polymer is then added until precipitation occurs. Shu and co-workers[234,235] developed a method whereby the solubility parameter could be determined from these data. As described above Klar and Urbanetz[195] showed good correlation between the solubility parameter for HPMCAS determined by inverse gas chromatography and turbidity titration. In addition, Schenderlein *et al.*[233] reported the turbidity titration to be more precise relative to the swelling approach when investigating different proportions of lactide to glycolide for poly(d,l-lactide-co-glycolide) (PLGA).

Carvalho SP *et al.*[237] used several methods to determine the solubility parameter for naphthalene, phenanthrene and pyrene and reported UV-vis as the most suited method for a wider molar mass range. For compounds with a low molar mass determination of the vapour enthalpy by DSC was argued to be better based on the similar results and a lower quantity of compound consumption, whereas the µDSC method still required some optimisation. Miecszkowski[205] used refractive index in several solvents to determine the partial solubility parameter for polystyrene and compared these experimental results together with calculations according to the Van Krevelen approach. Ravindra *et al.*[206] derived the solubility parameter of chitosan from intrinsic viscosity, surface tension, and the dielectric constant for data comparison including different group contribution calculations. The average of the calculation

methods yielded 43.1 $MPa^{1/2}$ for chitosan, while the experimental data provided 41.5 $MPa^{1/2}$, 39.8 $MPa^{1/2}$, and 37.0 $MPa^{1/2}$ when determined by viscosity, surface tension, and dielectric constant, respectively. This demonstrates the variation that might be seen across methods. All of the mentioned approaches have their specific assumptions and limitations both with experimental design and data evaluation.

3.3.7 Group contribution methods to calculate partial solubility parameters

The partial solubility parameters describe the ability of a molecule to interact with another molecule *via* intermolecular forces. Given that molecules contain several structural fragments/groups that can contribute to such molecular forces and volume, group contribution methods are meaningful to estimate solubility parameters based only on the chemical structure. The most frequently applied methods are the approaches described by Hoy,[239] Fedors,[240] and Van Krevelen and Hoftyzer,[241] however newer approaches have also been reported, e.g. by Stefanis and Panayiotou.[164,242] An example of solubility parameter calculation is given for lacidipine according to Hoftyzer/Van Krevelen (Table 3). Group contribution calculations are attractive as they require pure *in silico* approach, which demands less computation time compared to, for example, molecular dynamics simulations.

Table 3. Example of the parameters required for solubility parameter calculation for lacidipine according to Hotfyzer and Van Krevelen (modified from Forster [243]). Whereas *z* indicates the functional group, F_{di} is the group dispersion component giving δ_d, F^2_{pi} is the group polar component, E_{hi} the hydrogen bonding component and *V* the molar volume.

Group$_z$	**F_{di}**	**F^2_{pi}**	**E_{hi}**	**$\Sigma^z V/cm^3\ mol^{-1}$**
(7) CH_3	2940	0	0	234.5
(2) CH_2	540	0	0	32.2
(1) NH	160	210	3100	4.5
(1) C	-70	0	0	-19.2
(1) CH	80	0	0	-1.0
(4) C =	280	0	0	-22
(1) Phenylene	1270	110	0	52.4
(2) HC =	400	0	0	27
(3) COO	1170	1470	21000	54
(1) Ring (6)	190	-	-	16
Σ	**6960**	**1790**	**24100**	**378.4**

A solubility parameter from calculations or modelling is typically a bulk property of a liquid or of a supercooled melt. For that reason, it is essential to know whether a compound or polymer

is completely amorphous or contains crystalline parts, which may affect precision of the calculation. Computational concepts assume values for atomic or group contributions to the total cohesive energy. Most of the computational methods are related to the molar volume V_m of a substance, thus V_m has to be either known or calculated. Therefore, some researchers published values of group contributions to V_m, since in some cases reliable values of solubility parameters can be calculated best, when using two complementary methods. Whereas, other concepts e.g. the concept by Hoy, are suited to be combined V_m ascertained by experimental techniques.[239] Especially for high molecular materials as polymers, experimental determined V_m can provide more precise values for solubility parameters, although an experimental determined V_m is not recommended in all cases. For example, the method proposed by Fedors can only yield concise results when using the correlated calculation concept for V_m, since V_m of Fedors' method is often different to other calculations or experimentally determined V_m. Based on such differences it would be pragmatic approach to use different *in silico* methods to work with the median of these predictions.[190,206]

Based on these group contribution components the partial solubility parameters can be calculated;

$$\delta_d = \frac{\sum F_{di}}{V} = \frac{6960}{378.4} = 18.4\ MPa^{1/2} \quad (34)$$

$$\delta_p = \frac{\sqrt{\sum F_{pi}^2}}{V} = \frac{\sqrt{1790}}{378.4} = 0.11\ MPa^{1/2} \quad (35)$$

$$\delta_h = \sqrt{\frac{\sum E_{hi}}{V}} = \sqrt{\frac{24100}{378.4}} = 7.98\ MPa^{1/2} \quad (36)$$

From which the total solubility parameter can be calculated:

$$\delta_t = \sqrt{\delta_d^2 + \delta_p^2 + \delta_h^2} = \sqrt{18.4^2 + 0.11^2 + 7.98^2} = 20.1\ MPa^{1/2} \quad (37)$$

The ease of the calculations has seen group contribution approaches being widely adopted, e.g. Shah and Agrawal[244] used the Van Krevelen and Hoftyzer method to estimate the partial solubility parameters for a number of lipid excipients, including. Dynasan 114, Capmul MCM, Migloyol 812N and others. This approach has also been used for the calculation of solubility

parameters for drug substances,[184,185,190,196,243] which are often compared to experimentally obtained data. Besides the classical group contribution methods it is in principle also possible to employ, for example, the COSMO-RS[245] approach, molecular dynamics simulations,[246] or quantitative structure property relationships. Future research may compare such a modern approach to classical group contribution methods for pharmaceutical dataset.

3.4 Applications of solubility parameters in pharmaceutics

3.4.1 Organic solvent selection

Knowledge of solubility in pure solvents and solvent mixtures is crucial for designing the crystallisation process of drug substances. The first step in finding the optimal crystallisation conditions is usually a solvent screening. To minimise time and resource investment, it would be desirable to conduct *in silico* screenings using solubility parameters or other modelling approaches to reach educated first guess.[247] For this purpose, the use of solubility parameters is simpler than more advanced and complex theoretical models such as COSMO-RS (conductor-like screening model for real solvents), which is computation intensive, and PC-SAFT (perturbed-chain statistical associating fluid theory), which requires extensive parameter determination.[247,248] Thus, *in silico* solubility parameter determination is not the only way to rank solvents for further experiments however, it is significantly more straightforward, especially when considering group contribution methods.

Furthermore, solvent selection can be essential when considering these processes. For example, Rogers and Marangoni[249] reported that changes in solvent chemistry affected nucleation and crystal growth events and therefore defined the physical properties of obtained crystals. In addition, solvent selection can change, solvent−gelator compatibility, affecting the degree of undercooling, chemical potential, kinetics of gelation, and crystal morphology. These parameters are all inter-related and can be correlated to partial solubility parameters. Liu *et al.*,[219] studied crystallisation behaviour of two anhydrous as well as the monohydrate form of piroxicam. Interestingly, additives with a similar hydrogen bonding pattern to piroxicam facilitated crystallisation of anhydrous form I. It was argued that such additives would affect the formation of the different molecular clusters in the supersaturated solution. As a consequence, these additives had a higher ability to influence the nucleation of the different polymorphs. These data suggested that the HSP could indeed be used for preliminary screening of additives for the solid form control of piroxicam during the crystallisation processes.[219] Zhu *et al.*[250] used the partial solubility parameters to select the optimum solvent system for aerogels, which are open-porous predominantly mesoporous solids with a wide range of applications, including oil-spill clean-up and CO_2 capture. A HSP based search method was used to target a specific gel system and because the solvent in this case had a functional influence, its selection was of crucial importance.[250] Solubility parameters can also be used for defining extraction processes, as described by Masurel *et al.*[251] for the removal of tar from flue gas, but also other

publication focus on the use of solubility parameters for liquid extraction,[252–255] even though the applications are not necessarily pharmaceutical. In particular, the partial solubility parameters seem to have several applications within the space of organic solvent selection for either crystallisation or extraction. These processes are especially important for the final steps of drug substance manufacture and even though a solubility parameter approach, however more can be done to harness the power of the HSP in the area of pharmaceutical solvent selection.

3.4.2 Co-crystal and salt screening

Solubility as well as dissolution rate can be significantly influenced by the selection of a suitable solid-state form. Generally high solubility and fast dissolution rate is realised by usage of an amorphous solid-state form.[256] However, a direct use of the amorphous form, e.g. in a capsule or tablet, bears the risk of uncontrolled conversion to the crystalline solid-state form, which has inferior solubility and dissolution behaviour. Therefore, amorphous APIs are not normally used directly but stabilised by suitable formulation techniques,[257] which will not be discussed in this section. Instead, we focus on optimisation of solubility and dissolution by choosing advantageous crystalline solid-state forms. Generally, these comprise pharmaceutical salts, polymorphs – including pseudo-polymorphs such as hydrates and solvates – and co-crystals. Optimisation of aforementioned properties by polymorph selection comes with the same risks as discussed for the amorphous form. Selection of metastable polymorphs increases solubility, but bears the risk of uncontrolled conversion to the thermodynamically stable form. Therefore, a thermodynamically stable polymorph is typically chosen for clinical development, and only in rare cases or when there is limited knowledge of the APIs polymorph landscape, is the metastable form selected. Examples of cases where metastable polymorphs have been used in clinical development can be found in the literature.[258–260] Additionally, compared to the amorphous state, metastable polymorphs provide a much lower increase in solubility, which is why they are less attractive to develop. A schematic summary of the enthalpic processes involved in the dissolution process is given in Figure 3.

For this reason, optimisation of solubility, dissolution rate and consequently bioavailability can be best realised by selecting an appropriate pharmaceutical salt or co-crystal. Even though salt-selection is well established in the pharmaceutical industry, co-crystals have also emerged during recent years as part of more educated solid form engineering.

A comprehensive summary of salt-selection is given by Stahl[261] as well as Neau.[262] Historically, there have also been a few publications which summarize the use of pharmaceutical salts.[263–

267

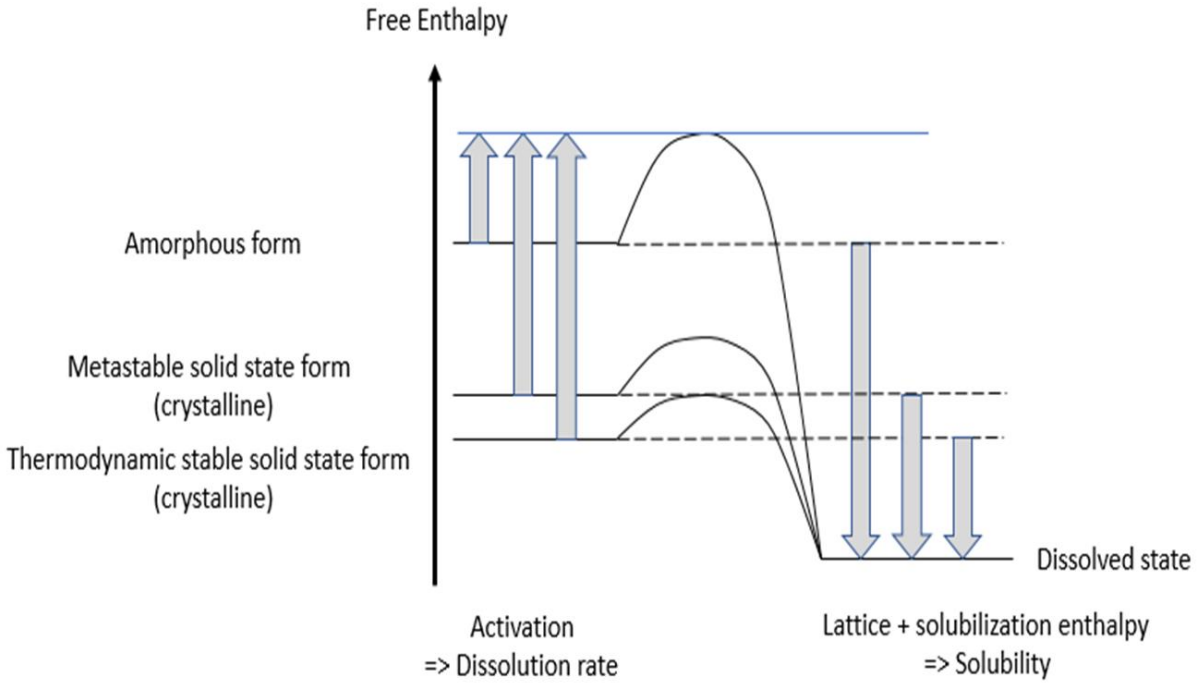

Figure 3 Enthalpic processes involved in the dissolution process.

From such analysis, it is clear that hydrochlorides historically represented the most frequently used pharmaceutical salts for basic APIs and the same was true for sodium if acidic APIs were used. However, in recent decades, it has been clearly recognised that these "one-fits-all" counterions did not always lead to the desired properties intended by the salt formation. This is in line with the observation that new drug candidates entering clinical development, in addition to newly approved drugs, exhibit significantly lower solubility (BCS class II and IV) and require more individualized solutions to optimize their physicochemical behaviour. This does not only include abovementioned solubility and dissolution aspects, but also further parameters such as hygroscopicity, melting point, chemical and physical stability as well as crystal habit. Several examples of optimizing such properties can be found in the literature.[268–271] In many cases, sulfonate salts such as e.g. mesylates, tosylates, napsylates, edisilates showed far better performance with regards to increased solubility and dissolution rate[272] compared to other salt forms. Lower dissolution rate of the parent (either free base or free acid) compared to pharmaceutical salts can be easily explained by the presence of ions in the crystal lattice of a pharmaceutical salt, leading to stronger interactions between the crystal lattice and water as the dissolution medium. However, a similar explanation as to why, for example, sulfonate salts

generally show excellent dissolution rate so far is not available. This phenomenon remains unexplained at least by simple chemical reasoning.

However, there are other more systematic approaches to improve solubility by usage of pharmaceutical salts, which are based on mechanistic understanding: as solubility depends on crystal lattice energy, and high lattice energy will generally result in low solubility, reducing the lattice energy represents a means to improve solubility. For pharmaceutical salts, Coulomb interactions contribute with a major part to the lattice energy. Use of large, "non-coordinating" counterions with low charges (one positive charge or one negative charge) are useful in designing such pharmaceutical salts with improved solubility.[273] In the extreme case, such pharmaceutical salts do not even represent solid APIs anymore, but become liquids.[274–277] As stability can be more challenging for such ionic liquids compared to solids due to increased mobility, this certainly has to be assessed critically. Moreover, toxicological assessment and regulatory acceptance represent the major hurdles for the use of such non-coordinating ions in humans, as none of these salt formers are currently used in human beings or "generally regarded as safe" (GRAS) by the FDA.[278] Therefore, this promising conceptual work on non-coordinating ions has not yet led to approved drugs on the market nor in clinical development.

From a more practical standpoint, several aspects must be considered for selection of pharmaceutical salts or co-crystals. The process steps include salt- or co-former screening and physicochemical characterisation with a typical focus on solubility and dissolution rate but also regarding chemical and physical stability while considering toxicological aspects of the selected salts or co-formers. This screening stage represents the starting points for the selection of a salt or co-crystal, respectively. Earlier, such screening was carried out as a typical synthesis process in lower gram-scale. Today salt or co-former screening is conducted on the lower mg-scale which saves API and allows conductance of such screens earlier during the research process. For this purpose, different screening approaches exist in the pharmaceutical industry. A salt or co-crystal screening might be carried out in an automated way using robotic systems that employ different solvents and solvent mixtures according to a fixed protocol. Alternatively, salt or co-crystal screens can be based on a rationale, non-automated process where small-scale crystallisation trials are performed and crystallisation is closely observed. This allows information to be obtained sequentially from one experiment to another. Even though for a single trial, larger amounts of API are required compared to the automated approach a repetition of unsuccessful experiments is avoided. A useful comparison of different screening approaches can be found in the literature for salt selection.[279]

Following initial screening of possible salt and co-crystal formation, characterisation of solid state properties, including melting point, hygroscopicity and stability is important; as well as analysis of solubility, dissolution and supersaturation. The aforementioned steps to salt and co-crystal formation offer different opportunities to use solubility parameters. One application is certainly the selection of organic solvents or anti-solvents for solid form screening, which is in line with the previous section. Other applications of partial solubility parameters are selection of ionic liquids even though they are still currently quite toxic or not sufficiently characterised leading to regulatory hurdles in pharmaceutical development. More important therefore, are applications to the field of co-crystals where it has been attempted to predict formation based on HSP.[280] A recent study conducted co-crystal search of itraconazole during which the HSP was used to rank different amino acids as potentially suitable co-formers.[281] In spite of such reports, there are also typical limitations of solubility parameters because they cannot account for specific aspects of the crystal lattice. There are currently methods in structural informatics that can use the Cambridge Structural Database to assist *in silico* screening of the energy landscape of possible crystals. These approaches together with other computational methods used in pharmaceutical solid state chemistry have been recently reviewed in an excellent book.[282] Therefore, partial solubility parameters can be applied successfully in the field of salt and co-crystal screening, however in cases where details of a crystal lattice energy landscape should be considered, alternative methods of solid state modelling are recommended.

3.4.3 Solubility parameter concept in lipid-based formulations

Lipid based formulations have been an important part of the toolbox to formulate low water-soluble compounds for over 50 years. Additionally, an increased prevalence of such poorly soluble drug candidates in the last two decades has also intensified the interest in lipid-based drug delivery systems (LBDDS). The biopharmaceutical advantages of LBDDS include the potential to enhance bioavailability, decrease pharmacokinetic variability as well as food effects, promote lymphatic absorption, and support controlled drug release.[283]

A key element of LBDDS is that the drug substance is dissolved within the lipid excipients before administration, hereby presenting the drug in a pre-solubilised state in the gastrointestinal tract. The level of solubility in the LBDDS is, hence, important to achieve the above-mentioned biopharmaceutical advantages. Therefore, options to predict and rank drug solubility in lipid excipient mixtures are of high interest to guide LBDDS formulation

development. Generally, the solubility in lipid excipients is determined experimentally; however, these experiments are costly, time-consuming, resource-intensive and the experimental protocols vary substantially between different research groups.[284] Also, LBDDS are often mixtures of different excipients, e.g. lipids, surfactant and co-solvents, so the number of typical solubility studies required can be very extensive.[284,285] Recently, the utility of empirical models to predict drug solubility in lipids has been explored, using multivariate data analysis with several molecular descriptors.[284–286] A disadvantage of any such multivariate approach is that the size and quality of the calibration dataset highly influences the accuracy of the prediction. Thus, an alternative to complex computational models, is the HSP approach that has been proposed to guide lipid-excipient selection. Dumanli *et al.*[287] used the HSP to rank compound solubility and miscibility in/with lipids. The required solubility parameters can be obtained either from experiments or from calculations as previously outlined in section 2. For lipid-based excipients, vapour pressure and boiling point determinations, miscibility of reference liquids (with known cohesive energy), inverse gas chromatography, and calculations using group contribution methods are of particular interest to determine HSP.[288] Solubility parameters have been commonly employed for this purpose, especially for characterisation and release of raw materials for cosmetics[289–291] and in the oil and textile industry.[292] However, there are not many applications of solubility parameters for lipid-based systems in the pharmaceutical field. Most studies determine the solubility parameter using theoretical group contribution approaches and often only consider simple mixtures, i.e. compound A in oil B.[46,244] De La Peña-Gil and co-workers[293] investigated methods to predict and calculate HSP of complex lipidic mixtures (i.e. vegetable oils) by using the HSPiP software.[194] Two approaches were used to determine HSPs. In one approach it was assumed that each functional group (fatty acids, fatty acids + glycerol and fatty acid methyl esters) present in triglycerides, had an additive contribution to the dispersion, dipole-dipole, and hydrogen bonding interactions. Therefore, the composition of triglycerides was divided into different functional groups and each component of the total HSP (δ_t) was calculated (i.e. δ_d, δ_p and δ_h). The second approach assumed that vegetable oils are mixtures of simple triacylglycerols in the same mass fractions as the fatty acids.[293]

Two studies by Shah and Agrawal[244,294] investigated the utility of HSP as a predictor for optimal carrier and solvent system selection:[294] firstly to describe the solubility behaviour of a drug (ciprofloxacin HCl) and lipid excipients and secondly, for the design of solid lipid nanoparticles (SLNs).[244] Both studies used the Van Krevelen/Hoftyzer group contribution approach to

calculate the HSP for different solvents, polymers and lipids by using the Molecular Modeling Pro software. Calculation of the solubility parameter was based on at single repeating polymeric unit for the polymers whilst, for lipids consisting of mixture of glycerides the calculation was carried out based on an average predominant ratio.[294] With the Van Krevelen approach, the molar attraction constant (*F*) was calculated and all the extended HSPs determined. The calculated values of the total HSP were matched between different lipids, organic solvents and drug compounds and when similar values were observed then the systems were considered miscible. Shah and Agrawal[244] validated the mathematical model used by experimental testing of drug solubility in the selected excipients and solvents. Both studies[244,294] succeeded in qualitatively predicting the solubility of ciprofloxacin HCl in different lipids and subsequently the solubility of lipids in various organic solvents by using the HSP determination/calculation. This approach resulted in identifying the most promising lipid candidates for maximum drug loading in SLN formulation consisting of glyceryl monocaprylate and glycerol monostearate 40-55. These studies demonstrate the possibility of using the HSP for optimal selection of excipients in designing SLNs and qualitative prediction of excipient-drug compatibility.

Another application of the HSP was suggested by Li *et al.*[295] to estimate the compatibility between materials to facilitate the design of polymer-lipid hybrid nanoparticles (PLN). Specifically, the enthalpies of mixing for a drug-polymer complex (i.e. verapamil in dextran-sulfate-sodium) and 15 different lipids including triglycerides, fatty acids, glycerol esters and mixtures of glycerol esters were predicted by accounting for the volume fractions of components in the mixture. The study also used the Van Krevelen/Hoftyzer group contribution approach to calculate HSP and showed the suitability of the HSP theory in the screening of lipid carriers for PLN design of verapamil.[295]

While useful to determine how a lipid or lipid mixtures may behave as solvent(s) and the possibility to predict how some compounds solubilize in lipids, the HSP concept has also some limitations. Firstly, the concept only considers the energies derived from direct contact of components and does not account for the entropy effects and the free volume of, for example, amorphous solids.[244] The free volume is defined as an empty space in a solid or liquid that is not occupied by the molecules. Generally, amorphous solids are inefficiently packed and present a considerable amount of free volume compared to ordered materials. Additionally, it was mentioned before as a disadvantage that a given crystalline solid-state form is not

accounted for. By contrast, experimental HSP determinations are generally conducted with the most stable polymorph. Studies have suggested that HSP calculations based on group contribution methods provide accurate predictions if materials with similar structures are compared, as the calculation does not account for the dependencies on conformation, concentration and specific intermolecular interactions that might occur in binary mixtures.[46] Finally, another limitation of the theoretical model is that it disregards specific self-association of molecules, which is also the case with further thermodynamic approaches other than SAFT (statistical associating fluids theory) calculations.

The HSP approach within LBDDS has only been investigated to a limited extend, potentially due to the variability and complexity of the lipid excipient composition and the multitude of drug excipient interactions. However, there are further pharmaceutical applications that are to some extent linked to lipids in general such as intestinal drug absorption,[296] skin penetration of topically applied drugs,[297] and prediction of drug-nail interactions.[298] The available studies suggest that partial solubility parameters have the potential to be a useful tool in early development of LBDDS.

3.4.4 Solid dispersions

3.4.4.1 Amorphous solid dispersions

Modification of the solid drug form to increase solubility and dissolution rate has been mentioned before (section 3.2.).In this endeavour, the high energy that the amorphous state can provide is especially interesting.[38,161,299,300] However, the amorphous state is thermodynamically unstable and tends to revert to a crystalline polymorph. The amorphous drug state can be stabilised by solid dispersion,[20,301] complexation with large (e.g. cyclodextrins)[302] or small molecules,[303] and spatial confinement (e.g. absorption on silica).[304,305]

Solid dispersions involving the immobilisation of amorphous API in polymer have been studied extensively in the literature[109,301,306,307] and are one of the most widely employed approaches to formulate an amorphous drug form. Amorphous solid dispersions (ASD) is an umbrella term for different types, which can be glass solution, glass suspension and solid solutions of drug in the carrier.[301,308] Drug-polymer miscibility is key to consider when formulating solid dispersions[89,309] and to obtain a single phase system, both the API and the carrier have to be miscible. Such miscibility can be calculated using advanced thermodynamic models, such as the previously mentioned PC-SAFT and COSMO-RS theories or the simpler Flory-Huggins

model may be applied.[310] The advantages of suitable prediction accuracy of advanced thermodynamic approaches have to be balanced against drawbacks like either extensive computation time or the need for parameters that have to be based on extensive experimentation. This makes the simpler solubility parameter approach very attractive and either the total Hildebrand solubility parameter can be considered or partial solubility parameters. Thus, HSP has been extensively used to identify drug-excipient miscibility with a general rule of thumb that molecules with similar δ values are assumed to be miscible.[89,102,190,280] This method considers the dispersion and polar interactions of a system as well as the hydrogen bond contributions of the test molecules. We emphasise again that HSP hereby addresses the main limitation of the conventional Hildebrand solubility parameter, which does not discriminate the different partial contributions to cohesive energy density.[160]

However, ASD formulation miscibility has been investigated with both the Hildebrand[28] as well as the Hansen[243,311–313] approach. It was proposed by Greenhalgh and co-workers[89] that systems with a difference in solubility parameters from 1.6 to 7.0 $MPa^{0.5}$ present no miscibility problems. However, substances with a difference of 10.8 to 18.0 $MPa^{0.5}$ were considered immiscible. Further practical measurements showed that systems with a difference of 1.6 to 7.5 $MPa^{0.5}$ could be considered miscible in the molten stage. Systems with a difference of 7.4 to 15 $MPa^{0.5}$ were slightly immiscible in the liquid state. Total immiscibility was observed in systems with differences greater than 15 $MPa^{0.5}$.[89]

With the Hansen approach similar observations were made when testing the miscibility of 2 drugs in 11 excipients.[243] Systems that were predicted to be miscible using the Greenhalgh values formed glass solution *via* hot melt extrusion while those combinations that were predicted to be immiscible formed solid dispersions in which the amorphous drugs was dispersed in crystalline carriers. On the other hand, when the Hildebrand approach was utilised in combination with log*P*, pK_a and T_g considerations, amorphous miscibility between additives and polymers failed to be predicted for systems in which acid-base interactions took place.[28] Systems which were predicted to be immiscible, but showed acid-base interactions, still resulted in ASD formulations. Contrastingly, this approach accurately predicted miscibility and ASD formation for systems produced *via* a solvent evaporation method without acid-base interactions. This underlines again that the Hildebrand concept with a single value for total solubility parameter cannot adequately account for specific or hydrogen bonding interactions.

As mentioned previously, the HSP concept offers a 3-D solubility parameter concept that can

be visualized in the Hansen space (Figure 1). A way to project a 3-D solubility parameter in a two-dimensional plane was proposed by Bagley *et al.*[314] It was argued that the thermodynamic contribution to the solubility parameter of the polar and dispersion interactions are often similar, and therefore a combined solubility parameter (δ_v^2) can be derived from Equation 8 to yield the following Equation:[314]

$$\delta_{\mathrm{d}}{}^2 + \delta_{\mathrm{p}}{}^2 = \delta_{\mathrm{v}}{}^2 \quad (39)$$

The plot of δ_v versus δ_h, simplifies the 3-D Hansen space into the 2-D plane, which is referred to as a Bagley plot. Analogues to the previously discussed Hansen space, it is assumed that molecules in vicinity of each other are more likely to be miscible.[190,309] The Bagley plot has been utilised to evaluate and predict miscibility between molecules using the $R_{a(v)}$ parameter, which gives an idea of the 'area of miscibility' around a molecule, and should be ≤5.6 $MPa^{1/2}$ for miscibility. This parameter is analogous to the R_a in Equation 21 but uses the simplification of Equation 39 to a drug polymer system:

$$R_a(_v)^2 = [4(\delta_{v2} - \delta_{v1})^2 + (\delta_{h2} - \delta_{h1})^2] \quad (40)$$

Bagley plots are highly versatile and have been used to investigate the miscibility of polymers in solvents,[241] drugs in excipients[102,190,309] and polymers in polymers.[315] It is important to consider the selected method when calculating solubility parameters, as different methods can give rise to different Bagley plots, which was highlighted by Meaurio and colleagues.[315]

These theoretical considerations were applied to ASD formations by different authors.[102,309] One study tested 84 drug molecules for their miscibility in PEG and demonstrated a good correlation between the group of drugs forming ASDs with PEG with the plot region around PEG derived from theoretical solubility parameter calculation.[309] Alhalaweh *et al.*[102] compared experimentally derived miscibility data of indomethacin and excipients with predicted miscibility data. The Bagley plots of these data sets were almost identical and the predicted data showed a good correlation to the ASD formation.

Another prerequisite for the formation and stability of successful ASDs is that the change in the free energy of the system upon mixing should be negative. Because ideal mixing increases the entropy of the system, the entropy contribution should facilitate mixing. Consequently, it is the enthalpy contribution that may prevent free mixing energy ΔG_m to be negative. In drug-polymer systems the Flory-Huggins equation has been adapted to align with the lattice-based equation (41) used for the dissolution of polymers in solvents[316–319] as previously described in Equation 5.

$$\Delta H_{\mathrm{m}} = V_{\mathrm{dp}}\varphi_{\mathrm{d}}\varphi_{\mathrm{p}}(\delta_{\mathrm{d}} - \delta_{\mathrm{p}})^2 \quad (41)$$

where subscript *d* and *p* describe drug and polymer respectively, while ΔH_m can, also, be given by the van Laar expression according to Equation 42:

$$\Delta H_m = \chi_{dp}\varphi_d\varphi_p RT \quad (42)$$

From Equation 42 it can be seen that the value of the drug-polymer interaction parameter, χ_{dp}, could be a surrogate for the enthalpy of the system, for given conditions. By combining equations (41) and (42), the drug-polymer interaction parameter can be given by Equation 43 (neglecting β) which is in line with the previously discussed Equation 6:

$$\chi_{dp} = \frac{V_{dp}(\delta_d - \delta_p)^2}{RT} \quad (43)$$

Where V_{dp} is volume of mixture, φ_d, φ_p are volume fractions of drug and polymer, δ_d, δ_p are solubility parameters of drug and polymer.

Similar to the total (or Hildebrand) solubility parameter, the HSP has also been linked to the drug-polymer interaction parameter (χ_{dp}) by consideration of partial contributions to cohesive energy density.[241]

The drug-polymer interaction parameter has been used widely for the investigation of binary mixtures especially, miscibility based on a negative ΔG_m. Although this parameter can be determined by melting point depression,[90,317,319,320] there are also some studies that use the 3-D solubility parameter approach[309,319,320] to investigate drug-excipient miscibility in a more quantitative way. Such construction of a phase diagrams shows the differentiation of single and two phase system at equilibrium (binodal line) and kinetic decomposition of metastable mixtures (spinodal line) can be estimated.[18,321] It is attractive to construct entire phase diagrams but this objective is more ambitious than use of the solubility parameters to simply rank excipient selection based on rules of thumb, such as based on the proximity of drug and excipient representations in the Hansen space or Bagley plot. A key strength of the solubility parameter is that such approaches are in general rather simple. A more ambitious quantitative calculation of entire phase diagrams can suffer from the simplifications of the thermodynamic approach as well as from lacking prediction of solubility parameter estimates. Phase diagrams constructed *via* solubility parameters might therefore be better considered as a first approximation only.

3.4.5 Mesoporous silica

Recent developments suggests mesoporous silica as a new and promising material to formulate poorly water-soluble drugs with the intent to increase dissolution rate and solubility.[305,322–326] Loaded mesoporous silica is prepared *via* adsorption of API from a concentrated organic solution followed by evaporating the solvent. This adsorption into the porous network stabilises the API in the amorphous state, due to steric effects. Upon administration, this amorphous API is then released and the dissolution is increased.[323]

Utilisation of the solubility parameter in the development of amorphous mesoporous silica is still largely unemployed without commercial formulations that are globally on the market. This represents a key gap in the literature, as solubility parameters can guide the selection of suitable solvent to maximize the penetration efficiency of API into mesoporous silica, which was demonstrated by Hideo Hata and co-workers.[327] They showed that, of six different solvents used to incorporate taxol onto mesoporous silica, only two resulted in effective loading of the API. They concluded that solubility parameter was a key factor in this observation; where solvents that interacted strongly with taxol resulted in the most effective loading, whereas those with weak interaction showed poor loading efficiency. Such interaction can be determined using solubility parameter approach.[327] However, the range of solvents suitable for use with formulation development is limited. Those solvents that show the strongest solubilisation power are often seen as 'no-go' solvents based on ICH guidelines.[328] Therefore, most instances of mesoporous silica use in the literature are carried out with either ethanol, acetone or dichloromethane, with even the latter being less utilised due to toxicity considerations.[305] The ICH list certainly limits solvent selection but not to the extent as it is currently reflected in the literature on mesoporous silica so there is potential to access a wider range of solvents by employing with a rank-order based protocol based on *in silico* solubility parameter calculation.

ASD systems have proved to be a useful formulation tools in battling the solubility issues of pharmaceutical molecules. However, because of their limitations in stability, miscibility of the system is of crucial importance for a successful formulation. This makes the identification of tools to evaluate miscibility in the development phase, not only useful, but imperative. Herein the application of solubility parameter concepts to assess miscibility has been reviewed and discussed in the previous section 3.4.1. It should be emphasised again that a consideration of partial solubility parameters is preferred to a simple comparison of total (i.e. Hildebrand) solubility parameters. Moreover, the need of a complete database for partial solubility

parameter either for drug and polymer was highlighted when using HSP. A limited number of data is not only available with respect to experimentally determined values but also for group contributions as used for *in silico* prediction of solubility parameters. The latter limitation can be especially troublesome in case of HSP estimation for more complex drug molecules. Application of the modified solubility parameter approach was applied by Piccinni[329] and even though the usefulness for early excipient ranking was recognised, it was also emphasised that physical screening tests should not be replaced by the *in silico* method until more robust prediction methods are available. This supports what was discussed in the previous sections that solubility parameters can be calculated *in silico* to rank excipients for a subsequent experimental screening. Such a screening phase can therefore be designed in a more focused and cost-effective way rather that be entirely replaced.

3.4.6 Application of solubility parameters in the formulation of nano- and microparticulate systems

One of the most used methods for dissolution improvement of poorly water-soluble drugs is particle size reduction. The decrease in size increases the surface to volume ratio, which accelerates dissolution kinetics. Especially interesting here are sizes well below 1µm, which have the highest potential increase the kinetic drug solubility[330,331] in addition to the dissolution rate enhancement. Thus, by bringing particle size to the nanoscale, solvation pressure increases and facilitates the disruption of the intra-solute bonds thus promoting solubilisation.[332]

Micronisation and nanosizing methods can be grouped into two categories: the top-down methods that entails size reduction of bigger particles by the use of shear forces and the bottom-up methods that involve the isolation of drug particles after recrystallisation from a highly supersaturated drug solution.[331] Although traditional micronisation techniques, such as dry-milling, are still being used, bottom-up approaches are becoming increasingly sophisticated, gaining merit as techniques that can circumvent typical process limitations.[333] These limitations may involve unwanted amorphisation, disruption of the crystal lattice and unpredictable particle size distributions.[334] However, bottom-up approaches also face their individual limitations. Due to the fact that they rely on the controlled precipitation of particles from supersaturated solutions, miscibility and solubility considerations should be taken into account for the optimal choice of formulation combinations.

Moreover, technical developments in both top-down (e.g. “pearl” milling and high-pressure

homogenisation) and bottom-up techniques (e.g. new-generation spray dryers, supercritical fluid technology and freeze drying) have broadened the availability of nanosizing approaches. As nanoparticles exhibit high surface cohesive energies, they are especially prone to aggregation,[335,336] making their stabilisation indispensable. The use of various stabilizers, often surfactants and/or polymers, has been reported. It is proposed that they work by sterically or ionically stabilizing the surface of nanoparticles, in order to limit aggregation.[337] The choice of appropriate stabilizers seems to greatly depend on the physical characteristics of the surface of drug molecules.[338] Consequently, the need for reliable tools to estimate possible candidates for nanoparticle formulations is evident.

Several attempts for nano- and micronised formulations have been reported in literature using a variety of materials including proteins, lipids and polymers.[339] We considered here not only the classical top-down and bottom-up approaches but more broadly reviewed also micro- and nanoparticle formation. Calculated solubility parameters are used eventually here as an early evaluation of miscibility of solvent-solute combinations as well as miscibility between molecules. However, evidence of using solubility parameters later during formulation development is very limited. To the best of our knowledge only few relevant literature references exist, i.e. where a solubility parameter approach has been used for choosing the appropriate lipids in drug-polymer-lipid nanoparticles,[295] for choosing the drug-polymer combinations for the construction of polymeric micelles and for predicting drug loading.[340,341] Furthermore, Mahmud *et al.*[341] and Dwan'Isa *et al.*[340]used the HSP to calculate the Flory-Huggins interaction parameter of drug-polymer combinations (χ_{dp}) and considered it as a measure of miscibility.[83] Dwan'Isa *et al.* tested 19 drugs for their interactions with a diblock co-polymer (MePEG-*b*-(PCL-*co*-TMC)), while Mahmud *et al.* studied the interactions of one anticancer drug (curcubitacin I) against a variety of core-forming polymers. In both studies, the calculation of the χ_{dp} parameter was able to reveal the optimal drug-polymer combinations, as well as to predict the drug loading capacity of the polymer micelle formulations. Even though the calculation of the interaction parameter provided a reasonably accurate method for the qualitative prediction of drug solubilisation in the polymeric micelles, a definite rank-order of combination miscibility among the variations tested could not be achieved, which may be attributed to the limitations of the Flory-Huggins theory as well as lacking accuracy of estimating the interaction parameter. Simplifications included the disregard of polymer molecular weight and polymer solvent interactions.[83] Nevertheless, the calculations of the HSP and the Flory-Huggins interaction parameter have been proven to be adequate tools for the

primary selection of potentially miscible nano- and microparticulate systems, which helps in reducing the number of early screening experiments.

3.5 Conclusions

Solubility parameters have proven to be useful in diverse scientific fields and this review has outlined the different applications concerning oral delivery of poorly water-soluble compounds. These compounds typically require bioenabling formulation for successful development and solubility parameters can help, for example with ranking of solvents and excipients to achieve a more focused formulation development. Herein, predictions based on chemical structure are particularly interesting since only limited compound is available in early development. Despite the usefulness of applying solubility parameters in pharmaceutics, there are also some gaps. Especially drugs in a solid crystalline state or also rather complex molecules in general may result in erratic predictions of solubility parameters. However, it is promising that new theoretical developments have been reported that present conceptual improvements. Moreover, experimental methods like high-throughput solubility testing or greater availability of inverse gas chromatography will help in generating more data. Important is to obtain more comparative data of experimental and computational methods to better learn about variability of results. This can in turn help to further improve *in silico* predictions of solubility parameters and a just accepted article has been following this research direction.[94] Therefore, it can be expected that solubility parameters will also in the future rank among the mostly used thermodynamic approaches in pharmaceutics

4 Towards a better understanding of solid dispersions in aqueous environment by a fluorescence quenching approach

Summary

Solid dispersions (SDs) represent an important formulation technique to achieve supersaturation in gastro-intestinal fluids and to enhance absorption of poorly water-soluble drugs. Extensive research was leading to a rather good understanding of SDs in the dry state, whereas the complex interactions in aqueous medium are still challenging to analyze. This paper introduces a fluorescence quenching approach together with size-exclusion chromatography to study drug and polymer interactions that emerge from SDs release testing in aqueous colloidal phase. Celecoxib was used as a model drug as it is poorly water-soluble and also exhibits native fluorescence so that quenching experiments were enabled. Different pharmaceutical polymers were evaluated by the (modified) Stern-Volmer model, which was complemented by further bulk analytics. Drug accessibility by the quencher and its affinity to celecoxib were studied in physical mixtures as well as with in SDs. The obtained differences enabled important molecular insights into the different formulations. Knowledge of relevant drug-polymer interactions and the amount of drug embedded into polymer aggregates in the aqueous phase is of high relevance for understanding of SD performance. The novel fluorescence quenching approach is highly promising for future research and it can provide guidance in early formulation development of native fluorescent compounds.

Aleandri, S., Jankovic, S., & Kuentz, M. (2018). Towards a better understanding of solid dispersions in aqueous environment by a fluorescence quenching approach. *International journal of pharmaceutics*, *550*(1-2), 130-139.70

4.1 Introduction

Solid dispersion (SD) is a widely employed approach to orally deliver poorly water-soluble drugs. The compound is mostly formulated in an amorphous high-energy state, which should be kinetically stabilized throughout the targeted shelf-life of the product. Especially critical for poorly soluble compounds is dispersion in aqueous medium, which comes naturally with the oral route of administration and bears a risk of drug crystallization from the amorphous state (Newman, 2015). To fully benefit from SD formulations, physical instability must be therefore hindered, for example, by using polymers [20,38,109,301] The results of most studies indicate that polymers decrease the crystallization tendency of an amorphous drug due to a reduction of molecular mobility [52], as well as by breaking of the interconnections between drug molecules and the formation of specific drug-polymer interaction [342,343] These molecular interactions and their biopharmaceutical consequences are of major interest within the field of SDs. A majority of research focuses on drug-polymer interactions in the dry bulk state employing Fourier transform infrared (FT-IR), Raman spectroscopy, differential scanning calorimetry (DSC), X-ray powder diffraction (XRPD) and solid state NMR spectroscopy [23,344,345]. Among the different characterization techniques to study the dry state of SDs, transmission electron microscopy was also deemed as highly relevant. [346–349]

It seems more complex to understand and study drug excipient interactions upon aqueous dispersion because there is often a complex phase separation involved. Indeed, previous studies reported that in contact with an aqueous solution simulating the gastro-intestinal media, SDs rapidly disperse and thereby provide a broad range of drug and excipient assemblies [4,11,18,101,350] Release from these particles and colloids provide the free drug concentration that is the true supersaturation driving absorption. [18,100] The above investigations were conducted not only in simulated intestinal medium but also in mere buffer systems because simulated intestinal media make the interpretation more difficult due to the various colloidal states present even without dispersing ASDs.[103]. Already aqueous solution of lipophilic drug alone can exhibit complex behavior where a critical transition leads to a drug-rich and water-rich phase, which is known as a liquid-liquid phase separation (LLPS). [105,351,352] In this context, different authors [4,104,353,354] have employed fluorescence probes as marker for the polarity of the molecular environment. The study reported by Tho *et al*. (2010) is one of few reports on fluorescence as a tool in SD analysis. [355] Solid drug particles were differentiated from a liquid and drug rich phase and nano- as well as micro-sized solid particles were formed (isolated and analyzed by X-Ray) on

dispersion of SDs in buffer media. [355] Moreover, Frank *et al*., 2012b reported a phase separation phenomenon during the dissolution of a commercial SD, including the formation of solid amorphous particles, which were isolated, dried, and analyzed by XRPD. [11]

Given the wide range of established applications of fluorescence in the life sciences, it is rather surprising that fluorescence methods have not been more harnessed in pharmaceutical analysis of SDs. A notable exception is the very recent work on fluorescence lifetime and steady-state fluorescence spectra measurements, which were successfully employed to differentiate and characterize phase transformations in supersaturated aqueous solutions of poorly water-soluble drug [125]. Interesting is in the context of fluorescence analysis of poorly soluble compounds also another work that employed pyrene to elucidate a drug dissolution enhancement effect of stevia-G. [356] Moreover, a study on fluorescence resonance energy transfer (FRET) is noteworthy, which aimed at differentiation of compound distribution in SD as either in the form of molecular dispersion or as larger amorphous clusters.[357] Fluorescence analysis is highly sensitive and can provide valuable information of a probe molecule regarding its immediate environment (*i.e.* polar molecules in polar solvents), rotational diffusion, distances between the sites on biomolecules, conformational changes, and binding interactions. It seems that fluorescence analysis could be further exploited in the field of solid dispersions and it may particularly help with the scientific challenges of analyzing the formulations on release in aqueous media.

In aqueous dispersion, the evolving complex multiphase systems of SDs are inherently difficult to study. There are different approaches reported in the literature to study release from SDs [313], but no single technique alone appears to be sufficient to characterize both the solid particles as well as the aqueous colloidal phase that is formed during release. The evolving phases from SDs could therefore be analyzed separately using complementary analytical approaches. This work reports on a fluorescence analysis to assess the drug-polymer interactions in the aqueous colloidal phase on drug release. In particular, we introduce a method based on fluorescence quenching and size-exclusion chromatography to investigate such systems. Celecoxib (CX), a native-fluorescent poorly soluble compound was studied in physical mixtures with various polymers (at different concentrations) as well as with SDs where the 1:1 (w/w) CX: polymer ratio was selected in order to have a high drug loading. The combined analysis of the (modified) Stern-Volmer plots and size-exclusion chromatography enabled unique insight into how the selection of polymer affected the accessibility of drug by the quencher as well collisional affinity in the aqueous colloidal phase. Such information is highly attractive to learn about the

molecular interactions of drug with formulation components that take place during the dissolution in the aqueous colloidal phase.

4.2 Materials and methods

4.2.1 Materials

Celecoxib (CX) was purchased from AK scientific, Inc. (USA), hydroxypropyl methyl cellulose acetate succinate, L grade (HPMCAS-LG) was obtained from Shin-Etsu AQOAT, polyvinylpyrrolidone vinyl acetate (PVP VA64) and Soluplus® were purchased from BASF, Poloxamer 188 and potassium iodide (KI) were purchased from Sigma Aldrich. PD MidiTrap G-25 M was purchased from GE healthcare life science. All solutions were prepared using Mill-Q water (18.2 MΩ cm^{-1}).

4.2.2 Methods

4.2.2.1 Preparation of solid dispersions and physical mixtures

SDs were prepared by using a solvent evaporation method as described in literature (Chiou and Riegelman, 1969). Briefly, CX and polymer were taken in ratio of 50:50 (w/w) and dissolved in an adequate amount of methanol. The solvent was then rapidly evaporated under reduced pressure using a mild heating bath (up to about 50 °C) to form a uniform solid mass. The co-precipitate was crushed and desiccated under vacuum for 24 h, then pulverized and vacuum desiccated again for a day. In case of the physical mixtures, CX and the different polymers were mixed in a ratio of 90:10, 80:20, 70:30, 50:50 and 30:70 (w/w) by trituration with a pestle-mortar, and were then stored in a desiccated environment. CX based SDs and physical mixtures were prepared using HPMCAS-LG, PVP VA64, Poloxamer 188 and Soluplus.

4.2.2.2 Powder x-ray diffraction (XRPD)

Powder X-ray diffraction was used to characterize the solid form of the physical mixtures and of SDs at ambient temperature using a Bruker D2 PHASER (Bruker AXS GmbH, Germany) with a PSD-50 M detector and EVA application software version 6. Samples were prepared by spreading powder samples on PMMA specimen holder rings from Bruker. Measurements were performed with a Co Kα radiation source at 30 kV voltage, 10 mA current and were scanned from 10–35 2θ with 2θ being the scattering angle at a scanning speed of 2θ /min.

4.2.2.3 Differential scanning calorimetry (DSC)

A DSC 4000 System, from PerkinElmer (Baesweiler, Germany) was calibrated for

temperature and enthalpy using indium. Nitrogen was used as the protective gas (20 mL/min). Samples (approximately 5 mg) were placed in 40 μL aluminum pans with pierced aluminum lids. The midpoint glass transition temperatures (T_g), was determinate by a single-segment heating ramp of 5 °C/min from 25 °C to a maximum temperature of 200 °C. All DSC measurements were carried out in triplicate.

4.2.2.4 Dynamic light scattering (DLS) for particle sizing

The size of the obtained aggregates was measured with NanoLab 3D (LS instruments, Freiburg, Switzerland) equipped with a 45 mW at 685 nm, vertically polarized laser, having the detector at 180° with respect to the incident beam at 37 ± 0.1 °C. Disposable polystyrene cuvettes of 1 cm optical path length were rinsed several times (at least five) with the solutions to be analyzed and finally filled with the same solution under a laminar flow hood to avoid dust contamination. At least three independent samples were taken, each of which was measured 10 times. Measurements were done in auto correlation mode and the obtained values are reported as an average ± standard deviation (STDV). Each measurement had a duration of 30 seconds with the laser intensity set on 100%. For the fitting of the correlation function, third order cumulant fits were performed with the first channel index and the decay factor being 15 and 0.7 and analyzed according to the cumulant method (Frisken, 2001).

4.2.2.5 Diffusing wave spectroscopy (DWS)

DWS RheoLab (LS Instruments AG, Fribourg, Switzerland) was used as optical technique for microrheological measurements as reported previously. [118] The theory of DWS-based microrheology was already explained in detail in our previous work. [153] The DWS was calibrated prior to each measurement with a suspension of polystyrene particles, PS, (Magsphere Inc., U.S.A) in purified water (10 wt. %). The PS particles have a mean size of 250±25 nm with a solid content of 0.5 wt. % in dispersion. This suspension was filled in cuvettes with a thickness L of 5 mm prior to measuring for 60 s at 25 ˚C. The value of the transport mean free path, l^* (microns) was determined experimentally as reported previously.[358] The transmission count rate was measured several times until a constant value was reached and the cuvette length, L, was considerably larger than the obtained values for l^* ($L \gg l$) ensuring diffusive transport of light. The transport mean free path of the sample l^* is needed for the determination of the correlation intensity function and thus for the microrheological characterization. Viscosity measurements were performed on 0.5 mg/mL

HPMCAS-LG, PVP VA64, Soluplus and Poloxamer 188 solutions in PBS at pH 6.5. Thus, 0.5 wt. % polystyrene (PS) nanoparticles were added to the clear samples to ensure the correct regime (guarantee a L/l^* ratio larger than 7). [118] 5 mm quartz cuvettes were employed and data acquired for 60 s and each sample was measured 5 times. The viscosity measurement of polymer solutions was determined in a broad frequency range by DWS, where an average reference viscosity (expressed as G''/frequency) at high frequencies (from 100000 to 150000 rad/s) is reported in table S1.

4.2.2.6 Preparation of aqueous colloidal phase

10 mL of PBS at pH 6.5 were added to 10 mg of freshly prepared SD or physical mixture of CX and different amounts of polymers. The obtained mixtures were kept under stirring (400 rpm) at 37 °C for 4 hours in the dark. The time period was arbitrarily selected to represent a pseudo-equilibrium that is of physiological relevance for the absorption process. The aqueous phase of the dispersed samples containing the solubilized CX and polymer was then collected as supernatant (called here aqueous colloidal phase, ACP) and separated from the above mentioned mixtures. Subsequently, an aliquot from the ACP was taken out and used for further experiments. The amount of solubilized drug and its concentration in the ACP (CX concentration in aqueous phase) was based on high- performance liquid chromatography (HPLC) and calculated by using a calibration curve (both HPLC method and calibration curve are shown in SI). Measurements were carried out in triplicate (n=3) and the results are shown (Table 1 to 5). It has to be noted that such percentage values refer to the solubilized amount of drug in the aqueous colloidal phase (in the pseudo-equilibrium after 4 h), while the residual part of the total drug amount was unreleased in a solid phase.

4.2.2.7 Fluorescence quenching experiments

Fluorescence quenching experiments on the above mentioned ACP were performed using iodide (I^-) as collisional quencher. All fluorescence experiments were carried out at room temperature on solutions with optical densities smaller than 0.05 to minimize inner filter effects. Fluorescence quenching experiments were performed by adding small aliquots of 1 M KI (containing small amount of $Na_2S_2O_4$ to avoid the oxidation of the quencher) solution to the samples.

Table 1. Physical mixtures of CX and HPMCAS-LG used for fluorescence quenching experiments.

Drug-polymer ratio (w/w)	**CX concentration in aqueous phase (µg/mL)**	**% Dose in aqueous phase**	K_D **(1/M × s)** [a]	***fa*** [b]	R^2 [c]
100:0	2.3 ± 1.1	0.5 ± 0.2	17.9 ± 0.7	1 ± 0.02	0.991
90:10	9.1 ± 3.2	1.8 ± 0.6	7.1 ± 0.3	1 ± 0.01	0.996
80:20	7.1 ± 1.0	1.4 ± 0.2	6.8 ± 0.2	1 ± 0.02	0.997
70:30	6.8 ± 1.5	1.3 ± 0.3	0.21 ± 0.002*	0.52 ± 0.027	0.998**
50:50	7.4 ± 1.3	1.5 ± 0.3	0.15 ± 0.002*	0.32 ± 0.023	0.996**
30:70	10.2 ± 1.9	2.0 ± 0.4	0.15 ± 0.003*	0.32 ± 0.030	0.993**

[a] Quenching constant (± standard error obtained by the fitting, SE), [b] accessible fraction (± SE) and [c] Coefficient of determination (i.e. R-squared) of the Stern-Volmer plot fitting. * Quenching constant of accessible fraction (*Ka*, 1/M, ± SE). ** R^2 of the modified Stern-Volmer plot fitting.

Table 2. Physical mixtures of CX and PVP VA 64 used for fluorescence quenching experiments.

Drug-polymer ratio (w/w)	CX concentration in aqueous phase (□g/mL)	% Dose in aqueous phase	K_D (1/M × s) [a]	*fa* [b]	R^2 [c]
100:0	2.3 ± 1.1	0.5 ± 0.2	17.9 ± 0.7	1 ± 0.02	0.991
90:10	13.5 ± 0.5	2.7 ± 0.1	8.0 ± 0.3	1 ± 0.01	0.987
80:20	17.4 ± 2.6	3.5 ± 0.5	8.1 ± 0.4	1 ± 0.03	0.982
70:30	15.7 ± 0.8	3.1 ± 0.2	8.6 ± 0.5	1 ± 0.04	0.979
50:50	16.8 ± 2.9	3.3 ± 0.6	9.0 ± 0.5	1 ± 0.03	0.983
30:70	15.4 ± 0.9	3.0 ± 0.2	9.0 ± 0.6	1 ± 0.04	0.990

[a] Quenching constant (± SE), [b] accessible fraction (± SE) and [c] R^2 of the Stern-Volmer plot fitting.

Table 3. Physical mixtures of CX and Soluplus used for fluorescence quenching experiments.

Drug-polymer ratio (w/w)	CX concentration in aqueous phase (□g/mL)	% Dose in aqueous phase	K_D (1/M × s) [a]	*fa* [b]	R^2 [c]
100:0	2.3 ± 1.1	0.5 ± 0.2	17.9 ± 0.7	1 ± 0.02	0.991
90:10	5.0 ± 2.3	1 ± 0.4	9.7 ± 0.4	1 ± 0.03	0.987
80:20	6.8 ± 2.2	1.8 ± 0.4	9.5 ± 0.2	1 ± 0.01	0.982
70:30	6.6 ± 1.2	1.7 ± 0.2	9.8 ± 0.4	1 ± 0.02	0.991
50:50	5.8 ± 2.8	2.0 ± 0.6	7.9 ± 0.3	1 ± 0.04	0.991
30:70	8.1 ± 1.2	2.0 ± 0.2	7.4 ± 0.5	1 ± 0.04	0.988

[a] Quenching constant (± SE), [b] accessible fraction (± SE) and [c] R^2 of the Stern-Volmer plot fitting

Table 4. Physical mixtures of CX and Poloxamer 188 used for fluorescence quenching experiments.

Drug-polymer ratio (w/w)	CX concentration in aqueous phase (□g/mL)	% Dose in aqueous phase	K_D (1/M × s) [a]	*fa* [b]	R^2 [c]
100:0	2.3 ± 1.1	0.5 ± 0.2	17.9 ± 0.7	1 ± 0.02	0.991
90:10	19.4 ± 1.8	3.8 ± 0.4	16.4 ± 0.4	1 ± 0.01	0.997
80:20	16.5 ± 1.2	3.3 ± 0.2	15.3 ± 0.2	1 ± 0.02	0.993
70:30	24.2 ± 4.3	4.8 ± 0.9	14.7 ± 0.5	1 ± 0.03	0.986
50:50	32.9 ± 5.3	6.6 ± 1.1	15.5 ± 0.4	1 ± 0.03	0.982
30:70	28.8 ± 4.4	5.7 ± 0.9	15.6 ± 0.6	1 ± 0.04	0.985

[a] Quenching constant (± SE), [b] accessible fraction (± SE) and [c] R^2 of the Stern-Volmer plot fitting

Table 5. CX solid dispersions (drug-polymer ratio 50:50, w/w) used for fluorescence quenching experiments.

CX SDs	CX concentration in aqueous phase (□g/mL)	% Dose in aqueous phase	*Ka* (1/M) [a]	*fa* [b]	R^2 [c]
HPMCAS-LG	28.8 ± 0.5	5.7 ± 0.1	0.038 ± 0.006	0.33 ± 0.07	0.990
PVP VA 64	38.0 ± 0.7	6.7 ± 1.0	0.020 ± 0.001	0.45 ± 0.06	0.999
Soluplus	6.1 ± 0.8	1.2 ± 0.2	0.017 ± 0.0004	0.86 ± 0.01	0.999
Poloxamer 188	40.1 ± 2.5	8.2 ± 0.5	16.2* ± 0.6433	1 ± 0.04	0.990

[a] Quenching constant (± SE) of the accessible fraction, [b] accessible fraction (± SE) and [c] R^2 of the modified Stern-Volmer plot fitting. * Quenching constant (K_D, 1/M × s ± SE).

Decrease of the CX fluorescence intensity was monitored at 380 nm by exciting at 250 nm using Greiner® UV-transparent microplates and a SpectraMax® M2 plate reader (Molecular devices, San Jose, CA, USA). Quenching of fluorescence is described by the Stern-Volmer equation and quenching data were presented as plots of F_0/F versus quencher concentration [KI], were F_0 and F are the fluorescence intensity in absence or in presence of the quencher, respectively. [121] The plot of F_0/F versus [KI] is expected to be linearly dependent upon the concentration of quencher and it yields an intercept of one on the y-axis and a slope equal to the Stern-Volmer quenching constant K_D (1/M × s) when the quenching process is dynamic. The K_D is given by $kq \times \tau_0$ where kq is the bimolecular quenching constant and τ_0 is the lifetime of the fluorophore in the absence of quencher. When the Stern-Volmer plots deviate from linearity toward the x-axis (i.e. downward curvature) a modified Stern-Volmer equation (Eq.1) was used to calculate the amount of accessible fraction (fa) and its affinity to the quencher (Ka, 1/M) [121] A plot of $F_0/(F_0-F)$ versus 1/ [KI] yields fa^{-1} as the intercept on the y-axis and $(fa \times \mathrm{Ka})^{-1}$ as the slope. The K_D, Ka and fa values are the coefficient of the curves obtained from six point's linear regression and the coefficient of determinations, *i.e*. R-squared (R^2) of the fittings are reported in the Tables. Each fitted value was reported as mean ± standard error (SE) that was obtained by the regression analysis using Sigma Plot (Systat Software, Inc. San Jose, CA, USA).

$$F_0/\Delta F = 1/(f_a \times K_a \times [KI]) + 1/f_a \quad (1)$$

4.2.2.8 Size exclusion chromatography

0.5 mL of the ACP containing only the solubilized CX and polymer was filtered at room temperature through a PD MidiTrap G-25 M, a Sephadex G-25 packed column. According to size exclusion chromatography (SEC), small molecules (such as the free CX) that are able to enter into the resin pores are retained longer in the column, while large molecules (such as aggregates) which are bigger than the pore size are eluted firstly. Therefore, this technique enables to discriminate between free drug and the drug embedded in aggregates. The elution profile was retrieved plotting either the value of the mean count rate (Kcps), obtained by DLS measurements or the percentage of CX present in the fractions eluted from the column *vs* the elution volumes (mL). The percentage of CX in the fractions (% CX) was evaluated according to Eq. 2.

$$\% \text{ CX} = (F_{fr} / F_{nf}) \text{ x } 100 \quad (2)$$

$$\% \text{ CX free} = 100 - \% \text{ CX-Polymer} \quad (3)$$

Where F_{fr} is the fluorescence intensity value of the fractions eluted from Sephadex filtration and F_{nf} is the fluorescence intensity value before Sephadex filtration. The total percentage of CX embedded in polymer aggregates (% CX-Polymer) is given by the sum of the percentage of CX (% CX) present in the fractions where DLS shown presence of aggregates. On the other hand, the percentage of free CX (% CX free) was calculated according to the Eq. 3. All experiments were carried out consecutively (n=3) at room temperature, the % CX free is reported as mean ± STDV.

4.3 Results

4.3.1 Bulk characterization of physical mixtures and solid dispersions

Prepared SDs were analyzed by powder X-ray diffraction (XRPD) at 25°C to verify the amorphous nature of the dispersions and the results were compared with those of the corresponding physical mixtures. As shown in Figure 1A, CX based SDs manufactured with HPMCAS-LG, PVP VA64, and Soluplus (at 50% (w/w) drug loading) were X-ray diffraction amorphous. However, the SD prepared with Poloxamer 188 showed diffraction peaks and a substantial crystallinity was verified in the physical mixtures as well as with pure drug. The SDs were further characterized by DSC to confirm the physical state of drug in the matrix. As shown in Figure 1B, the SD with HPMCAS-LG, PVP VA 64 and Soluplus display a single glass transition temperature (T_g) and the absence of a drug melting temperature (T_m). On the other hand, the SD based on Poloxamer 188 shows two different thermal events, one corresponding to melting of the eutectic mixture and the second to the T_m values indicate suspended CX present in the eutectic melt. As very different types of polymers were selected deliberately, it was expected that not all SDs of CX would result in an entirely amorphous system.

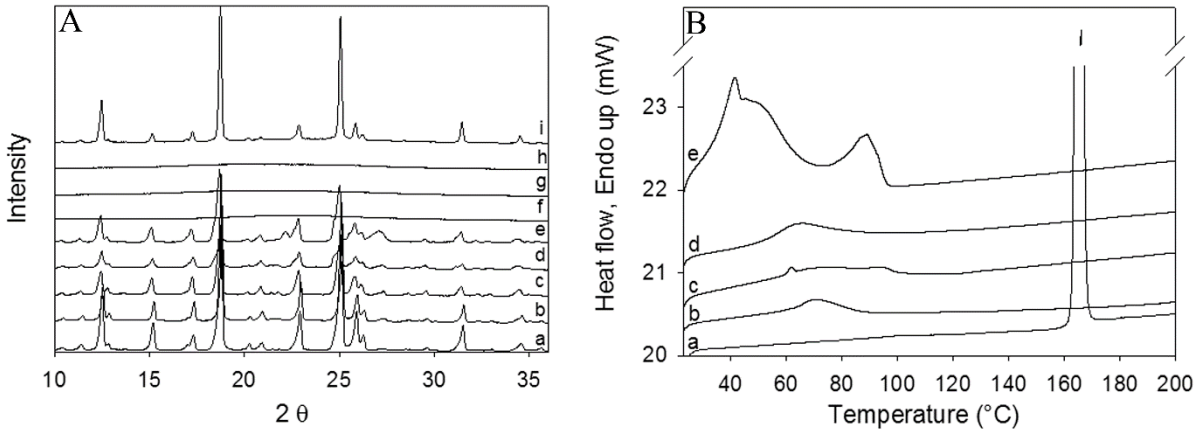

Fig. 1. Powder X-ray diffraction (XRPD) plots of CX alone (a), physical mixtures with HPMCAS-LG (b), PVP VA 64 (c), Soluplus (d), and Poloxamer 188 (e). CX solid dispersions (SD) are shown with HPMCAS-LG (f), PVP VA 64 (g), Soluplus (h), and Poloxamer 188 (i) (A). DSC thermograms of CX alone (a), SDs with HPMCAS-LG (b), PVP VA 64 (c), Soluplus (d) and Poloxamer 188 (e).

4.3.2 Characterization of drug-polymer interactions

Fluorescence quenching experiments were employed to gain information about the molecular environment of the model drug CX in the aqueous colloidal phase. The study of accessibility of drug to the quencher was therefore of interest in the physical drug-polymer mixtures as well as in SD formulations.

The freshly prepared SDs or physical mixtures of CX with different amounts of polymers were added to PBS at pH 6.5 and kept under stirring at 37 °C for 4 hours in the dark. The duration was selected as physiologically-relevant time scale which typically allows a SD to reach a pseudo equilibrium. The obtained aqueous colloidal phase, containing the solubilized CX (CX concentration in aqueous phase) and polymers were used to study drug-polymer interactions that take place in the aqueous solution. Even though the study focused on this aqueous phase, one should keep in mind that this phase contained only a part of the dose since 4 h release (i.e. pseudo- equilibration) resulted in multiphase system in which some drug was either not released or it precipitated from supersaturation. Therefore, any given percentages in the fluorescence experiments are understood as relative to the drug amount solubilized in the aqueous phase. However, the exact amount of drug (CX concentration in aqueous phase) present in the aqueous colloidal phase (and the percentage of dose) used for quenching experiments were evaluated by HPLC and the results are shown in tables from 1 to 5.

Moreover, CX quenching is established to be dynamic and the fluorescence of the drug decreased linearly with the concentration of KI that is a commonly used collisional quencher (see SI, Figure S2).

As shown in Figure 2A and summarized in Table 1, the quenching of fluorescence is described by the Stern-Volmer equation in the cases of CX alone (black circles) and the physical mixtures with 10 (black upper triangles) and 20 (white diamonds) % (w/w) of HPMCAS-LG. Thus, fluorescence quenching data, presented as plots of F_0/F versus [KI], show a linear behavior. Already the presence of 10 or 20 w/w % polymer led to a decrease CX quenching as seen from decreased values of the quenching constant (K_D). Interestingly, addition of 30 w/w % polymer or more (see Figure 2B) resulted in Stern-Volmer plots that clearly deviated from linearity. Indeed, CX quenching decreases by an increasing amount of HPMCAS-LG from 30 (white upper triangles) to 70 (black down triangles) w/w %. As shown in Figure 2C and summarized in Table 1, a modified Stern-Volmer equation was used to calculate the amount of accessible fraction (*fa*) and its affinity to the quencher (*Ka*).

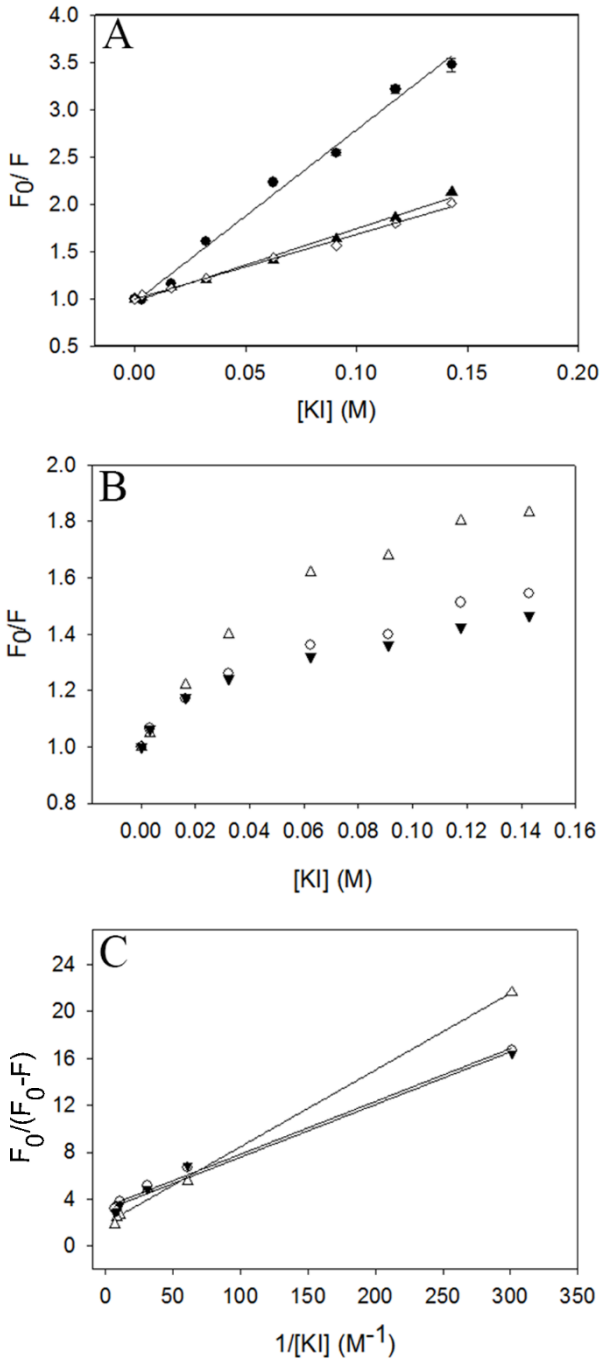

Fig. 2. Physical mixtures: Stern–Volmer plots (A and B) and modified Stern–Volmer plots (C) for fluorescence quenching of CX in the presence of 0 (black circles), 10 (black upper triangles), 20 (white diamonds), 30 (white upper triangles), 50 (white circles) and 70 (black down triangles) w/w % of HPMCAS-LG.

On the other hand, when in the physical mixture, HPMCAS-LG is replaced with PVP VA64, Soluplus, or, Poloxamer 188, the Stern-Volmer quenching plot did not deviate from linearity by a clear downward curvature (see SI, Figure S3) even not at highest polymer concentration (*i.e.* 70 w/w %). Similar as for HPMCAS-LG, was for PVP VA64 (Table 2) or Soluplus (Table 3) that a decrease of the quenching constant (K_D) was noted with added polymer in physical mixtures. By contrast, Poloxamer 188 did not exhibit any changes in the quenching of CX and the obtained K_D values for different drug-polymer mixture ratios are comparable with the one for CX alone (Table 4).

Moving from the physical mixtures to SDs of drug and polymer revealed that except for the Poloxamer 188 based SD, the Stern-Volmer plots deviated from linearity (downward curvature) for all the other formulations (see SI, Figure S4). As summarized in Table 5, the HPMCAS-LG based SD shows the lowest value of *fa,* while using Soluplus in SD, the accessible fraction rises up close to 0.9. As already mentioned in the case of Poloxamer 188, the obtained K_D value (Table 5) was comparable with those obtained in the physical mixture and in the case of CX alone. This was different in the case of HPMCAS-LG (Figure 3) because the quenching constant in the physical mixtures was higher than in the SD while *fa* was about the same. Differences between SD and physical mixture were found also in the case of PVP VA64. As shown in Figure 4, in the case of the physical mixture, the quenching of fluorescence is described by the Stern-Volmer equation. This plot in case of SD deviated from linearity and the modified Stern-Volmer equation (inset Figure 4) was used to calculate the amount of accessible fraction (*fa*) and its affinity to the quencher (*Ka*). The same behavior was also observed in case of Soluplus (see SI, Figure S5).

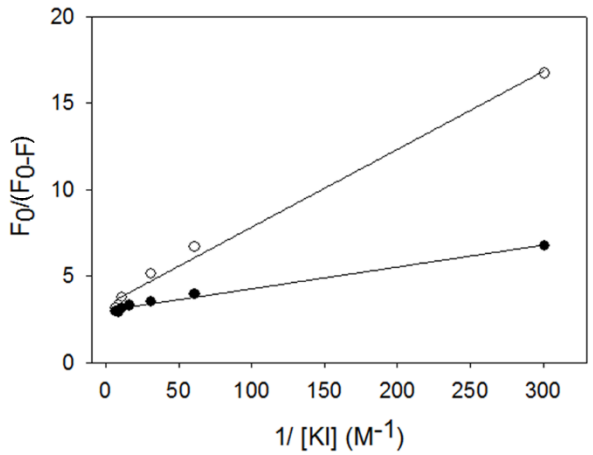

Fig. 3. Modified Stern–Volmer plots for fluorescence quenching of CX with HPMCAS-LG as either SD (black circles) or physical mixture (white circles).

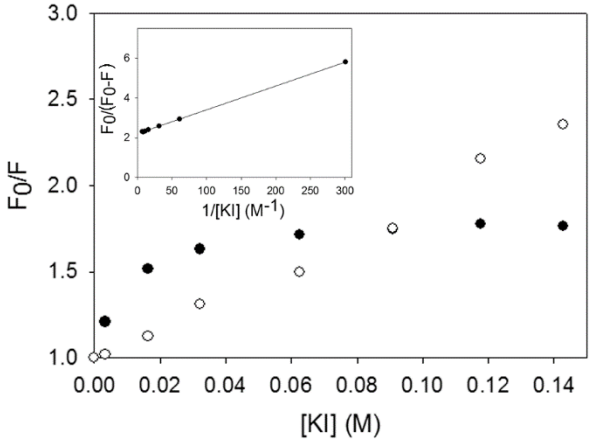

Fig. 4. Stern–Volmer plots for fluorescence quenching of CX/ PVP VA 64 as either SD (black circles) or physical mixture (white circles). The inset in the figure shows the modified Stern–Volmer plots for a comparative fluorescence quenching of CX/ PVP VA 64 SD

After the fluorescence quenching experiments, the ACP was filtered through a Sephadex G-25 packed column (Figure 5) to quantify the amount of free dug (% CX free) as well as the drug embedded in polymer aggregates (% CX-Polymer). Drug percentages obtained in the size exclusion chromatography experiments are again understood as relative to solubilized compound in ACP, which holds only for a part of the dose.

Table 6. Solid dispersion (drug-polymer ratio 50:50, w/w) results from size exclusion elution profiles.

CX solid dispersion	% CX free [a]	Size (nm)[b]
HPMCAS-LG	24 ± 6	2800 ± 45
PVP VA 64	53 ± 10	2000 ± 75
Soluplus	85 ± 5	615 ± 22
Poloxamer 188	95 ± 4	850 ± 35

[a] The values were obtained according to the equation 2, [b] Size analysis of fractions containing the CX embedded in polymer (% CX-Polymer) obtained by DLS. The % CX free and size measurements are reported as mean ± STDV (n=3).

As summarized in Table 6, the HPMCAS-LG based SD shows the lowest value of free drug, indicating that most of the drug is embedded in polymer aggregates. Moreover, the HPMCAS-LG aggregates, analyzed by DLS, were the biggest with respect to the SD prepared with the other polymers. By contrast, in the case of SD of Poloxamer 188, the aggregates were about three times smaller than in the SD using HPMCAS-LG and almost the entire compound was in the free drug fraction. It has to be noted that the values of accessible fraction (*fa* in Table 5) and the values of percentage of free CX (% CX free in Table 6) were comparable for all the investigated SDs.

4.4 Discussion

Formulations based on SD technology generally target enhanced dissolution and sustained supersaturation of drug for optimal performance following oral administration.[109] However, the aqueous formulation dispersion leads to phase changes and emergence of different particle species from which drug release takes place. The mechanisms of how polymers affect such drug release from SDs are still not thoroughly understood. Much current research is directly toward individual mechanistic aspects, for example how polymers can sustain drug supersaturation.[359–361] Interesting is further the mechanism that an enhanced dissolution rate was found to be partly due to the stabilization of drug in nanosized particles formed by precipitation.[362,363] These different mechanisms of drug release provide a better understanding of drug-polymer interactions in aqueous environment. To gain such insights into the aqueous phase of SDs in a pseudo-equilibrium at a physiologically relevant time scale (4 h) was the primary objective of the present work.

Celecoxib (CX) a Biopharmaceutics Classification System (BCS) class II drug was selected as model because it exhibits fluorescence. We introduced quenching analysis as a tool to explore drug-polymer interactions in SDs that take place in the aqueous colloidal phase during release, which was meant to complement existing analytics for this type of drug delivery systems.[364] First, we analyzed different SDs by means of XRPD and DSC to determine their amorphous nature.

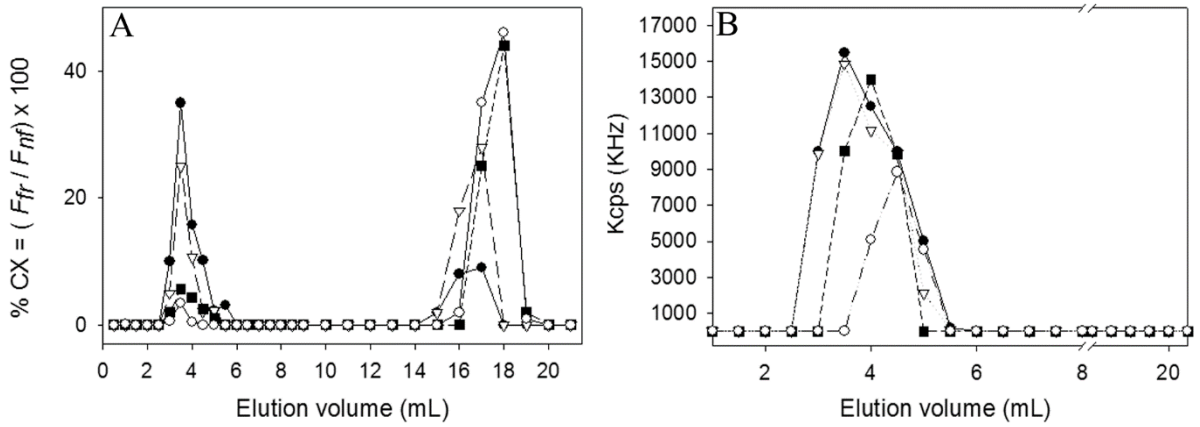

Fig. 5. Elution profile obtained by SEC: Percentages of CX (A) and the mean count rate, expressed by Kcps (B) present in the eluted fractions were plotted *vs* the elution volumes. CX SD with HPMCAS-L (black circles), PVP VA 64 (white triangles), Soluplus (black squares), and Poloxamer 188 (white circles).

Within this work, the ratio between CX and polymer (50:50, w/w %) was selected arbitrarily to reflect a rather high loading. In the case of SDs prepared with HPMCAS-LG, PVP VA64, and Soluplus, no distinct peaks were observed in the diffraction patterns. The case of SD prepared with Poloxamer 188 was different (but in agreement with previous results in the literature [10], because peak positions similar to CX were evidenced, indicating that notable amounts of drug were crystalline. These results were confirmed by DSC studies. As shown in Figure 1B in the SD formulated with HPMCAS-LG, PVP VA64, and Soluplus, the absence of melting point (T_m) of CX and the presence of single peak of glass transition temperature (T_g) indicate the conversion of drug to an amorphous state and its miscibility with the polymer. A broad peak in the case of PVP VA64 SD is likely due to strong interaction between the carrier matrix and CX even though this effect may have been confounded by the presence of water. On the other hand, as already reported in literature,[20] Poloxamer 188 and CX form an eutectic, which exhibits a T_m at 40 °C and the second broad peak at 88 °C was attributed to the excess amount of the suspended CX present in the molten eutectic.

It has to be noted that the four polymers have been selected to cover a broad variety of excipients: from the most hydrophobic and negatively charged at pH 6.5 HPMCAS-LG, to the nonionic triblock copolymers Poloxamer 188 that shows a rather high water solubility (>100 g/l).[365] Therefore it was already expected that not all of them would result in completely amorphous dispersions of CX.

Fluorescence quenching was then used to obtain information about the environment that surrounds the model drug in the aqueous colloidal phase (ACP). Quenching of fluorescence is

presented as a Stern-Volmer plot where the ratio F_0/F is plotted versus the quencher concentration [*KI*].[121] The extrapolated quenching values, such as K_D or *fa*, are independent from the absolute values of F and F_0 and therefore also from the concentration of CX in ACP. However, the exact CX concentration in the ACP used for the quenching experiment was evaluated by HPLC. As already mentioned, it only contained a part of the dose because any pseudo-equilibrium of drug release from solid dispersion typically results in either some unreleased or precipitated drug in the course of supersaturation.[306] Any given percentages in the fluorescence experiments are understood as relative to the drug amount solubilized in the ACP. The reference value of crystalline CX (4 h pseudo-equilibrium) was in line with literature.[96] The physical mixtures showed drug concentrations in ACP that were higher than solubility of pure CX, which was attributed to excipient solubilization effects (Tables 1 to 4). This effect was particularly notable for Poloxamer 188 (Table 4). As for SD formulations Table 5 indicates elevated concentrations of CX with exception of Soluplus. Perhaps the Soluplus (at least at the CX/polymer ratio used here) resulted in extensive drug precipitation after the equilibration time in accord with literature.[366] An increase in Soluplus/ CX ratio could have decreased drug precipitation.[367]

In the case of CX alone, the solubilized drug is totally accessible to the quencher and its fluorescence intensity decreased by increasing [*KI*]. However, when a polymer is added, different scenarios are observed and quenching measurements reveal important information about the polymer spatial arrangement around the drug.

As already known from literature and as experimentally evaluated herein, the presence of polymers at the same concentration used within this work (see SI, Figure S6) increases the viscosity of the system. [358] The quenching, a diffusion-limited process, is inversely proportional to the viscosity of the solution,[368] since an increase of viscosity decreases the mobility of the quencher and therefore the number of collisions with the drug.[369]

In the case of physical mixtures of CX with HPMCAS-LG, PVP VA64, and Soluplus either the drug-polymer interactions or the increase of viscosity could lead to a decrease in quenching efficiency. However, it has to be noted that even though Poloxamer 188, PVP VA64 and Soluplus solutions exhibit comparable viscosity values (0.83, 0.84 and 1.1 mPa s respectively), the extent of quenching did not decrease by using Poloxamer 188. Furthermore, the most viscous HPMCAS-LG (2.12 mPas s) displays a comparable decrease of quenching with the less viscous PVP VA64 (0.84 mPas s). This suggests that drug-polymer interactions predominantly contributed to the fluorescence quenching decrease, whereas viscosity was a factor of lesser

importance.

Given that a polymer can form aggregates able to surround the drug, the latter would be totally protected from the quencher and hence quenching cannot occur. Additionally, two populations of drug in the aqueous phase can be present simultaneously: one which is accessible to quencher (*fa*) while the other one is inaccessible or buried in polymer aggregates. In this scenario, *fa* is the drug fraction that is not sequestered by the polymeric network. As a consequence, the more the polymer is able to bury the drug by forming aggregates surrounding it, the more the *fa* decreases. Interestingly, increasing the HPMCAS-LG concentration up to 30 % (w/w) in the physical mixture, the excipient was able to surround a fraction of CX. The drug interacting with polymer could have either become buried due to conformational change of the macromolecule or because of polymer aggregation. By contrast, the other polymers were not able, at least as physical mixtures, to protect CX from the quencher either by conformational change or by forming aggregates even not at a higher amount (70 %, w/w). CX was likely to interact with either hydrophobic side chains as well as via polar interactions, or hydrogen bonding with HPMCAS-LG.[109] Especially the comparatively lipophilicity of polymer led in combination with the lipophilic model drug was likely to result in pronounced drug embedding. [51]

As known from the literature, electric charge either on the quenchers or on the polymers' surface can have a dramatic effect on the extent of quenching. [370] In general, charge effects might be present with charged polymers such as HPMCAS-LG, and might be absent for neutral like PVP VA64.[371] For instance, a negative charge on HPMCAS-LG could prevent a negatively charged quencher from coming in contact with the drug. However, it is clear from our results (see Table 1 to 4) that the decrease of quenching was not mainly due to the electrostatic repulsion, because the neutral PVP VA64 showed almost the same extent of quenching as the negatively charged HPMCAS-LG.

Interestingly, except for Poloxamer 188, SDs in aqueous environment displayed at least two drug populations: one which is accessible to the quencher and the second that was inaccessible as it was buried in a polymeric conformation or in aggregated macromolecules. In the case of HPMCAS-LG (see Figure 3) the physical mixture showed a higher *Ka* as compared to SD. The quenching constant measures the stability of the quencher-fluorophore complex, and it is related to the accessibility of the fluorophore to the quencher, in particular to the separation distance within the excited-state complex, affected by diffusion and steric shielding of the fluorophore.[372] Therefore, despite of the same values for *fa* (0.3 for both SD and physical

mixture), in the case of SD, the drug was bound to a microenvironment less suitable for the interaction with the quencher compared to the physical mixture. This was obviously the results of different spatial arrangement of drug in polymer matrix as the SD was prepared by a solvent-evaporation method. This preparation must have facilitated a higher extent of polar interactions and hydrogen bonding of drug-HPMCAS-LG compared to physical mixture.[373] However, also more frequent hydrophobic interactions (due to succinoyl substituent) could have occurred. [51] In the case of PVP VA64 (Figure 4) and Soluplus (SI, Figure S5), the polymer was able to embed the drug only when it was formulated as SD. Even in this case, a possible explanation can be the capability of the polymer to strongly interact with the drug trough H-bonds between amide protons of CX and carbonyl C=O of polymers only in an amorphous state, as reported in literature. [374,375]

A problem of classical drug release studies from SDs is that drug free in aqueous solution or interacting colloids in different forms is typically not differentiated at all. Few research articles emphasized the different drug forms emerging from SDs in aqueous environment. [11,18,99] Different analytical tools are in this context of interest to study how the drug is present in solution. While dialysis methods or ion selective electrodes can study free drug in solution, the asymmetric flow field flow fraction (AF4) is an approach to investigate colloidal and particulate forms that contain drug. [103,376,377]

In this study, the use of an SEC method enables to discriminate between the percentage of drug embedded in polymer aggregates (% CX-polymer) and the percentage of free drug (% CX free) present in the aqueous phase (i.e. ACP). As for the quenching experiments, it has to be kept in mind that a part of the initial drug was not in the colloidal aqueous phase and hence, the term free drug refers to the amount of solubilized drug in ACP, which was not buried or embedded in polymer aggregates. This should not be confused with the total amount of free CX relative to an initially administered dose.

As shown in Table 6, the HPMCAS-LG is able to entrap around 76 % of the drug (% CX-polymer) and only 24% of CX is free (% CX free) according to Eq. 3. It has to be noted that the values of accessible fraction (*fa* in Table 5) and the values of percentage of free CX (Table 6) were comparable for all the investigated SDs. In the case of SD, the polymer aggregate protected the drug and therefore only the free fraction was reachable by the quencher.

However, drug release is a dynamic process and different populations of drug can coexist. The amount of free CX present in the ACP, will change over time, since a percentage of it can be

either released or sequestered by the polymer. We considered a rather long but reasonable equilibration time for oral drug absorption so that the percentage of free CX would be either at or comparatively close to a pseudo- equilibration in the case of SDs. Studying the accessibility of the drug to a fluorescence quencher is a powerful and new method to investigate and elucidate the drug-polymer interactions upon drug release from SDs. In one formulated solubilization mechanism, the drug particles dissolve rapidly generating a highly supersaturated solution followed by the formation of drug nanoclusters within the polymer matrix. [363,378] It has been emphasized, for example by Ricarte et al. (who studied SDs of HPMCAS) that emergence of nanostructures from polymeric SDs can determine the kinetics of drug supersaturation. [349] Accordingly, the present study suggests the presence of the polymer aggregates in the aqueous colloidal phase, which is able to interact and embed a solubilized drug fraction. We know that absorption is driven by free drug but it is unclear if buried drug in polymer from the aqueous solution phase is lost for absorption or if it merely acts as a reservoir of drug in the sink of absorption. It will be a matter of individual colloidal partitioning kinetics regarding how much of the drug in the solubilized form is finally available for intestinal permeation.

4.5 Conclusions

The molecular and supramolecular interactions of drug and excipients are of critical relevance for the performance of oral solid drug dispersions. Traditional release testing offers only limited characterization and more recent approaches attempted to better understand particles and colloids formed in aqueous environment. Various physical methods can be used to either study the solid phase that is typically formed on release from SDs or an aqueous colloidal phase is studied following a physiologically-relevant equilibration time. The current work introduced a fluorescence quenching method to study drug-polymer interactions in such an aqueous phase. Information was obtained regarding the accessible fraction of drug by the quencher and about the affinity to the quencher, which offered insights into molecular interactions with the polymer. An improved understanding of solubilization behavior was achieved by a comparison with results from size exclusion chromatography and dynamic light scattering. Depending on the polymer, a fraction of drug can obviously be buried in the macromolecule. This reduces free drug in solution, which leads to lower absorptive flux but also reduces the risk of undesired drug precipitation. Thus, it will depend on the partitioning kinetics of a given system between buried and free drug if such embedded drug can act as a favorable reservoir of drug absorption or if it adds to the dose fraction that is lost for absorption. There is certainly more research

needed but it seems that fluorescence quenching analysis can greatly contribute to a better understanding of drug -polymer interactions *in vitro*, which ultimately can guide development of oral solid dispersions.

5 Biphasic drug release testing coupled with diffusing wave spectroscopy for mechanistic understanding of solid dispersion performance

Summary

Amorphous Solid dispersions (ASDs) represent an important formulation technique to achieve supersaturation in gastrointestinal fluids and to enhance absorption of poorly water-soluble drugs. Drug release from such systems is complex due to emergence of different colloidal structures and potential drug precipitation, which can occur in parallel to absorption. The latter drug uptake from the intestinal lumen can be simulated by an organic layer in a biphasic *in vitro* test, which was employed in this work to mechanistically study the release of ketoconazole from ASDs produced by hot melt extrusion using different HPMCAS grades. A particular aim was to introduce diffusing wave spectroscopy (DWS) to biopharmaceutical testing of solid dispersions. Results indicated that amorphous formulations prevented crystallization of the weakly basic drug upon transfer into the intestinal medium. Microrheological differences among polymer grades and plasticizers were revealed in the aqueous phase, which affected drug release and subsequently uptake into the organic layer. The results indicate that DWS can be employed as a new non-invasive tool to better understand drug release from solid dispersions. This novel light scattering technique is highly promising for future biopharmaceutical research on supersaturating systems such as solid dispersions.

Jankovic, S., O'Dwyer, P. J., Box, K. J., Imanidis, G., Reppas, C., & Kuentz, M. (2019). Biphasic drug release testing coupled with diffusing wave spectroscopy for mechanistic understanding of solid dispersion performance. *European Journal of Pharmaceutical Sciences, 137*, 105001.93

5.1 Introduction

Amorphous solid dispersions (ASDs) are one of the most widely employed methods to formulate poorly water-soluble drugs. To increase the apparent solubility and/or dissolution rate of a poorly soluble compound, it is encouraged to consider the amorphous form of a drug. The compound in an amorphous high-energy state is usually formulated in a polymer matrix system, which should be kinetically stabilized throughout the targeted shelf-life of the product. [23] Thus, polymers should have a stabilizing function in the formulation to prevent drug crystallization in solid dispersions [20,38,109,301] by means of specific interactions with the active compound and via a general reduction of molecular mobility. [52,342,343] A large number of polymers employed for solid dispersion are water soluble in all pH conditions, but there are also enteric polymers that contain acidic groups that become ionized at higher pH to facilitate swelling and some water solubility. The latter group of polymers includes hydroxyl propyl methylcellulose acetate-succinate (HPMCAS) and methacrylate-based enteric coating polymer systems, such as the Eudragits. [23,30]

Biopharmaceutical classification system (BCS) class II drugs are characterized by low solubility and high permeability. [24,379,380] In addition, weakly basic drugs have higher solubility values in the acidic environment of the stomach compared with the more neutral environment of the small intestine, thereby leading to a susceptibility to precipitate in the intestine. Precipitation of poorly water soluble drugs can result in erratic absorption and decreased bioavailability. Although the rate of transfer from stomach to the intestine will affect precipitation rates, various authors have shown that the presence of an absorptive compartment under conditions simulating the environment in the small intestine is crucial for predicting the precipitation of a weak base. [381–384] Therefore, biphasic dissolution testing has been proposed, which includes dissolution of drug in an aqueous phase and drug partitioning into an organic phase. [382,385] The *in vitro* biphasic test use of a lipid layer, such as octanol or decanol, in dissolution testing has been employed to act as a 'quasi-sink' since unionized drug can partition from the aqueous layer into this organic compartment to mimic drug absorption in the intestine. This allows to study simultaneously how a drug is released and taken up.

The dissolution of drug in the aqueous phase determines the amount of drug available for partitioning into the organic phase, which acts as a sink. [350,382,385,386] Such two phase dissolution tests can offer several advantages due to the presence of a second layer reflecting drug absorption from the intestine. First of all, in the presence of the organic layer, the dissolution

profile of the dosage form can be different compared to single phase dissolution systems. A key aspect of the biphasic dissolution is that it mimics the *in vivo* absorptive sink following drug release. The molecularly dissolved drug provides the driving force for partitioning into the organic layer and the concentration of the drug in the organic phase is a marker of *in vivo* absorption. This is supported by recent studies in which drug concentrations in the organic layer of a biphasic test were found to correlate with *in vivo* drug absorption. [385,387] These findings are encouraging even though the degree of correlation may depend on the used drug, formulation as well as test conditions.

A particular advantage of biphasic release testing is that direct *in-situ* determination of drug concentration in the organic phase is often less challenging than analytics in the aqueous phase. This is because of the lack of turbidity compared to the aqueous phase in which particles can originate from non-dissolving excipients or precipitated drug.

Apart from analytics of drug concentrations, it would be of interest to monitor physical changes occurring during drug release from a formulation. In particular, measurement of polymer swelling and microrheology upon dissolution testing presents an unmet research need in drug release analysis from solid dispersions. This study introduces diffusing wave spectroscopy (DWS) to ultimately gain a deeper understanding of drug release from polymeric matrices. DWS is an optical technique based on light scattering that investigates the microrheological properties of the fluid based on the intensity correlation function. DWS is a fast and non-contacting method in which the sample is probed by a laser beam over a large frequency range that is partially inaccessible to classical mechanical rheology. It has been just recently introduced into pharmaceutics to characterize lipid-based formulation, but to the best of our knowledge, this is the first time it has been used for amorphous solid dispersions. [118,153] Ketoconazole (KCZ), a poorly soluble drug and a weakly basic drug (basic pKa = 2.9 & 6.5, log P =3.9), was selected as a model compound. Similar to other such bases, KCZ is rather soluble in acidic gastric fluid, but precipitates in human upper intestine [388] as well as in simulated intestinal media [30,380]. In order to reduce or avoid precipitation in the intestinal environment, HPMCAS was employed since it is a polymer that dissolves at pH values higher than 5.5. A number of researchers have highlighted the unique properties of HPMCAS since the polymer is partially ionized above pH 5.5 and therefore becomes a hydrated polyelectrolyte. [18] The presence of the charges influences polymer conformation in solution; on one hand it

inhibits the formation of big polymer coils, while on the other hand, HPMCAS facilitates the stabilization of small drug/polymer aggregates that allow the drug to stay in solution. [18] These unique characteristics make HPMCAS a particularly interesting candidate for ASDs.

The aim of this article is to assess the performance of the KCZ ASDs employing a biphasic dissolution test further incorporated a pH shift and to correlate it with microrheology and in particular the swelling of the polymer dispersion by using DWS.

5.2 Materials and methods

5.2.1 Materials

Ketoconazole (KCZ) was purchased from BOCSI, Inc. (USA), hydroxypropyl methyl cellulose acetate succinate (HPMCAS) L,M,H grades were obtained from Shin-Etsu Chemical Company (Tokyo, Japan) (**Table 1)**, triethyl citrate (TEC), sodium chloride, sodium acetate trihydrate and sodium dihydrogen phosphate monohydrate was purchased from Sigma Aldrich, (St.Louis MO, USA). The lipid Gelucire 50/13 (Stearoyl macrogol-32-glycerides) was kindly donated by Gattefossé (Luzern, Switzerland). FaSSIF V2 was purchased from Biorelevant.com. (UK) All solutions were prepared using Mill-Q water (18.2 MΩ cm^{-1}).

Table 1. Characteristics of HPMCAS L, M and H grades

Grade	MeO	HPO	Acetyl (%)	Succinoyl (%)	Dissolving pH
AS-L	20.0–24.0	5.0–9.0	8	15	>=5.5
AS-M	21.0–25.0	5.0–9.0	9	11	>=6.0
AS-H	22.0–26.0	6.0–10.0	12	7	>=6.5

5.2.2 Preparation of solid dispersions and physical mixtures

ASDs were prepared by using a hot melt extrusion (HME) method as described in the literature. [389,390] Briefly, KCZ, polymer and plasticizer (Gelucire 50/13 or TEC) were employed in a ratio of 20:80:10 w/w and mixed with the spatula. The different compositions of the extrudates were

prepared by the HME process using a Thermo Scientific Haake MiniLab II, which is a conical, co-rotating, twin- screw microcompounder (Thermo Electron, Karlsruhe, Germany). The premix was manually fed into the extruder hopper and the temperature of the barrel was set to 150°C. The screw speed during the feeding step was 150 rpm. Subsequently, the extrudate strand was allowed to exit from the flat die by opening the bypass valve. The strands were then stored in the desiccator until analysis. Extrudate strands were pelletized using a Thermo Scientific Process 11 (Karlsruhe, Germany) producing pellets of 2mm employed for dissolution.

5.2.3 Powder X-ray diffraction (PXRD)

PXRD was used to characterize the solid form of the physical mixtures and of freshly prepared ASDs at ambient temperature using a Bruker D2 PHASER (Bruker AXS GmbH, Germany) with a PSD-50 M detector and EVA application software version 6. Samples were prepared by spreading pellets from HME or powder of the physical mixture or collected after filtration at the end of the USP II dissolution test on PMMA specimen holder rings from Bruker. Measurements were performed with a Cu K α radiation source at 30 kV voltage, 10 mA current and were scanned from 6–40 2θ with 2θ being the scattering angle at a scanning speed of 0.016 2θ /min.

5.2.4 Differential scanning calorimetry (DSC)

A DSC 4000 System, from DSC 3 (Mettler Toledo, Greifensee, Switzerland) was calibrated for temperature and enthalpy using indium. Nitrogen was used as the protective gas (20 mL/min). Samples (approximately 5 mg) were placed in 40 µL aluminium pans with pierced aluminium lids. The midpoint glass transition temperature (T_g), was determined by a single-segment heating ramp of 10 °C/min from 25 °C to a maximum temperature of 200 °C. All DSC measurements were carried out in triplicate.

5.2.5 Biphasic dissolution test

The biphasic dissolution experiments were carried out using the inForm (Pion Inc., Billerica, MA) platform, with the experimental setup shown in **Figure 1**. The UV detection wavelengths for ionized (pH 2) KCZ were between 260 and 280 nm, for unionized (pH 6.8) KCZ between 280 and 300 nm and in the organic layer the selected range was 285 -315 nm. A linear relationship (R^2>0.99) was established between absorbance and concentration in each of the

media tested. KCZ formulations were added into the gelatin capsules and delivered via the sample holder into a cylindrical vessel (diameter 49.9mm, height 74.9mm). Crystalline KCZ and KCZ ASD formulation were delivered at a dose equivalent to 20mg of KCZ. Initially, samples were introduced into 36 mL of 0.01M acetate phosphate at pH 2. After 30 minutes to replicate the transition into the upper small intestine, a layer of decanol (40mL) and 4 mL of 10 x concentrated FaSSIF V2 were added, with the pH of the aqueous layer adjusted to pH 6.8. The duration of the intestinal sector was 240 minutes. Concentration of KCZ in both layers was quantified every 2 minutes using two *in situ* multi-wavelength fiber optic UV dip probes. The pH was monitored throughout the experiment using an *in situ* pH probe and controlled to ± 0.1 pH unit using 0.5M HCl or 0.5M NaOH. Temperature was monitored using the temperature probe and controlled to 37^{o}C using a heating block. The stirring speed of the paddles was set to 100 rpm. Stirring was temporarily stopped, while the layer of decanol was added into the vessel**.**

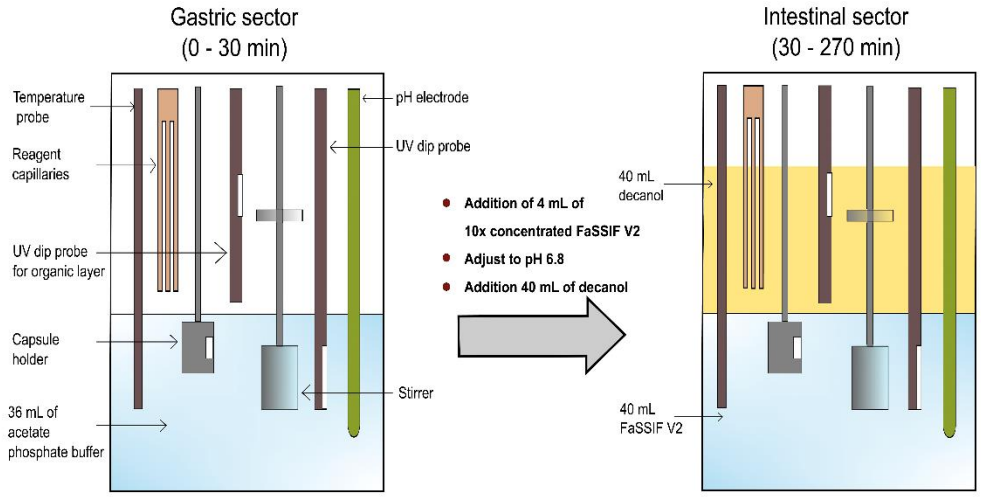

Figure 1. Schematic representation of the biphasic dissolution setup

5.2.6 USP II dissolution test

In order to investigate polymer swelling in the aqueous layer with DWS, a dissolution testing using the same proportion between drug amount and the dissolution volume in the biphasic method was carried out using an Erweka USP II dissolution apparatus (Heusenstamm, Germany). Temperature was set to 37^{0}C and initial release testing was in 225 ml of 0.01M acetate phosphate buffer at pH 2 for the first 30 minutes, with a stirring speed of 100 rpm. After

30 minutes, undissolved pellets were withdrawn and transferred in 225 mL of biorelevant fasted state medium FaSSIF V2 at pH 6.8, with the temperature maintained at 37 ^{0}C ± 0.5 and stirring speed of 100 rpm. [24] The biorelevant media were prepared using FaSSIF V2 based on instructions from www.biorelevant.com. Gelatine capsules containing 225 mg of ASDs, equivalent to 45 mg of KCZ were tested. A 5 mL aliquot was withdrawn at appropriate time intervals and replaced with fresh dissolution media. Microrheology of withdrawn samples was determined using DWS as described in the following section.

5.2.7 Diffusing wave spectroscopy (DWS)

DWS RheoLab (LS Instruments AG, Fribourg, Switzerland) was used as optical technique for microrheological measurements. [118,391,392] The theory of DWS-based microrheology has already been explained in detail in previous works. [118,153] The DWS was calibrated prior to each measurement with a suspension of polystyrene particles, PS, (Magsphere Inc., U.S.A) in purified water (10 wt. %). The PS particles have a mean size of 250± 25 nm with a solid content of 0.5 wt. % in dispersion. This suspension was filled in cuvettes with a thickness L of 5 mm prior to measuring for 60 s at 37 ˚C. The value of the transport mean free path, l^* (microns) was determined experimentally, as reported previously. [358] The transmission count rate was measured several times until a constant value was reached and the cuvette length, L, was considerably larger than the obtained values for l^* ($L \gg l$) ensuring diffusive transport of light. The transport mean free path of the sample l^* is needed for the determination of the correlation intensity function and, thus for the microrheological characterization. Microrheological characterization (l^* and complex viscosity) were performed on the samples withdrawn from the USP II dissolution test at different time points.

Thus, 0.5 wt. % PS nanoparticles were added to the clear samples to ensure the correct regime (guarantee a L/l* ratio larger than 7). [118] Quartz cuvettes (5 mm) were used and data acquired for 60 s. Each sample was measured 5 times as previous measurements**.** The microrheological characterization of polymer solutions was measured in a broad frequency range by DWS, whereas an average of the complex viscosity, at high frequencies (90 000rad/s) was selected.

5.2.8 Statistical analysis

Analysis of the variance (ANOVA) and regression analysis were calculated using Statgraphics (v16.1.11, Statpoint Technologies, Inc., Warrenton, Virginia). A multi factor ANOVA was used

to assess possible effects of polymer grades, plasticizers, and time on drug uptake into the organic phase. A multi factor analysis of variance (ANOVA) was calculated with respect to the uptake of drug amounts into the organic phase, *Q* (%). Thus, effects of the polymer, plasticizer, time and their factor interactions on *Q* (%) were evaluated statistically. This analysis was focused on the organic layer due to its likely relevance for drug absorption and because of lack of particles, which avoided the analytical complication of turbidity that otherwise occurred in the aqueous phase.

5.3 Results

5.3.1 *In vitro* characterization of crystalline KCZ

Figure 2 shows the biphasic dissolution profile of KCZ in aqueous and organic phase, represented as drug concentration (µg/mL) versus time. Drug concentration reaches a peak in the gastric compartment after 0.5h, while at simulated intestinal conditions, the drug concentration decreased due to precipitation caused by the lower solubility at intestinal pH (pKa 2.9 and 6.5). Precipitation of the drug was assessed using DWS. The parameter monitored was the transport mean free path *l**, that can be viewed as a measure of sample turbidity. More specifically, *l** is a critical length scale in the case of diffuse light propagation and is described as the distance a photon travels in the sample before its direction of propagation is randomized. Therefore, the lower the value of *l**, the more turbid is a sample. In **Figure 3,** a decrease of *l** indicated turbidity due to precipitated drug upon change to intestinal medium. X-ray diffractograms at 25°C (**Figure 4b**) revealed that after 4.5h of dissolution time, KCZ existed in a crystalline state when compared with the KCZ reference material (**Figure 4a**).

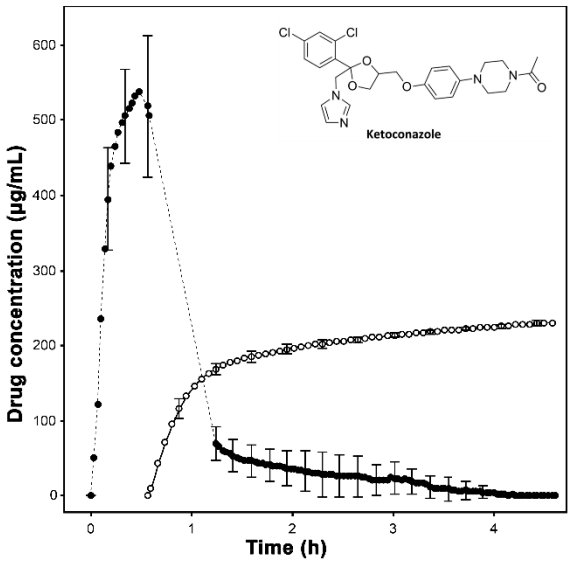

Figure 2. Dissolution profile of KCZ in the biphasic dissolution test: aqueous profile (filled circles) and organic profile (opened circles). Broad error bars and the connecting dotted line are an indication of UV blackout occurring in the aqueous phase due to rapid KCZ precipitation.

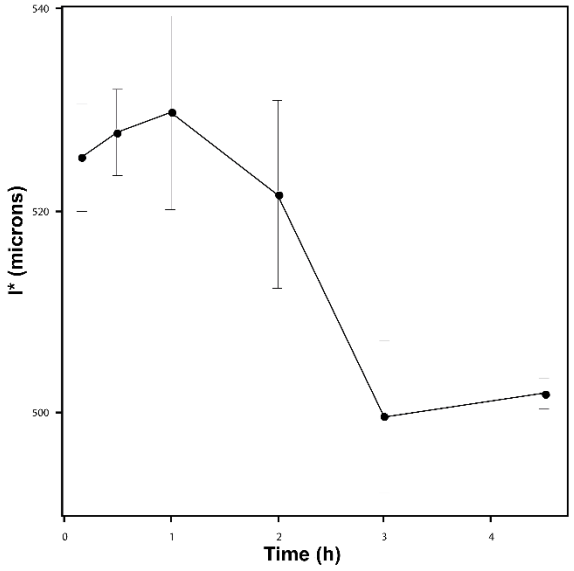

Figure 3. Microrheological characterization of the aqueous dissolution profile of pure KCZ with DWS in the USP II apparatus

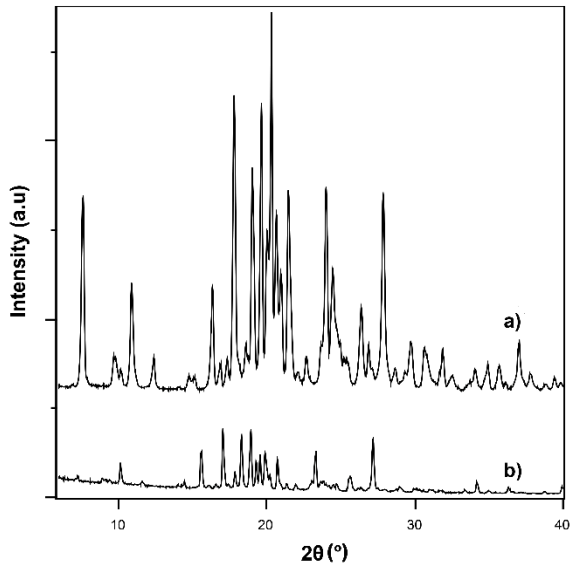

Figure 4. KCZ raw material (a), ketoconazole precipitate after 4.5h of dissolution test at 37 degrees (b)

5.3.2 Bulk characterization of crystalline material and solid dispersions

Prepared ASD, physical mixtures and raw materials were analyzed by PXRD at 25°C to verify the amorphous nature of the dispersions, and the results were compared with those of the corresponding physical mixtures. As shown in **Figure 5,** KCZ based ASDs manufactured with HPMCAS-L, HPMCAS-M and HPMCAS-H grade were amorphous at 20% (w/w) drug

loading. In contrast, physical mixtures and raw materials were crystalline, as expected. ASDs were further characterized by DSC (**Figure 6)** to confirm the solid form of the drug in the physical mixture and in the ASDs. All ASDs showed an absence of the KCZ melting peak, while the physical mixture had a melting peak of the drug (T_m).

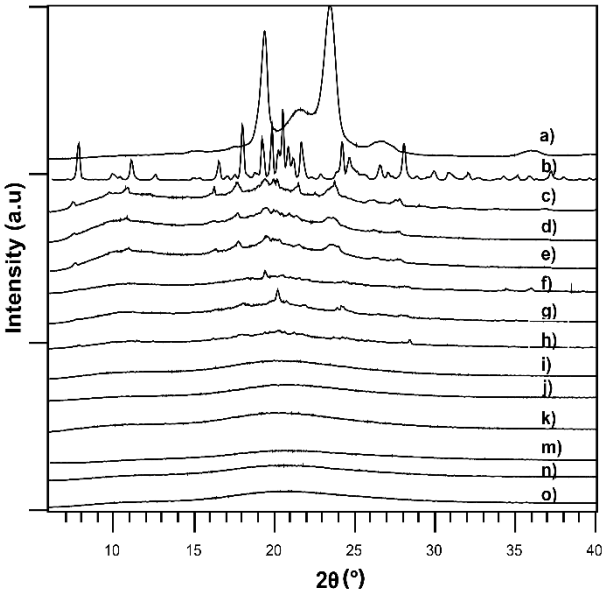

Figure 5. X-ray powder diffraction patterns of Gelucire (a) KCZ (b), physical mixtures of HPMCAS H, Gelucire, and KCZ (c) Physical mixtures of HPMCAS M, Gelucire, and KCZ (d), physical mixtures of HPMCAS L, Gelucire, and KCZ (e), physical mixtures of HPMCAS H, TEC, and KCZ (f), physical mixtures of HPMCAS M, TEC, and KCZ (g), physical mixtures of HPMCAS L, TEC, and KCZ (h), ASD HPMCAS H, Gelucire, and KCZ (i), ASD HPMCAS M, Gelucire, and KCZ (j), ASD HPMCAS L, Gelucire, and KCZ (k), ASD HPMCAS H, TEC, and KCZ (m), ASD HPMCAS M, TEC, and KCZ (n), ASD HPMCAS L, TEC, and KCZ (o).

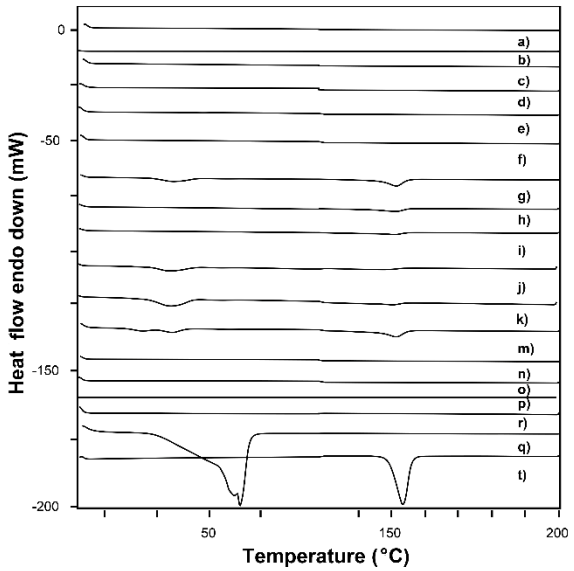

Figure 6. DSC thermograms of ASD HPMCAS L, TEC and KCZ (a), ASD HPMCAS M, TEC, and KCZ (b), ASD HPMCAS H TEC and KCZ (c), ASD HPMCAS L, Gelucire, and KCZ (d), ASD HPMCAS M, Gelucire, and KCZ (e), ASD HPMCAS H, Gelucire, and KCZ (f), physical mixtures of HPMCAS L, TEC, and KCZ (g), physical mixtures of HPMCAS M, TEC, and KCZ (h), physical mixtures of HPMCAS H, TEC, and KCZ (i), physical mixtures of HPMCAS L, Gelucire, and KCZ (j), physical mixtures of HPMCAS M, Gelucire, and KCZ (k), physical mixture HPMCAS H, Gelucire, and KCZ(m), HPMCAS L (n), HPMCAS M (o), HPMCAS H (p), TEC(r), Gelucire (q), KCZ alone (t)

5.3.3 Biphasic dissolution experiment of ASDs

Figure 7a depicts dissolution profiles of six different ASDs formulation in the aqueous layer. As mentioned before the first 0.5h of the dissolution test were in a gastric environment and during this time, no relevant differences were observed between formulations. By contrast, in the intestinal sector, differences between formulations and polymer grades were observed. As a trend, the L polymer grade resulted in comparatively highest amounts of KCZ in solution, followed by the M and H grades even though the given plasticizers appeared to play a role as well. The absolute concentrations in the aqueous phase result in kinetics that is essentially confounded by the overlapping processes of drug release, supersaturation, and potential precipitation. It was therefore important to compare the concentrations profiles also with those obtained from the organic layer, simulating the amount of absorbed drug. **Figure 7b** demonstrates again clear differences between the formulations depending on polymer grade and plasticizer used.

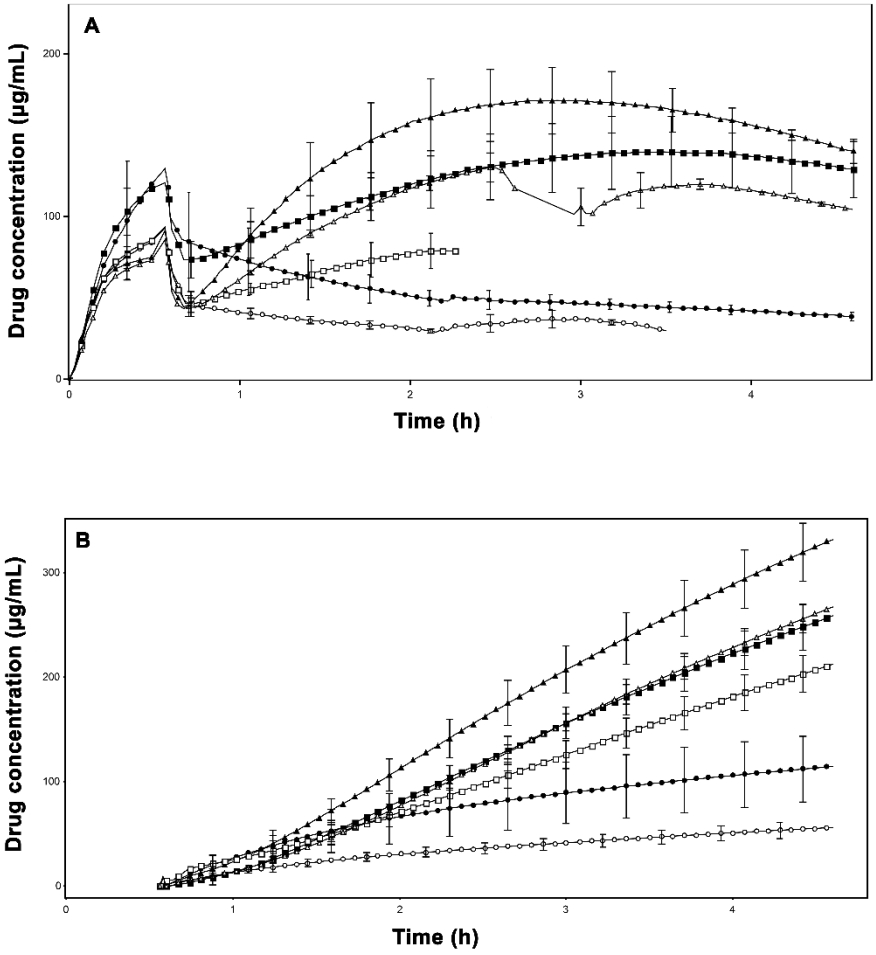

Figure 7. Biphasic dissolution test in aqueous (a) and in organic layer (b). Mean (SD) (n=3) biphasic dissolution data of ASD Gelucire formulation (filled symbols) with L grade (triangle), M grade (square), H grade (circles) ASD TEC formulation (opened symbols) with L grade (triangle), M grade (square),H grade (circles). Some aqueous layer dissolution profiles appear not complete because of the strong turbidity blocking UV light reaching the detector.

5.3.4 Microrheological characterization

Analysis of biphasic dissolution test results revealed differences between grades of the HPMCAS polymer. The behavior of the different solid dispersions was further studied in a USP II dissolution vessel using DWS. This microrheological technique allowed even at low polymer concentrations to monitor the mechanical sample dynamics over a large range of time scales (10^{-7} s to 10s) and local displacements. Using DWS, it was possible to correlate the decrease of complex viscosity with an increase of KCZ concentrations over dissolution time in the aqueous layer. The dissolution test was performed at pH 6.8 using the same biorelevant medium FaSSIF

V2 and polymer concentration as compared to the biphasic *in vitro* experiment. Sample differences were specific for given grades and plasticizers, and the residue of the ASDs were studied by PXRD analysis after 4.5 h of dissolution which showed absence of crystalline drug precipitate. (Figure 8) In Figure 9 is shown that comparatively higher complex viscosity was noted in gastric conditions (0.5 h) with moderate differences between samples. More pronounced differences were seen depending on polymer grade and plasticizer following transfer into the intestinal medium. In Figure 10, it can be seen that values of *l** generally decreased over time, which meant an increase in turbidity.

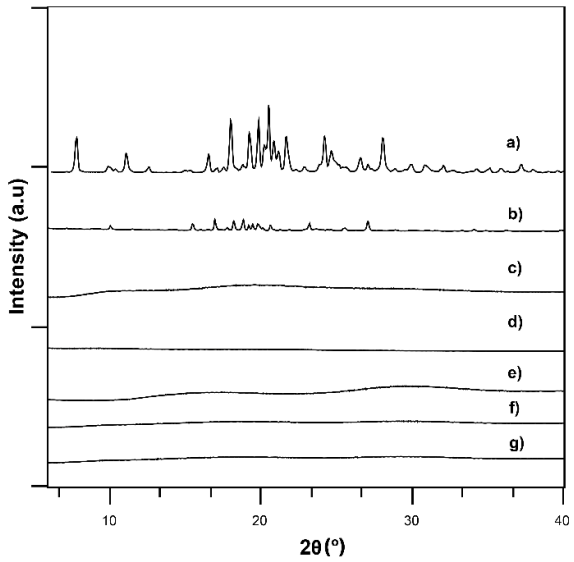

Figure 8. Representative X-Ray diffraction patterns of KCZ precipitates in the USP II dissolution test. KCZ reference material a), crystalline pattern collected from the intestinal sector (*in vitro*) that refers to pure KCZ after 4.5h of dissolution at 37 ^{0}C b), amorphous patterns that refer to collected solid from ASDs in the intestinal sector (4.5 h, 37°C) that indicate absent crystallization c),d),e),e),f),g).

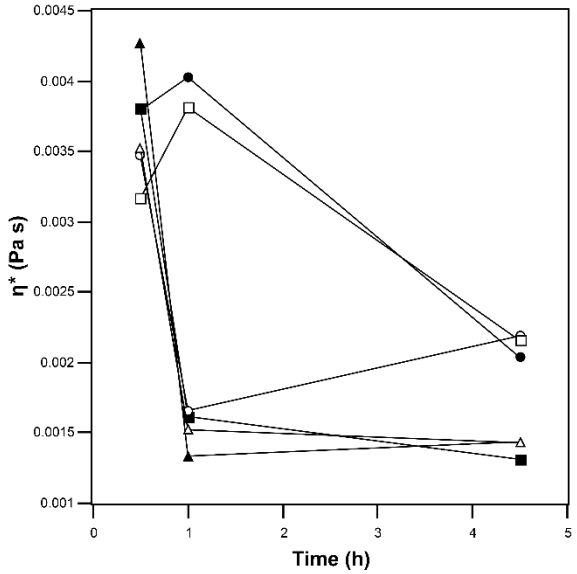

Figure 9. Mean (SD) (n=3) complex viscosity *(η*)* data versus dissolution time (h) for different grades of HPMCAS. Filled symbols indicate ASD Gelucire formulation L grade (triangle), M grade (square), H grade (circles) while opened symbols represent ASD with TEC L grade (triangle), M grade (square), H grade (circles).

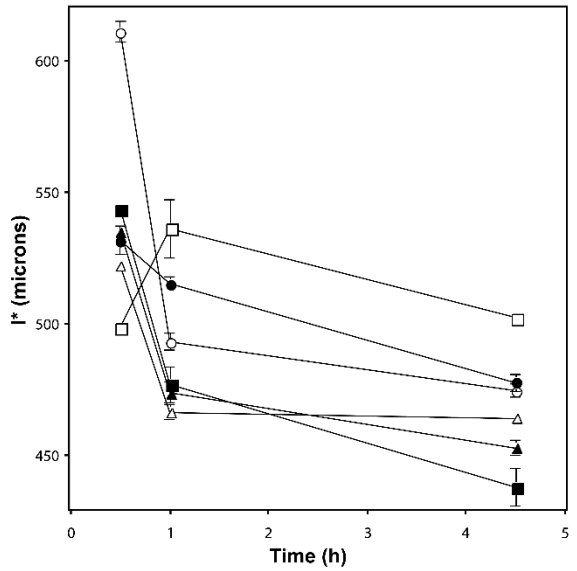

Figure 10. Mean (SD) (n=3) *l** data versus dissolution time (h) for different grades of HPMCAS. Filled symbols indicate ASD Gelucire formulation L grade (triangle), M grade (square), H grade (circles) while opened symbols represent ASD with TEC L grade (triangle), M grade (square), H grade (circles).

5.3.5 Statistical analysis

The statistical analysis revealed a significant influence of the polymer grades on drug release into the organic phase, as well as another effect of the plasticizer on drug release as indicated by the obtained *p*-values. (**Table 2**) The ANOVA table decomposes the variability of *Q* (%) organic phase into contributions due to various factors. Since type III sums of squares (the default) have been chosen, the contribution of each factor is measured having removed the effects of all other factors. Different factor effects as well as interactions were found to be significant with *p*-values lower than 0.05 (i.e. 95% significance level) regarding the drug amount taken up into the organic phase Q (%). (**Table 2)** Inspecting means of drug uptake into the organic layer provided highest values for L grade, then the M grade, and finally the H grade of HPMCAS. The interaction of polymer grade and dissolution time revealed that the above ranking was primarily due to the drug uptake at 4.5h. A comparison of the means for plasticizer effect showed on the average higher uptake for formulations containing Gelucire instead of TEC.

Table 2. Analysis of variance for Q (%) organic phase - Type III sums of squares

Source	Sum of squares	Df	Mean square	F-ratio	*p*-value
A:HPMCAS	1605.5	2	802.8	108.9	0.0000
B:Plasticizer	190.3	1	190.3	25.8	0.0000
C:time (h)	15696.4	2	7848.2	1065.2	0.0000
INTERACTIONS					
AB	17.9	2	8.9	1.2	0.3074
AC	3212.0	4	803.0	109.0	0.0000
BC	319.7	2	159.9	21.7	0.0000
RESIDUAL	294.7	40	7.4		
TOTAL (CORRECTED)	21336.6	53			

Interesting was a regression of drug amounts in the organic layer versus the aqueous layer, which provided a correlation coefficient of $r = 0.50$ ($p = 0.0002$) if all data were considered and at the longest release time, the correlation was higher $r_{4.5h} = 0.83$ ($p < 0.0001$). These correlations were expected to be less than unity because partitioning into the organic layer is governed by thermodynamic activity rather than drug concentrations or amounts.

In the aqueous phase, the amount released can be compared versus the complex viscosity and

resulted in a correlation coefficient of $r = 0.50$ ($p = 0.0001$) and for the longest release time in $r_{4.5h} = 0.67$ ($p = 0.0024$). Interestingly, a negative weak correlation was found for drug amounts released into the aqueous phase versus l^* with $r = -0.31$ ($p = 0.0222$). This correlation coefficient became stronger for a consideration of endpoint data only, $r_{4.5h} = -0.73$ ($p = 0.0005$).

5.4 Discussion

To cope with the biopharmaceutical challenges of poorly soluble drugs, one of the current research needs is to improve mechanistic understanding upon release, while another important need is to have suitable analytical methods to study these aspects. This work studied amorphous solid dispersions of KCZ in a biphasic *in vitro* test and introduced DWS to elucidate mechanisms of sustained drug release from ASD.

From the data in Figure 7, it is apparent that the ASDs of KCZ displayed a dissolution behavior that was quite distinct from that of crystalline KCZ. (Figure 2) Crystalline KCZ completely dissolves in the gastric compartment (>99%) and upon transition into the intestinal medium, precipitation occurred. The dissolved amount in the aqueous phase readily partitioned into the organic layer, providing constant drug concentrations over the dissolution time (plateau is around 200 µg/mL). Obtained data suggested that drug precipitation in FaSSIF was relatively rapid compared to the partitioning rate into the organic layer. Precipitated fraction of the pure KCZ in the intestinal condition was found to be crystalline, in contrast to *in vivo* findings reported by Psachoulias et al. (2011) who found a limited fraction of amorphous precipitate.[388] (Figure 4). Furthermore, over predicted precipitation has been mentioned also by Ruff A et al. (2017) who studied formulated KCZ in an *in vitro* transfer model without an absorptive sink. Thus, it seems challenging to simulate a relevant degree of precipitation *in vitro.* [381] The present biphasic release test has here the advantage of an absorptive sink, but a direct correlation with *in vivo* data was beyond scope as the study focused on mechanistic understanding of the drug release performance from solid dispersion.

A weak base KCZ was selected as a model compound and combined with the enteric coating polymer HPMCAS to form solid dispersions. Release performance was assessed using biphasic dissolution testing, while mechanistic aspects were investigated by means of DWS. Considering the obtained dissolution profiles of ASDs, it is possible to observe that at the end of the simulated gastric phase, the majority of the KCZ (about >75%) from the ASDs remained undissolved. Thus, all ASDs provide significantly lower concentrations of KCZ under gastric conditions when compared with the crystalline KCZ. This was due to the poor solubility of the

HPMCAS polymers at gastric conditions at pH 2. The initial low release of KCZ from the ASDs during this gastric phase was hence expected to be mostly caused by KCZ close to the surface of the ASDs since the bulk of the polymer matrix would hardly swell and dissolve in the acidic environment. After transition to intestinal conditions, KCZ released by the ASDs partitioned into the decanol layer, with the L type HMPCAS ASDs resulting in the greatest release of drug whilst the H grade HMPCAS ASDs showing the lowest release of drug, as presented in Figure 7. Dissolution performance of each formulation is reflected with the mass of the residue collected at the end of the dissolution test. (Table 3) Indeed, H grade reported the highest solid amount undissolved (83.58 % of the ASD with TEC and 69.70% of ASD with Gelucire), while L grade presented the lowest solid amount (24.36% in ASD with TEC and just 3% in the ASD with Gelucire). In addition, ASDs using the Gelucire plasticizer showed a larger release of KCZ compared to the ASDs using TEC as a plasticizer. These higher concentrations of KCZ from the ASDs using Gelucire was a likely consequence of the surfactant properties of Gelucire resulting in greater solubilization of KCZ in the aqueous layer. [393] In accordance with the results in the aqueous layer, the partitioning rate into the organic layer differed greatly among the ASDs. The rank order of KCZ released from the ASDs in the decanol layer reflects the dissolution performance of the ASDs in the aqueous layer. It can be therefore be summarized that avoidance of high release in the stomach medium and the observed sustained release in the intestinal medium of the employed ASD formulations were advantageous to maximize absorptive drug uptake. This is in line with literature of other solid dispersions that a sustained drug release rate would lead to relatively longer induction times of crystallization, which thereby forms the basis of effective drug absorption. [11,99,374]

Table 3. Outline of the calculated percentage (w/w) KCZ in each layer at the end of the biphasic dissolution experiment; formulations with Gelucire as plasticizer are indicated with Gel, while the others with triethyl citrate are indicated with TEC

	Percentage of 20mg KCZ Dose (%)		
Formulation	Organic layer	Aqueous layer	Solid
L Gel	66.24	30.88	2.88
M Gel	51.72	28.41	19.87
H Gel	22.34	7.96	69.70
L TEC	53.38	22.26	24.36
M TEC	42.44	16.32*	41.24
H TEC	11.24	5.18*	83.58
Crystalline	45.76	2.99**	51.25

Since drug release and hence absorption is governed by rather complex mechanisms in the aqueous phase and the drug concentration in the aqueous phase is the driving force for partitioning into the organic layer, it was of interest to obtain complementary data to the kinetics of drug concentrations. We introduced DWS to gain knowledge about microrheological properties of the dispersed ASDs (such as the complex viscosity) and to study l^* over the dissolution time. The mechanism of drug release from ASDs is typically governed by polymer swelling and the dissolution of the carrier in the solvent medium. [99,374] Such swelling and dissolution is dependent on ionization state of the polymer as well as on how close its solubility parameter is to that of the surrounding medium. [84] The selected carrier, HPMCAS is practically not soluble in gastric media, while it starts to dissolve and swell at pH values higher than 5.5 depending on the ratio of succinoyl and acetyl moieties. (Table 1) The poor solvent conditions of the acidic medium would theoretically lead to undissolved dispersed polymer particles together with some initial polymer swelling. In addition, at lower pH values the polymer is not charged and the absence of repulsive charge might cause polymer particles aggregation. [18] Thus, large hydrophobic particles of the polymer and drug in the gastric conditions provide higher values of complex viscosity in the medium as evidenced by DWS. (Figure 9) The opposite situation is observed in FaSSIF, where the polymer exists as colloidal aggregates. [99] Indeed, in the simulated intestinal media, the colloidal nature of HPMCAS allows the drug to interact with hydrophobic moieties of the carrier providing drug polymer nanoaggregates and colloids as reported in literature. [18,349] The negative charge of the succinoyl groups present in the polymer

matrix in intestinal media provide stable nanoaggregates due to the repulsive forces and prevent aggregation of the polymer in big colloids causing a decrease in the complex viscosity in the intestinal conditions compared to the gastric. [18,349,394,395] Indeed, it is well known that viscosity is influenced by the particle size and smaller colloidal size have a lower resistance to flow, therefore providing lower complex viscosity values in solution (Barnes, 2003) As reported in literature upon contact with water, Gelucire forms micelles and their presence in solution likely influenced the drop in complex viscosity observed for these formulations. [64] It is known that micelles increase the solubility and wettability of poorly soluble compounds and these might be the reason of higher drug release from ASDs Gelucire formulations. [65] The same trend in complex viscosity values were also evidenced in comparative experiments with just polymer and plasticizer matrix, indicating that drug had a relatively lower influence on the microrheology compared to the excipients alone (data not shown). Critical for drug release are the particles and colloidal assemblies that emerge from ASDs and a recent study reported on different accessible drug fractions in the aqueous phase of HPMCAS-based solid dispersions. [396] This study about the accessible drug fraction used fluorescence and suggested that thermodynamic activity in such HPMCAS systems can clearly differ from nominal concentrations.

The present DWS study further considered the mean free path *l**, which has been used before to study microstructural changes in emulsion system. [118] The mean free path *l** describes the optical characteristics of the sample. In this study it has been employed to describe the appearance of the turbidity during dissolution. In case of pure KCZ, a decrease of the *l** values was observed during dissolution time probably due to the precipitation upon the transition into intestinal pH. The precipitation behavior of crystalline KCZ in the aqueous phase is also shown during the biphasic dissolution testing with the UV blackout. (Figure 2) Considering the dissolution of ASDs, an interesting finding is that in the case of ASDs, there was a drop in *l** at the end of the dissolution test compared to the initial values in gastric medium. (Figure 10) In the former systems, the increase of the turbidity is due to the increase of the polymer drug nanoaggregates occurring during the dissolution time in the aqueous phase. Indeed, it can be observed that lower values of *l** are provided with Gelucire formulations (L and M grade of the polymer) that are also performing better in the biphasic dissolution testing.

Overall the obtained results support the idea that HPMCAS is a good candidate for ASD formulation development of especially weak basic drugs. Indeed, the major advantage of the

ASDs formulations is the sustained drug release from the polymer matrix when compared to the performance of the crystalline KCZ. (Figure 2)

ASDs formulations with HPMCAS have been prepared employing solvent methods, but some researchers have also studied the utility of HPMCAS for HME. [50,312] Optimization of the process was meaningful to avoid degradation of drug or polymer in line with Sarode et al. (2014) who have investigated the stability of HPMCAS for HME. The present study accordingly extruded at a temperature (i.e. 150°C) that was deemed as uncritical from a degradation viewpoint, which was enabled by adding suitable plasticizers (i.e. Gelucire 50/13 or TEC). Process optimization might be critical for the miscibility of the system and therefore for the stability of the formulations. All ASDs formulations appear miscible at the molecular level, presenting just one single T_g. (Figure 6) Miscibility is an important factor for physical drug stability and all ASDs presented the drug in the amorphous form. (Figure 5) Even though ASDs can be technically produced by employing both TEC or Gelucire as plasticizer, the release results favored ASDs with the PEGylated lipid Gelucire. Increased drug release from these formulations might be due to the multiple interactions between the drug and polymer/lipid matrix compared to the polymer/TEC carrier. (Figure 7) [65,390,397]

5.5 Concluding remarks

Solid drug dispersions form complex and heterogeneous systems upon aqueous dispersions. Coarse as well as colloidal drug/polymer particles evolve and impact on drug release that in turn drives absorptive flux. Traditional release testing often neglect important aspects like an absorptive sink and they offer only limited physical characterization. More recent approaches attempted to better understand emerging particles that are formed in aqueous environment. The current work used a biphasic dissolution test with a pH shift method and introduced DWS as novel analytical tool to gain a deeper understanding of the dissolution process from ASDs. Information about the polymer matrix was obtained regarding the polymer swelling in aqueous media and differences between the grades and plasticizers were highlighted. The microrheological correlations with drug release provided valuable aspects that were in previous research neglected due to lack of data. More results of further solid dispersions should clarify how broadly the identified correlations hold but already now it can be concluded that DWS is a promising tool for *in vitro* testing of ASDs and potentially also further supersaturating formulations.

6 Broadband Diffusing Wave Spectroscopy reveals microstructuring of polymer-drug system

Summary

Microstructuring during a phase transition and crystallization in particular is critical for the physico-chemical properties of polymeric drug carriers and of the final dosage form. Extensive research has been dedicated to study polymeric matrices in drug delivery and despite of substantial progress, there are still unmet challenges such as a non-invasive mechanical analysis since classical rheological methods typically disturb the samples especially during a phase transition. This paper employs Diffusing Wave Spectroscopy (DWS) over a broad frequency band to study polymer-drug systems in a non-invasive way. Eutectic mixtures of polyethylene glycol (PEG) were investigated using two model drugs. While fenofibrate was barely interacting with the polymer, flurbiprofen provided a compound showing distinct molecular interactions with the carrier. Mechanical spectra were obtained during cooling of the molten polymer-drug systems. In conclusion, broadband DWS provided a better mechanistic understanding of the polymer-drug interactions and of macromolecular structuring during cooling of the eutectic melts. Such findings are relevant for a rationale design of pharmaceutical formulations during development and such knowledge would be also important for manufacturing to achieve drug products with reproducible quality characteristics.

Submitted to Crystal Growth and Design

6.1 Introduction

The rheological properties of pharmaceutically important materials such as polymer melts, colloids, gels, and dispersions are central to many fields of formulation development and manufacturing. Most mixtures exhibit complex rheological behavior since formulations include abundant polymers of different kinds.[398] Polymers that melt into a liquid are called to be thermoplastic and they are often processed by extrusion or molding. Polymeric crystallization may start when nuclei develop in a stochastic way and grow to a critical size in the cooling melt. Studies over the past two decades have provided important information on shear-induced crystallization and anisotropy in the direction of shear and show that crystallization proceeds as the nuclei grow into crystallites until all the melt has solidified.[399] When neighboring crystallites grow and segments of the chains forming these crystallites can no longer be incorporated into the crystalline domains, then amorphous regions start to form. This process is depending on the cooling rate so that a low cooling rate grants polymer chains more time to arrange or incorporate themselves into crystallites.[399]

Crystallization in synthetic polymers typically produces polycrystalline aggregates that are called spherulites given their spherical morphology. These spherulites are radially symmetric arrays of fibrillary crystallites ranging in diameter from less than one micron to several millimeters.[400] In pharmaceutical systems, previous research revealed that interactions between the polymer and a drug can influence the crystallization behavior of the polymeric matrix.[36] Indeed, molecular drug- polymer interaction can occur already in the molten state and may not be easily evidenced in the solid state.[401,402] Especially difficult is to study the crystallization process because such a phase transition is easily perturbed by the analytical method thereby leading to experimental bias.

Mechanical rheology has a long tradition in the study of polymer melts.[403] Shear stress controlled rheometers with high sensitivity allow measurement in the linear visco-elastic regime (LVR). Current rheological research on polymer crystallization attempts to combine the mechanical experiment with monitoring techniques such as nuclear magnetic resonance (NMR), small-angle X-ray scattering or dynamic optical microscopy.[404] However, any mechanical rheometry is not contact-free and it can be problematic to measure within the LVR when very dynamic changes occur such as during polymer crystallization. Shear stress controlled oscillatory measurements are further limited because of a narrow range of accessible

high frequencies (with a maximum of about 100 Hz) and most important for the herein system, by the flow induced crystallization.[135,405]

Modern microrheology based on Diffusing Wave Spectroscopy (DWS) has significantly extended the range of experimentally accessible frequencies and it is possible to measure non-ergodic samples such as gels and semi-crystalline materials in a non-invasive way.[130,131,406]DWS has been used previously in the field of Pharmaceutics to study self-emulsifying formulations, emulsions as well as solid drug dispersions.[118,153,391,396,407]

The present research explores, for the first time, the effects of crystallization in a pharmaceutical polymeric system using DWS. Two eutectic systems with polyethylene glycol (PEG) and fenofibrate or flurbiprofen were employed as models.[36,408] This polymer type is hydrophilic with a crystalline lattice structure and can form eutectic mixtures with an active pharmaceutical ingredient (API). Specific interactions between PEG and a drug can suppress the crystalline polymer lattice to some degree during cooling of the molten blend. The model mixtures were selected for their ability to either specifically interact with PEG (e.g. flurbiprofen) or as a model for which no specific interactions are known (e.g. fenofibrate).[35,36] A particular aim of this DWS pioneer study in polymer crystallization was to obtain insights into structure formation of the solidifying molten matrices upon cooling. This is not only of interest from a formulation perspective but also regarding manufacturing such as by hot melt extrusion.

6.2 Materials and methods

6.2.1 Materials

Fenofibrate was purchased from AK Scientific (30023 Ahern Ave Union City CA,USA), while poly(ethylene glycol) 6000, PEG was obtained from Sigma Aldrich (Riedstr. 2 D89559 Steinheim 497329970). Flurbiprofen was supplied by Acros Organics (New Jersey USA) and uniform $Ti0_2$ particles were obtained from LS Instruments (Fribourg, Switzerland).

6.2.2 Methods

6.2.2.1 Preparation of the eutectic mixtures

Eutectic mixtures were prepared by using the melting method as described in the literature.[301] Briefly, the PEG 6000 binary mixtures contained 24% (w/w) fenofibrate or alternatively 33%

(w/w) of flurbiprofen. These concentrations were obtained from previous DSC measurements, (i.e. as mixtures with one endothermic event) as reported in the literature.[36] The physical mixture was blended with a spatula in a metallic pan and heated up to 90˚C to assure complete melting. The obtained molten mixture was then cooled down to room temperature and kept in a desiccator before analysis. The heat exposure during preparation and analysis of the eutectic mixtures was not expected to cause any drug degradation of the two rather stable compounds in line with previous reports that employed hot melt extrusion.[409,410] The obtained molten mixture in the present work was then cooled down to room temperature and kept in a desiccator before analysis. Characteristics and compositions for various drug-PEG eutectic systems are described in Table 1**.**

Table 1. Characteristics and composition for various Drug-PEG eutectic systems

Compound	Molecular weight (MW)	T_m (°C)	ΔH_f (kJ/mole)	Molar volume (cm^3/mol)	cLog*P* (n-octanol/water)	Experimental eutectic composition with PEG 6000 (%)	References
Fenofibrate	361	80.2	34.0	310.7	4.43	24	[35]
Flurbiprofen	244	114.7	28.0	263.5	4.12	33	[408]
PEG	6000	58-63	-	-	-	-	

6.2.2.2 Powder x-ray diffraction (XRPD)

Powder X-ray diffraction was used to characterize the solid form of the physical mixtures and of solid dispersions at ambient temperature using a Bruker D2 PHASER (Bruker AXS GmbH, Germany) with a PSD-50 M detector and EVA application software version 6. Samples were prepared by spreading powder samples on PMMA specimen holder rings from Bruker. Measurements were performed at 25°C with a Cu Kα radiation source at 30 kV voltage, 10 mA current and were scanned from 6-40 2θ, with 2θ being the scattering angle at a scanning speed of 2 °/min.

6.2.2.3 Differential scanning calorimetry (DSC)

A DSC 3 system (Mettler Toledo, Greifensee, Switzerland) was calibrated for temperature and enthalpy using indium. Nitrogen was used as the protective gas (200 mL/min). Samples (approximately 5 mg) were placed in 40 µL aluminium pans with pierced aluminium lids. The melting point (T_m) was determined by a single-segment heating ramp of 10 °C/min from 25 °C to a maximum temperature of 200 °C. All DSC measurements were carried out in triplicate.

6.2.2.4 Fourier transform infrared spectroscopy

Attenuated total reflection Fourier transform infrared (ATR-FTIR) spectra of pure compounds and SDs were acquired in the 4000–600 cm^{-1} range using a Cary 680 Series FTIR spectrometer (Agilent Technologies, Santa Clara, USA) equipped with an attenuated total reflectance accessory. A scanning range of 4000–600 cm was selected with 42 scans and a resolution of 4 cm. The spectra were evaluated using the software ACD/Spectrus Processor 2016.1.1 (Advanced Chemistry Development Toronto, Canada).

6.2.2.5 Diffusing wave spectroscopy (DWS)

6.2.2.5.1 Measuring principle:

DWS is a light scattering technique that requires turbid samples to study the dynamic properties. In the transmission geometry, the sample is illuminated by an expanded laser light source and the transmitted light is analyzed on the opposite side.[129] The colloidal scattering particles can be present inside the sample, such for example oil droplets in emulsion, or they can be added in case of transparent sample such as, for example by dispersing titanium dioxide. Light detectors measure the intensity of the scattered light. The fluctuations of scattered light are characterized by the normalized intensity autocorrelation function (eq.1):[129]

$$g_{(2)}(t)=\langle I(t_0)I(t_0+t)\rangle/\langle I\rangle^2 \quad (1)$$

where the quantity $\langle I\rangle$ is the average intensity, while t represents the lag time.

Using the Siegert relation (eq.2), the intensity correlation function and the field autocorrelation are related:

$$g_{(2)}(t)=1+\beta|g_{(1)}(t)|^2 \quad (2)$$

where β is an instrumental factor given by the collection optics. Once the field correlation

function and l^* have been measured, the mean square displacement (MSD, $<\Delta r^2(t)>$) of a sample can be calculated employing (eq.3)[135,136]:

$$g_{(2)}(t)\text{-}1 \propto \left| \int_0^\infty P(s) exp\left[-\frac{1}{3} k^2 < \Delta r^2(t) > \frac{s}{l^*} \right] \, ds \right|^2 \quad (3)$$

where $k = 2\pi n/\lambda$ is the optical wavenumber including n as the refractive index of the medium and λ is the laser wavelength. $P(s)$ represents the distribution of the photon trajectories of length s in the sample of thickness L, while l^* is the transport mean free path which characterizes the typical step length of the photon random walk.

The data obtained for the MSD were analyzed employing the function proposed by Bellour and coworkers[411]:

$$< \Delta r^2(t) >= 6\delta^2 \left(1 - e^{-\left(\frac{D_0}{\delta^2} t\right)^\alpha} \right)^{1/\alpha} \left(1 + \frac{D_m}{\delta^2} t \right) \quad (4)$$

Where δ^2 represents the amplitude of particle motion, t is the lag time, D_o and D_m are the short and long-time diffusion coefficient while α is an additional parameter introduced to take into account the broad spectrum of relaxation times at the plateau onset time.

Eq. 4 has been recently extended to better describe the region of longer relaxation times in case of pharmaceutical emulsions.[412] On the other hand eq. 4 can also be simplified for other systems. Bellour et al. suggested the following eq. 5 for particles that are harmonically bound (i.e. "entrapped") to exhibit Brownian motion around a stationary mean position:

$$< \Delta r^2(t) >= 6\delta^2 \left(1 - e^{\frac{-D_0}{\delta^2} t} \right) \quad (5)$$

It is here possible to approximate the displacement value of the plateau with $6\delta^2$. The present work determined this plateau value based on the obtained MSD at the estimated inflection point.

6.2.2.5.2 Experimental setup:

All samples were measured in transmission mode using a DWS RheoLab instrument (LS Instruments AG, Fribourg, Switzerland). The theory of DWS-based microrheology was already explained in detail in our previous work.[153] In brief, the laser light was scattered from the ground glass and collimated by a single lens before illuminating the sample. To avoid time consuming measurements at low frequencies, the instruments uses the so-called echo technique. The echo completes the data set to obtain the ICF over a broad range of lag times. In the echo mode the

ground glass rotates during the measurement producing different illumination speckle pattern.[118] This feature is particularly important when working with non-ergodic samples, such as emulsions, gels and semi-crystalline polymers.[118,153] Samples were analyzed using a 5mm thickness cuvette. To ensure turbidity of the molten polymer and of the solid dispersion, 4.5 mg of titanium dioxide tracer particles with mean diameter of 360 nm were added and mixed with 2 g of sample. The mixture was poured into the cuvette to fill it up to 15-20 mm. The measurements were set in slow rotation mode at 300s with 30 s of echo mode. Five measurements of each temperature were done with two independent samples. The average of ten measurements is presented in all graphs.

6.2.2.6 Hot stage cross polarized microscopy

An assessment of the crystal nucleation and growth was based on polarized light imaging using a heating stage coupled with a microscope Axioskop 2 mot (upright). The latter had a Hamamatsu 5810 3CCD video camera and was equipped with phase contrast, polarized filters, and DIC. Physical mixtures were molten at 85° degrees and the crystallization was studied using a remained constant magnification throughout the whole measurement (scale bars are displayed in every image).

6.2.2.7 Molecular visualization by docking

To qualitatively analyze and depict drug interactions with the polymer, molecular docking was conducted. Chemical structures were obtained from the ChemicaElectrica Gateway (v. 4.01) and loaded into Molecular Modeling Pro Plus (v.8.2.1.) (both programs by Norgwyn Montgomery Software Inc., North Wales, USA). A relatively shorter chain for polyethylene glycol (i.e. PEG 400) was selected as model and this structure was drawn together with either the drug fenofibrate or flurbiprofen. Following a molecular mechanics minimization of the conformational energy (using the MM2 algorithm), partial charges of the molecules were calculated based on a semi-empirical quantum mechanical method (using a Complete Neglect of Differential Overlap, CNDO approach). Starting from 6 Angstroms distance between the molecular Van der Waals surfaces, a grid search algorithm proposed a molecular docking configuration of minimized energy. A relative permittivity of 18 was selected to approximate the PEG environment.[413] The final molecular association was depicted as combined wire frame and space filled model.

6.3 Results

6.3.1 Solid state characterizations

Raw materials and the eutectic mixtures of PEG 6000 with either fenofibrate or flurbiprofen were characterized initially. Solid state analysis such as by DSC, PXRD and FT-IR was performed to determine the physical state of the raw materials and of the eutectic mixtures as well as to study interactions in both the molten and solid state.

While the composition of eutectic mixtures and the respective melting point are presented in Table 1, the molecular docking of the two compounds with the carrier employed is presented in Fig. 1.

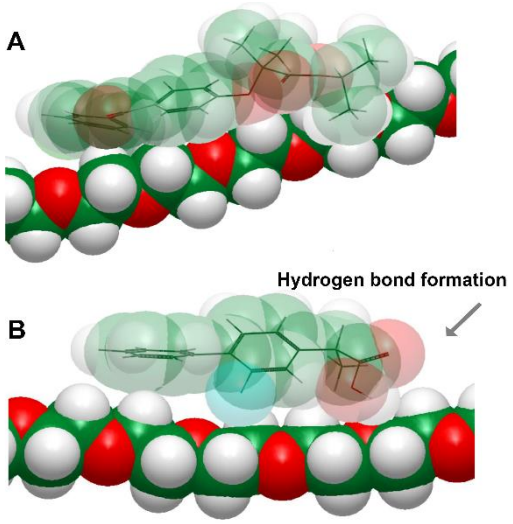

Fig. 1. Molecular docking of PEG 6000 with fenofibrate (A) and flurbiprofen (B)

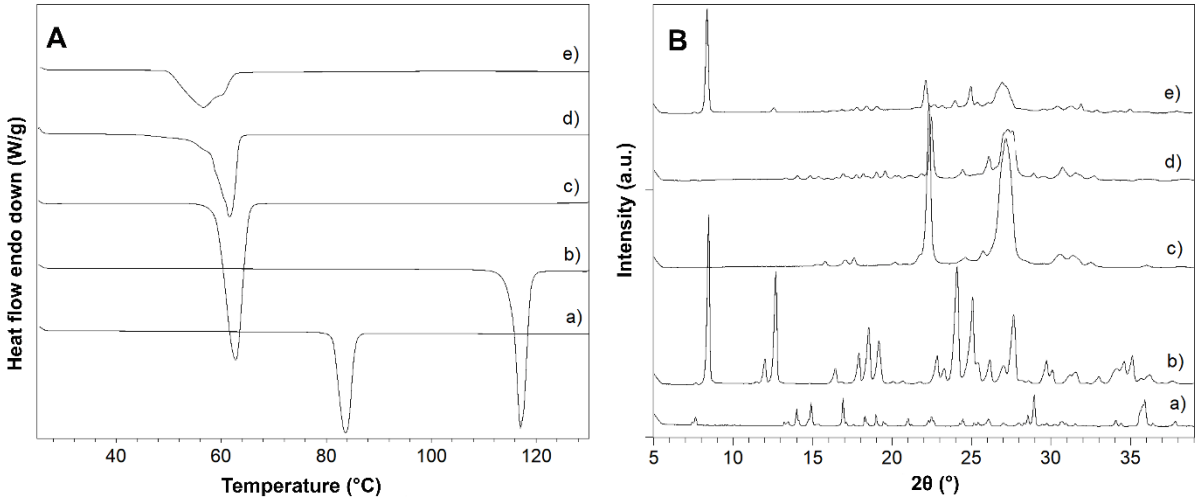

Fig. 2. Differential Scanning Calorimetry (DSC) (A) and Powder X-ray diffraction (XRPD) (B) plots of fenofibrate (a), flurbiprofen (b), PEG c) PEG –fenofibrate SD (d) and PEG- flurbiprofen SD (e).

The DSC thermograms of pure PEG 6000, fenofibrate and flurbiprofen, as well as of their eutectic mixture are shown in **Fig. 2A**. The analysis of pure PEG 6000 shows that the onset of the endotherm occurs at 58 °C, having a peak at 62.5 °C. While the pure drug fenofibrate had a melting point of 80.2 °C and flurbiprofen's melting point was 114 °C, the endothermic event of the eutectics was much lower compared to the raw materials. The eutectic composition for PEG and fenofibrate has been determined previously to comprise 24% (w/w) of drug and it was independent of the molecular weight of the carrier.[414] Due to a strong hydrogen bonding, the eutectic composition for PEG and flurbiprofen was much higher with 33% (w/w) of API and strongly influenced by the molecular weight of the polymer.[36,408] As eutectic systems, the crystallinity of the pure drugs was affected in mixture regarding form as well as extent, thereby resulting in the observed DSC endotherms. The molecular interaction of the two model drugs with a PEG chain was also visualized based on molecular modeling (i.e. molecular docking of API to a polymer chain).

Fig. 1 depicts the hydrogen bond that is formed in the case of flurbiprofen whereas no such strong interaction was possible in case of fenofibrate with PEG.

The crystalline state of the raw materials and of the eutectics was analyzed further by PXRD. As observed in **Fig. 2B**, raw material and eutectics present distinct Bragg peaks, indicating a crystalline nature. When comparing the spectra of the raw flurbiprofen with that of the eutectic mixture, a slight shift in the location of the peaks was observed.

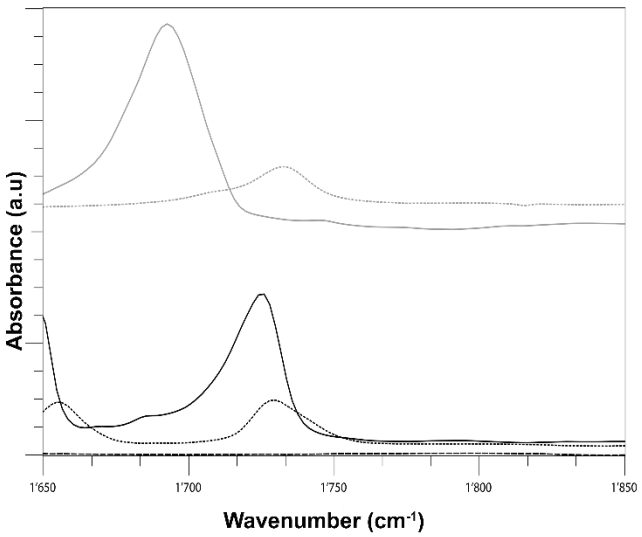

Fig. 3. FT-IR of flurbiprofen (gray solid line), solid dispersion with flurbiprofen (gray dots), fenofibrate (black solid line), solid dispersion with fenofibrate (black dots).

The interaction between flurbiprofen and PEG 6000 was further evaluated by FT-IR.

Pronounced shifts in the absorption bands of FT-IR are visible in Fig. 3 when comparing the spectra of flurbiprofen and fenofibrate as raw material and those obtained from the respective eutectic formulations. It can be seen that the carbonyl stretching band of flurbiprofen's carboxyl moiety at 1700 cm^{-1} band has shifted to a higher frequency in the eutectic mixture. It has been argued that flurbiprofen is able to both donate and accept hydrogen bonds via the carboxyl moiety depending on the molecular weight of the polymer.[36] It is likely that flurbiprofen is able to donate hydrogen bonds with PEG 6000, while it might also accept hydrogen bonds with much lower molecular weight PEG considering a more relevant influence of hydroxyl groups present at the chain ends.[415] This is according to the expected molecular interaction based on molecular docking (Fig. 1) and the previously reported changes in FT-IR spectroscopy in mixtures of flurbiprofen and PEG.[36,408] Such a shift was not observed in the case of the fenofibrate and the eutectic mixture of this drug. There were also not pronounced changes in the lower wave number vibrations in case of the pure fenofibrate compared to that of the eutectic mixture. This was again different for the system of flurbiprofen where at relatively lower wave numbers, some changes were observed in the spectra; especially a peak at 696 cm^{-1} that was shifted towards lower wavenumber (630 cm^{-1}) for the solid dispersion of flurbiprofen with PEG.

6.3.2 DWS

Analysis of polymer crystallization and macromolecular structuring was a central aim of this study. Recent progress in DWS allows measuring at changing temperatures in a dynamic way so that a solidification of eutectic melts with and without drug could be analyzed.

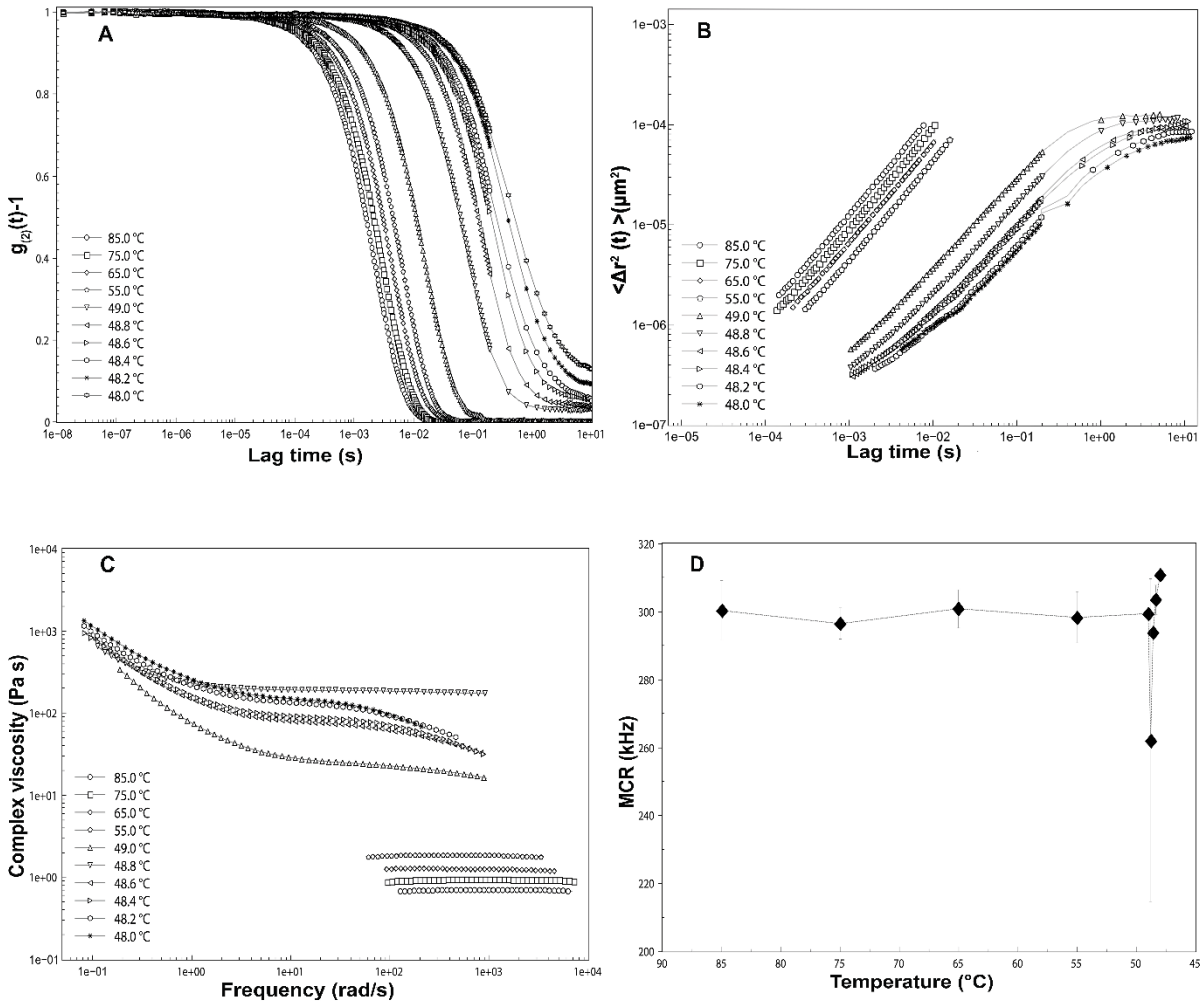

Fig. 4. Microrheological characterization of PEG 6000: ICF (A), MSD (B), complex viscosity (C) and MCR (D).

Fig. 4A presents the intensity correlation function (ICF) of PEG 6000 from 85 °C to 48 °C. At 85 °C when the polymer was completely molten, the intensity correlation function decayed to zero. Upon cooling, such decay occurred at longer lag time, and this abrupt shift was due to high viscosity increase that was expected by polymer nucleation and crystal growth since PEG 6000 is a semi-crystalline polymer at room temperature. The major changes in intensity correlation function were observed between 49 and 48 °C and the shift in lag time is displayed in Fig. 4B, where MSD is plotted. At relatively high temperature, the system was liquid and the

MSD was linearly increasing with lag time, while with temperature decreased, the MSD was reaching a plateau. Such a plateau means that tracer particles exhibit limited Brownian motion as they become entrapped. Complex viscosity versus the frequency is presented in Fig.4C. While at high temperature, the polymer was behaving as a Newtonian system with constant viscosity across a broad range of frequencies, this was different at lower temperatures, for which viscosity was changing with frequency thereby suggesting a structuring in the course of polymer crystallization leading to shear thinning. Mean count rate (MCR) represents the average intensity of light (proportional to the number of photons arriving at the detector) that is an indicator of sample transparency. At the higher end of measured temperatures, MCR was around 300 kHz, whereas with the onset of polymer crystallization there was a strong decrease of the MCR, indicating an increase of turbidity. (Fig. 4D). This provided a sensitive analytical approach to the macroscopic appearance of the polymer that was transparent at 85°C but white at room temperature. In PEG 6000 is a semi-crystalline polymer and the increase of turbidity was due to the crystallization of the polymer occurring around 48 °C.

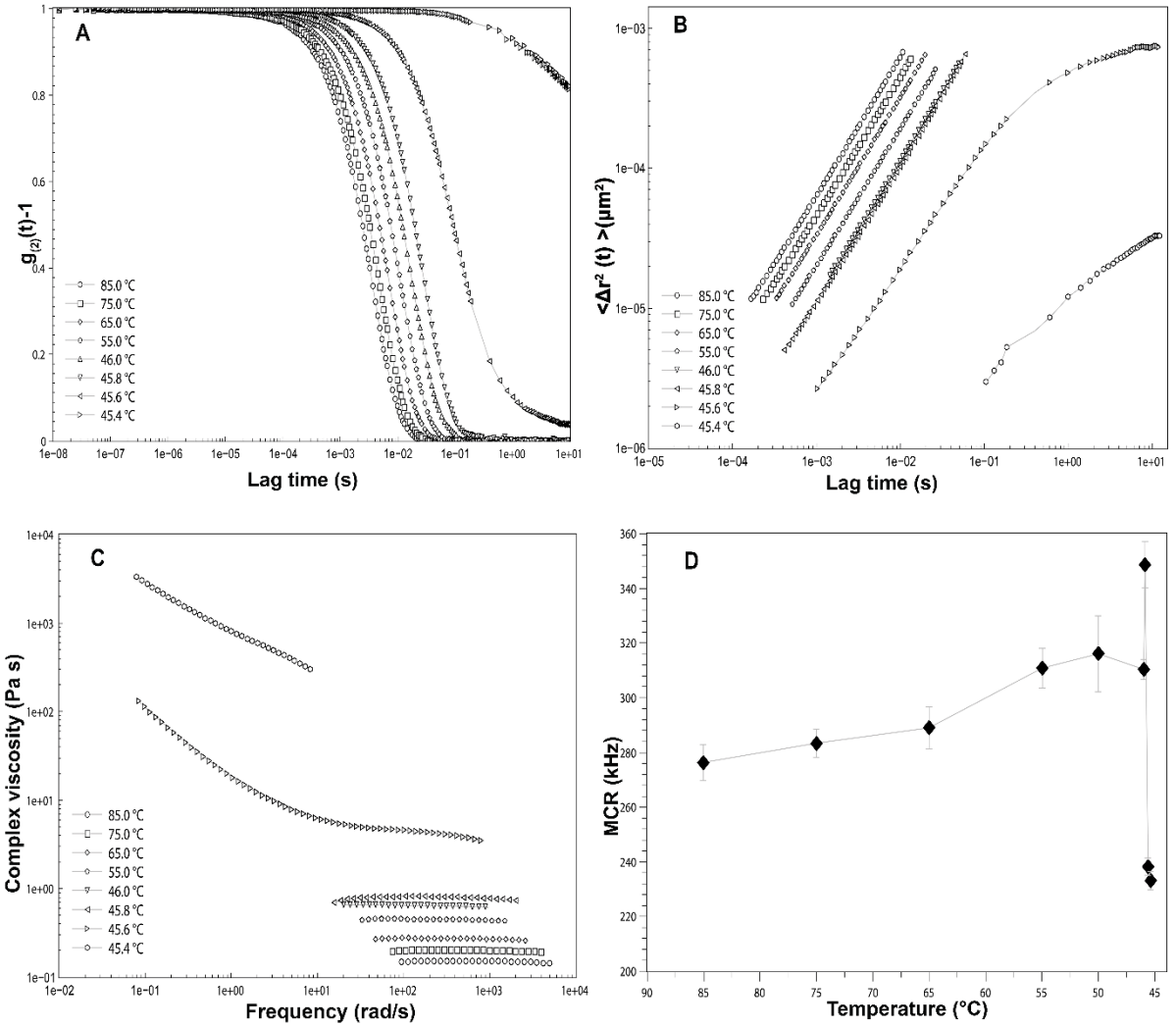

Fig. 5. Microrheological characterization of solid dispersion of PEG 6000 and fenofibrate: ICF (A), MSD (B), complex viscosity (C) and MCR (D).

The molten physical mixture of PEG 6000 and fenofibrate was then heated to 85 °C Fig. 5A compares the intensity correlation function (ICF) upon cooling to lower temperatures and 45.4°C can be identified as the temperature of crystallization. Thus, at 85 °C when the polymer was completely molten, the ICF decayed to zero, whereas the ICF started to no longer reach zero upon cooling. ICFs were shifted to higher values of lag time(s) and the viscosity was increasing. The major changes in intensity correlation function for the eutectics were observed between 46 and 45.4 °C. The shift in lag time is depicted in Fig. 5B, where MSD is plotted versus lag time. At high temperature for which the system is liquid, the MSD was increasing linearly with lag time, while upon decreasing the temperature, the MSD was reaching a plateau. Changes of the complex viscosity versus temperature are presented in Fig.5C. Similar to pure PEG 6000, the molten polymer mixture had a constant viscosity over the measured frequency

range, whereas at lower temperatures, there was a decrease of viscosity over the frequency range suggesting again shear thinning as previously observed with pure PEG 6000. Further analysis of the fenofibrate and PEG 6000 mixture is given by Fig. 5D that shows the decrease of the MCR over the temperature for this eutectic system. At higher temperatures, MCR was approximately 300 kHz and a strong decrease of the MCR, indicated an increase of turbidity in the course of matrix crystallization. The onset of crystallization was occurring at a temperature of about 45 °C and MCR reached approximately 220 kHz when the sample was completely solidified.

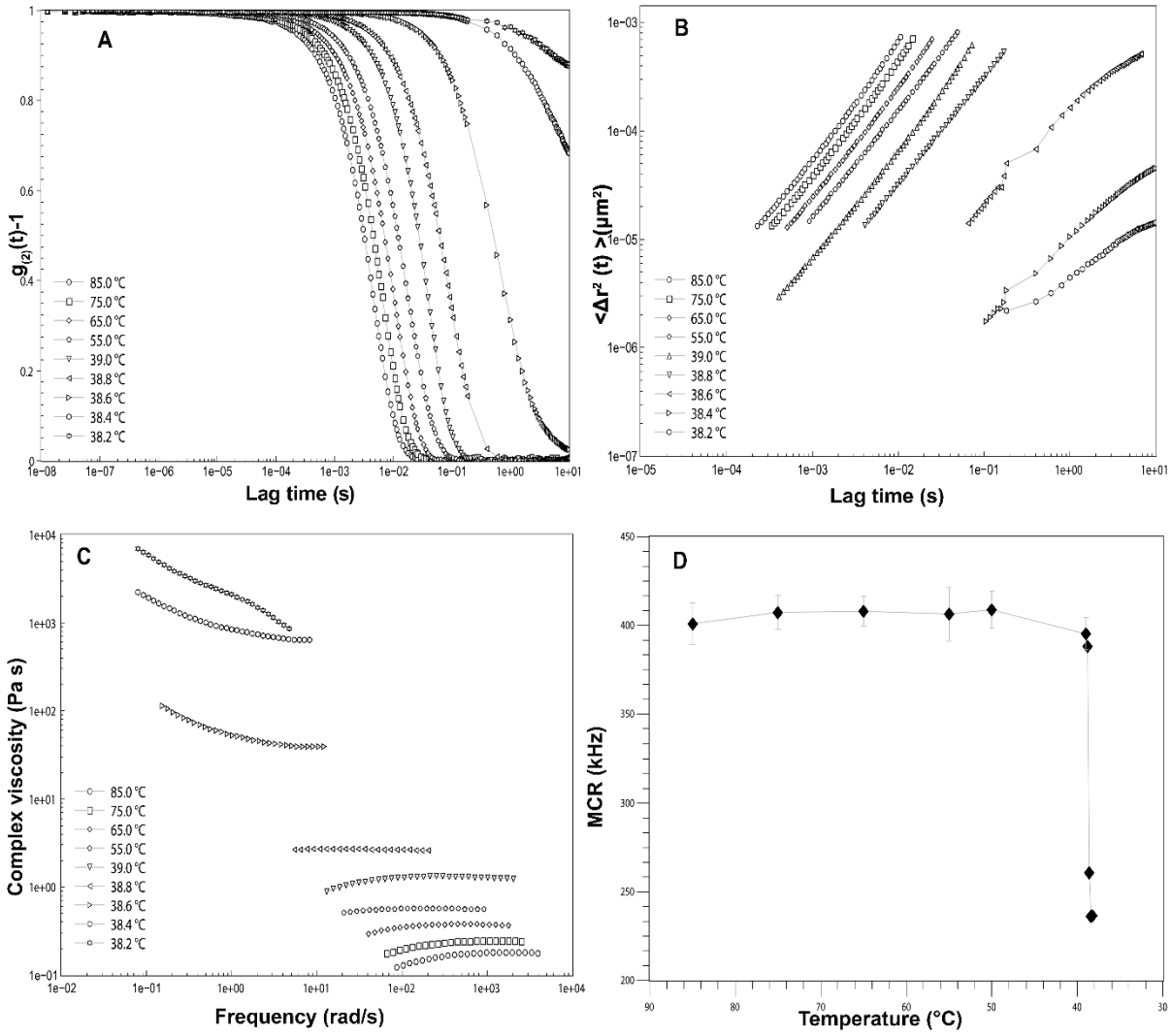

Fig. 6. Microrheological characterization of solid dispersion of PEG 6000 and flurbiprofen: ICF (A), MSD (B), complex viscosity (C) and MCR (D).

Finally, the model of the strongly interacting mixture was analyzed using PEG 6000 in combination with flurbiprofen. The molten mixture at 85 °C showed again an ICF that was decaying to zero. However, with a decrease of temperature there was again a shift to higher lag times, indicating a higher viscosity of the system as it can be seen in Fig.6A. For this eutectic mixture, no solidification was observed even close to the body temperature (38° C) in line with what has been reported before.[36] Again, the MSD provided again insights into the microstructure via the mean average distance that tracer particles were travelling. (Fig. 6B). In the liquid state, tracer particle were able to perform Brownian motion and therefore, there was a linear increase of MSD versus lag time. For a nearly constant MSD, tracer particles were apparently confined around their mean positions. When considering Fig 6C, the systems does

not exhibit an ideally viscous behavior at high temperature; therefore, an apparent shear thickening may have caused the observed frequency changes at 85°C, while cooling of the system was leading to a rheological behavior suggesting shear thinning similar to the previously analyzed samples. Such cooling led again to a strong decrease of MCR values due to the occurrence of crystallites as shown Fig 6D.

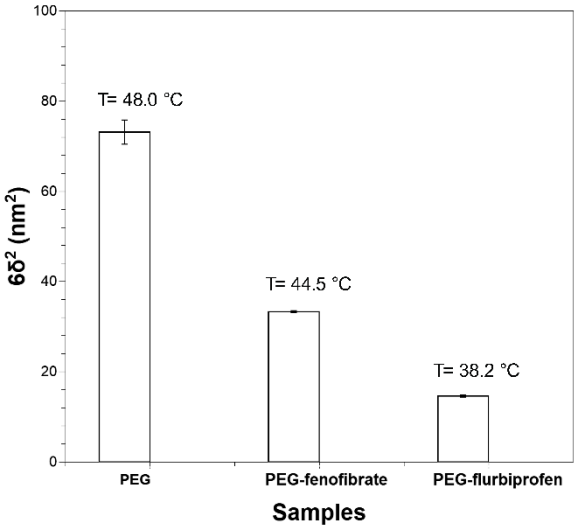

Fig. 7. Comparison of the apparent cage size (named as $6\delta^2$) in pure PEG, SD of fenofibrate and SD of flurbiprofen close to their solidification temperature.

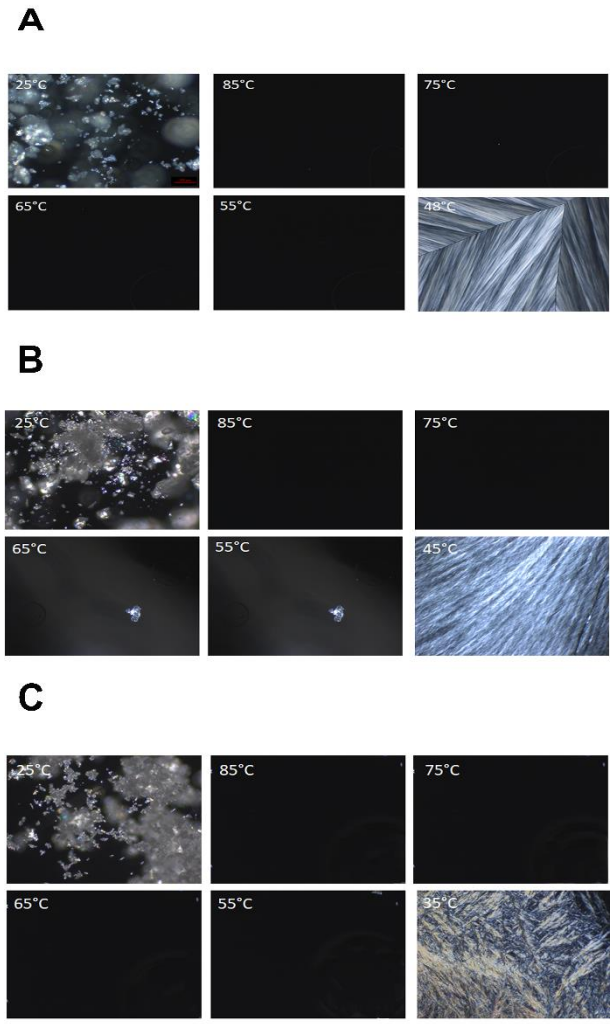

Fig. 8. Hot stage cross polarized light microscopy of PEG 6000 (A), SD of fenofibrate (B) and SD of flurbiprofen (C)

Since all samples showed a plateau regime of MSD, a comparison for this apparent confinement of the tracer particles due to microstructuring of the solidifying polymer matrix. Following the approach of Bellour et al.[411] (Eq. 5) for the present case of polymeric melts, the given confinement of the tracer particles can be plotted as a kind of "cage size" as displayed in Fig. 7. The dimension of this apparent confinement of tracer particles was biggest for polymer alone, followed by the eutectic mixtures with fenofibrate and finally that with flurbiprofen. The data of DWS were finally complemented by studies using hot stage cross polarized microscopy and the results are presented in Fig.8A, B and C respectively. As mentioned before, polymer drug interaction play a significant role in polymer chain folding during the crystallization and as highlighted in the Fig. 8C, the crystalline structure of the SD with flurbiprofen in the solid state appeared to be different compared to the polymer alone or also compared to the SD with fenofibrate that was less interacting with the polymer matrix. It is evident that the crystalline

structure was in the latter case rather disrupted in line with previous reports in the literature.[401,408,414]

6.4 Discussion

Crystallization of polymers is a complex topic and the classical of Hoffmann-Lauritzen theory provides a basic understanding of how polymeric chains exhibit surface crystallization into lamellae of a given thickness.[416] Since these pioneer days, several more refined theoretical models involving multistep crystallization have been proposed and a very recent review in the journal Macromolecules comes to the conclusion that even these days, important theoretical questions remain unanswered.[417] The theoretical complexity is of course even increased in presence of additives such as a drug and therefore, pharmaceutical research has mostly taken just a phenomenological approach to crystallization of polymeric drug formulations. However, any experimental study of a phase transition such as crystallization is also difficult because the analytics should not disturb the observed process, which is a concern with techniques such as mechanical rheology. The present work therefore used for the first time broadband DWS to study pharmaceutical eutectic model systems in the course of solidification upon cooling.

Previous work suggested that flurbiprofen is strongly interacting with PEG while fenofibrate is not.[36] Solid state characterization employing DSC, PXRD were performed and the results are shown in Fig. 2. Specific interactions such as hydrogen bonding between flurbiprofen and PEG 6000 have been studied with FT-IR and presented in Fig 3. The current study found that drug-polymer interaction played a key role in case of flurbiprofen during phase transition of the PEG-based solid dispersion. It can be well imagined that strongly attached flurbiprofen would affect polymer chain flexibility and its bulkiness so that crystalline packing of lamellae would be affected. This qualitative view may explain the observed effects on polymer matrix crystallization in case of this strongly interacting eutectic system. The solid dispersion comprising PEG 6000 and fenofibrate exhibited ideal viscous behavior at high temperatures and the frequency spectrum suggested some viscoelastic behavior at lower temperatures. (Fig. 4C and 5C). The high temperature regime can be imagined to hold for a typical melt with polymer chains that can arrange in random coils and thereby provide a rather homogenous system with practically ideal viscous behavior. Once polymer nucleation and growth occurs, the lamellar grow into crystallites and such spherulites can further aggregate. Since these aggregates provide suspended particles, there was turbidity noted as indicated by the MCR of

the DWS experiments. The frequency dependence of viscosity was analogues to shear thinning of a suspension and a recent study actually evaluated typical models of suspension rheology for such samples.[418] The authors pointed to the analogy of particle hierarchy between aggregated crystallites and other polymeric nanocomposites. The latter nanocomposites are typically agglomerates of small aggregates and these again consist of primary nanoparticles. Analogously, crystal aggregates (spherulites) are aggregates of crystal lamellae consisting of several individual lamellae.

Table 2. Temperatures and *G' G'* values at the intersection of curves

	Temperature (°C)	Frequency (rad/s)	Moduli *G'G"* (Pa)
PEG	48.20 48.00	0.63 0.70	120.00 150.60
SD of fenofibrate	45.60 45.40	2.69 0.50	19.54 398.58
SD of flurbiprofen	38.40 38.20	0.12 1.64	151.40 1958.76

Aggregated polymeric crystals can exhibit mechanical rigidity and therefore elastic behavior. Determination of the solidification point is obtained using the crossover point of *G'* and *G''* and the results presented in Table 2. Indeed, above the given crystallization temperature, samples were in molten state exhibiting *G''> G'*, while upon solidification, there was dominance of the elastic modulus with *G'* > *G''*. (data not shown)

Newtonian behavior at high temperatures was not found in case of the molten solid dispersion with flurbiprofen. (Fig. 6C) The changes along the differences frequencies suggested increasing viscosity at 85 °C, whereas upon cooling, data indicated again a shear thinning behavior. The latter behavior supports the view that occurrence of crystallites was leading to a suspension-type of rheology. However, the behavior at 85°C in the melt is particularly notable since PEG 6000 alone did not show such increased viscosity with frequency but was rather Newtonian. Polymers of higher molecular weight can show an increase of viscosity with rising frequency which is due to the entanglement of longer chains. Each detanglement is expected to require a specific relaxation time and for higher frequencies, transient bonds of entanglement would become permanent on the given time scale.[419] Even though a strongly interacting small-molecular drug like flurbiprofen would not greatly lengthen the chains of PEG 6000, the present

results still display some frequency dependency of the viscous melt caused by the presence of flurbiprofen.

The presence of strong molecular interactions between a drug and PEG 6000 was also studied by Van Duong et al. (2017). They outlined the view that in the melt, PEG chains are locked in hydrogen bonding with drug molecules and therefore no more than one repeated unit of helical structure can be folded. The crystallization process for the considered systems is taking place in a relatively narrow temperature range, and this may occur especially when the system is homogeneously dispersed. The model assumes that in the course of chain folding, drug-polymer hydrogen bonds are disrupted leading to a segregation of API. Some drug remains hydrogen bonded to the surface of the folded lamellae and is part of drug-rich domains. Such solidified polymer systems are typically semi-crystalline and the extent of crystallinity as well as the given microstructure were previously mentioned to likely affect quality attributes such as drug release.[36,401]

To gain a better understanding of how the presence of drug affected polymer crystallization, the average movement of the tracer particles as MSD grants insights into the microstructuring in the course of crystallization. The approach by Bellour et al. [411] has been previously used to describe other structured liquids such as a surfactant solution of worm-like micelles and it was qualitatively used in the present study to interpret the obtained data of the polymeric melts upon crystallization.[411] When tracer particles exhibit a nearly constant MSD for a regime of frequencies (or lag times), then there is a kind of apparent entrapment given. The so-called "cage size" grants indirect insights into the structure of the matrix that is surrounding the used tracer particles. It is noteworthy that the MSD decreases in presence of polymer drug interaction, which is also reflecting by the apparent cage size at the inflexion point (named as $6\delta^2$) as presented in Fig.7. Given that tracer particles were embedded in a matrix of crystallizing and aggregating lamellae, the differences in apparent cage size may suggest how finely meshed these networks of lamellae were. This would support the view that the strongly interacting flurbiprofen perturbs polymer crystallization thereby leading to relatively smaller lamellae compared with pure PEG 6000 or its SD with fenofibrate. Indeed, the presence of flurbiprofen attached to the PEG via hydrogen bonding would inhibit the crystallization of the polymer, because it induces defects in the PEG crystalline network, hindering it from growing and structuring in line with results depicted in Fig.8. The present findings show that microstructuring of polymer in presence of drug can be studied not only by small-angle X scattering but also with novel microrheological tool such as broadband DWS.[420,421]

These findings help us to understand the microstructuring during phase transition of the

polymer and of eutectic mixtures at high frequencies and in a non-invasive conditions. In addition, physicochemical properties and pharmaceutical performance of PEG-based solid dispersion depend on the drug-polymer interactions. Disruption of the crystalline lattice has also expected implications of drug release in that a relatively lower matrix crystallinity typically shows faster drug release compared to an eutectic system with a higher degree of crystallization. Therefore, the given microstructure is central for the quality attributes of the given SD formulations and present work may find applications in formulation development as well as in process development of a eutectic drug product.

6.5 Conclusions

The physico-chemical properties of polymeric drug carriers and of the final dosage form depend on the micro structuring during the crystallization process in case of polymer eutectics. DWS and MSD were employed to study macromolecular structuring during cooling of the PEG-based mixtures with two model drugs, fenofibrate and flurbiprofen. While the first compound was barely interacting with the polymer, flurbiprofen provided a distinct molecular interaction with the carrier. This interaction already present in the molten state was changing the rheological behavior of the otherwise pure polymer melt. The crystallization of polymer was monitored by studying complex viscosity and MSD parameters from DWS. Indirectly it was possible to gain insights into how lamellae may crystalize and aggregate in the different formulations. Given the importance of the microstructure of such eutectic systems on different pharmaceutical quality attributes, the present findings are of high relevance also for practical formulation development. Compared to classical rheological measurements where the directions of the crystallizing lamellae are influenced during the measurements, DWS offers insights into the microstructuring of crystallizing lamellae based on contact-free measurements over a broad frequency range. Such mechanistic analysis and understanding of microstructuring under non-invasive conditions is not only relevant for eutectic systems. Other solid drug dispersions could be studied in the future too and tracer particles should be added whenever a system does not provide sufficient light scattering on its own. Therefore, DWS is a quite versatile tool to study the solidification behavior of drug-excipient mixtures, which is important to properly understand phase behavior and microstructuring of pharmaceutical formulations.

Final remarks and outlook

Solid dispersion technology is one of the most employed technologies to enhance the performance of poorly soluble drugs. It employs not just polymer but also other excipients to enhance the solubility and dissolution rate of low solubility APIs. The selection of an appropriate excipient for the formulation is still challenging and involves a lot of trial and errors. Different approaches to characterize amorphous solid dispersions have been already presented. Indeed, solid-state analytical characterizations are widely employed to discern between the amorphous and crystalline physical state of the API, explore the system thermodynamics, changes and the effect of multicomponent systems within the amorphous solid dispersion. However, many aspects of solid dispersions are still unknown; in this regard, novel approaches for solid dispersion characterization can deepen our understanding of processes such as drug-polymer interaction during manufacturing, or upon water dispersion. This thesis aims to introduce two novel approaches for solid dispersion characterizations such as Diffusing Wave Spectroscopy (DWS) and Fluorescence Spectroscopy.

DWS is an advanced light scattering technique, which provides microrheological knowledge employing dispersed particles in a solvent. The main advantages of this technique are the broadband frequencies and low viscosity measurements in a non-invasive way. For the first time, it has been introduced in the solid dispersion field and it has been applied to mechanistically study the dissolution process from different solid dispersion formulations. It allowed us to measure very low viscous media during the dissolution process for example in Chapter 4 and correlate it to the dissolution mechanism. The polymer type employed in this study forms colloids upon water dispersion, and through viscosity measurements, it was possible to deepen our knowledge about the dissolution mechanism of complex solid dispersions mixtures.

Also, fluorescence spectroscopy together with size-exclusion chromatography aimed to study drug-polymer interactions that emerge upon water dispersion of the solid dispersion (Chapter 4). In this study celecoxib, a native fluorescent drug was combined with four different polymers; drug-polymer interactions in the physical mixture or solid dispersion were compared. The results of this study outline the amount of drug embedded into polymer aggregates and the amount of free drug in solution, which is the true supersaturation driving absorption.

Drug release from solid dispersions was also the topic in Chapter 5. For this purpose, different grades of HPMCAS were prepared and tested in a biphasic in vitro dissolution test. DWS was introduced to study microrheological differences among polymer grades and plasticizers in the aqueous phase; polymer swelling and drug-polymer nanoaggregates affected drug release and the uptake in the organic layer. DWS outlined its potential in the biopharmaceutical research on supersaturating systems, such as solid dispersions.
The last chapter emphasized the use of DWS for drug development and manufacturing, employing a fusion method. In Chapter 6 the microstructuring upon cooling of two different solid dispersions was studied and compared to the pure matrix. DWS highlighted differences in microstructuring upon cooling in the presence of and in the absence of molecular interaction.

This thesis offers interesting and promising characterization approaches for the formulation of solid dispersions, which can guide early formulation development of drug delivery systems. DWS, for example, might be used in the characterization for differently gelling drug delivery systems or in combination with fluorescence spectroscopy to gain a better understanding of the swelling and drug release mechanism.

7 Bibliography:

1. Shah, N. H., Sandhu, H., Choi, D. S., Chokshi, H. & Malick, A. W. *Amorphous Solid Dispersions (Theory and Practice)*. (Springer New York, 2014).
2. Butler, J. M. & Dressman, J. B. The developability classification system: application of biopharmaceutics concepts to formulation development. *J. Pharm. Sci.* **99**, 4940–4954 (2010).
3. Hu, J., Johnston, K. P. & Williams, R. O. Nanoparticle Engineering Processes for Enhancing the Dissolution Rates of Poorly Water Soluble Drugs. *Drug Dev. Ind. Pharm.* **30**, 233–245 (2004).
4. Taylor, L. S. & Zhang, G. G. Z. Z. Physical chemistry of supersaturated solutions and implications for oral absorption. *Adv. Drug Deliv. Rev.* **101**, 122–142 (2016).
5. Viernstein, H., Weiss-Greiler, P. & Wolschann, P. Solubility enhancement of low soluble biologically active compounds - Temperature and cosolvent dependent inclusion complexation. *Int. J. Pharm.* **256**, 85–94 (2003).
6. Van Den Mooter, G. The use of amorphous solid dispersions: A formulation strategy to overcome poor solubility and dissolution rate. *Drug Discov. Today Technol.* **9**, e79–e85 (2012).
7. Baird, J. A., Van Eerdenbrugh, B. & Taylor, L. S. A classification system to assess the crystallization tendency of organic molecules from undercooled melts. *J. Pharm. Sci.* **99**, 3787–3806 (2010).
8. Zografi, G. & Newman, A. Interrelationships Between Structure and the Properties of Amorphous Solids of Pharmaceutical Interest. *J. Pharm. Sci.* **106**, 5–27 (2017).
9. Janssens, S. & Van den Mooter, G. Review: physical chemistry of solid dispersions. *J. Pharm. Pharmacol.* **61**, 1571–1586 (2009).
10. Homayouni, A., Sadeghi, F., Nokhodchi, A., Varshosaz, J. & Afrasiabi Garekani, H. Preparation and characterization of celecoxib solid dispersions; comparison of poloxamer-188 and PVP-K30 as carriers. *Iran. J. Basic Med. Sci.* **17**, 322–331 (2014).
11. Frank, K. J. *et al.* The amorphous solid dispersion of the poorly soluble ABT-102 forms nano/microparticulate structures in aqueous medium: Impact on solubility. *Int. J. Nanomedicine* **7**, 5757–5768 (2012).
12. Vasanthavada, M., Tong, W. Q., Joshi, Y. & Kislalioglu, M. S. Phase behavior of amorphous molecular dispersions I: Determination of the degree and mechanism of solid solubility. *Pharm. Res.* **21**, 1598–1606 (2004).
13. Miyazaki, T., Yoshioka, S., Aso, Y. & Kojima, S. Ability of polyvinylpyrrolidone and polyacrylic acid to inhibit the crystallization of amorphous acetaminophen. *J. Pharm. Sci.* **93**, 2710–2717 (2004).
14. Qian, F., Huang, J. & Hussain, M. A. Drug-polymer solubility and miscibility: Stability consideration and practical challenges in amorphous solid dispersion development. *J. Pharm. Sci.* **99**, 2941–2947 (2010).
15. Mori, Y. *et al.* Theoretical and practical evaluation of lowly hydrolyzed polyvinyl alcohol as a potential carrier for hot-melt extrusion. *Int. J. Pharm.* **555**, 124–134 (2019).
16. Guzmán, H. R. *et al.* Combined use of crystalline salt forms and precipitation inhibitors to improve oral absorption of celecoxib from solid oral formulations. *J. Pharm. Sci.* **96**, 2686–2702 (2007).
17. Craig, D. Q. M. M. The mechanisms of drug release from solid dispersions in water-soluble polymers. *Int. J. Pharm.* **231**, 131–144 (2002).

18. Friesen, D. T. *et al.* Hydroxypropyl Methylcellulose Acetate Succinate-Based Spray-Dried Dispersions: An Overview. *Mol. Pharm.* **5**, 1003–1019 (2008).
19. Succinate-based, H. M. A. *et al.* Spray-Dried Dispersions : An Overview. **5**, 1003–1019 (2008).
20. Serajuddln, A. T. M. M. Solid dispersion of poorly water-soluble drugs: Early promises, subsequent problems, and recent breakthroughs. *J. Pharm. Sci.* **88**, 1058–1066 (1999).
21. Kwon, J. *et al.* Spray-dried amorphous solid dispersions of atorvastatin calcium for improved supersaturation and oral bioavailability. *Pharmaceutics* **11**, (2019).
22. Guns, S. *et al.* Comparison between hot-melt extrusion and spray-drying for manufacturing solid dispersions of the graft copolymer of ethylene glycol and vinylalcohol. *Pharm. Res.* **28**, 673–682 (2011).
23. Newman, A. *Pharmaceutical Amorphous Solid Dispersions*. (John Wiley & Sons, Inc., Hoboken, New Jersey, 2015).
24. Amidon, G. L., Lennernäs, H., Shah, V. P. & Crison, J. R. A theoretical Basis for a Biopharmaceutical Drug Classification:The Correlation of in Vitro Drug Product Dissolution and in vivo bioavailability. *Pharm. Res.* **12**, 413–20 (1995).
25. Rosenberger, J., Butler, J., Muenster, U. & Dressman, J. Application of a Refined Developability Classification System. *J. Pharm. Sci.* **108**, 1090–1100 (2019).
26. Rosenberger, J., Butler, J. & Dressman, J. A Refined Developability Classification System. *J. Pharm. Sci.* **107**, 2020–2032 (2018).
27. Wu, C. Y. & Benet, L. Z. Predicting drug disposition via application of BCS: Transport/absorption/ elimination interplay and development of a biopharmaceutics drug disposition classification system. *Pharm. Res.* **22**, 11–23 (2005).
28. Yoo, S. U., Krill, S. L., Wang, Z. & Telang, C. Miscibility/stability considerations in binary solid dispersion systems composed of functional excipients towards the design of multi-component amorphous systems. *J. Pharm. Sci.* **98**, 4711–4723 (2009).
29. Descamps, M. & Willart, J. F. Perspectives on the amorphisation/milling relationship in pharmaceutical materials. *Adv. Drug Deliv. Rev.* **100**, 51–66 (2016).
30. Warren, D. B., Benameur, H., Porter, C. J. H. & Pouton, C. W. Using polymeric precipitation inhibitors to improve the absorption of poorly water-soluble drugs: A mechanistic basis for utility. *J. Drug Target.* **18**, 704–731 (2010).
31. Vasconcelos, T., Sarmento, B. & Costa, P. Solid dispersions as strategy to improve oral bioavailability of poor water soluble drugs. *Drug Discov. Today* **12**, 1068–1075 (2007).
32. Hancock, B. C. & Parks, M. What is the True Solubility Advantage for Amorphous Pharmaceuticals? *Pharm. Res.* **17**, 397–404 (2000).
33. Hancock, B. C. & Zografi, G. Characteristics and Significance of the Amorphous State in Pharmaceutical Systems. *J. Pharm. Sci.* **86**, 1 (1997).
34. Vo, C. L.-N., Park, C. & Lee, B.-J. Current trends and future perspectives of solid dispersions containing poorly water-soluble drugs. *Eur. J. Pharm. Biopharm.* **85**, 799–813 (2013).
35. Law, D. *et al.* Properties of rapidly dissolving eutectic mixtures of poly(ethylene glycol) and fenofibrate: The eutectic microstructure. *J. Pharm. Sci.* **92**, 505–515 (2003).
36. Vippagunta, S. R., Wang, Z., Hornung, S. & Krill, S. L. Factors affecting the formation of eutectic solid dispersions and their dissolution behavior. *J. Pharm. Sci.* **96**, 294–304 (2007).
37. Newa, M. *et al.* Preparation, characterization and in vivo evaluation of ibuprofen binary solid dispersions with poloxamer 188. *Int. J. Pharm.* **343**, 228–237 (2007).
38. Leuner, C. Improving drug solubility for oral delivery using solid dispersions. *Eur. J.*

Pharm. Biopharm. **50**, 47–60 (2000).
39. Sethia, S. & Squillante, E. Solid dispersion of carbamazepine in PVP K30 by conventional solvent evaporation and supercritical methods. *Int. J. Pharm.* **272**, 1–10 (2004).
40. Okonogi, S., Oguchi, T., Yonemochi, E., Puttipipatkhachorn, S. & Yamamoto, K. Improved dissolution of ofloxacin via solid dispersion. *Int. J. Pharm.* **156**, 175–180 (1997).
41. Bhattacharya, S. & Suryanarayanan, R. Local mobility in amorphous pharmaceuticals - Characterization and implications on stability. *J. Pharm. Sci.* **98**, 2935–2953 (2009).
42. Kissi, E. O. *et al.* Glass-Transition Temperature of the β-Relaxation as the Major Predictive Parameter for Recrystallization of Neat Amorphous Drugs. *J. Phys. Chem. B* **122**, 2803–2808 (2018).
43. Dedroog, S., Pas, T., Vergauwen, B., Huygens, C. & Van den Mooter, G. Solid-state analysis of amorphous solid dispersions: Why DSC and XRPD may not be regarded as stand-alone techniques. *J. Pharm. Biomed. Anal.* **178**, 112937 (2019).
44. Lehmkemper, K., Kyerematen, S. O., Heinzerling, O., Degenhardt, M. & Sadowski, G. Long-Term Physical Stability of PVP- and PVPVA-Amorphous Solid Dispersions. *Mol. Pharm.* **14**, 157–171 (2017).
45. Xiang, T. X. & Anderson, B. D. Effects of Molecular Interactions on Miscibility and Mobility of Ibuprofen in Amorphous Solid Dispersions With Various Polymers. *J. Pharm. Sci.* **108**, 178–186 (2019).
46. Huynh, L., Neale, C., Pomès, R. & Allen, C. Computational approaches to the rational design of nanoemulsions, polymeric micelles, and dendrimers for drug delivery. *Nanomedicine Nanotechnology, Biol. Med.* **8**, 20–36 (2012).
47. Lübtow, M. M., Haider, M. S., Kirsch, M., Klisch, S. & Luxenhofer, R. Like Dissolves Like? A Comprehensive Evaluation of Partial Solubility Parameters to Predict Polymer-Drug Compatibility in Ultrahigh Drug-Loaded Polymer Micelles. *Biomacromolecules* **20**, 3041–3056 (2019).
48. Watts, Robert O. Williams III Alan B. Miller, D. A. *Formulating Poorly Water Soluble Drugs*. *Formul. Poorly Water Soluble Drugs* vol. 3 (2012).
49. Van Duong, T. & Van den Mooter, G. The role of the carrier in the formulation of pharmaceutical solid dispersions. Part II: amorphous carriers. *Expert Opin. Drug Deliv.* **13**, 1681–1694 (2016).
50. Tanno, F., Nishiyama, Y., Kokubo, H. & Obara, S. Evaluation of Hypromellose Acetate Succinate (HPMCAS) as a Carrier in Solid Dispersions. *Drug Dev. Ind. Pharm.* **30**, 9–17 (2004).
51. Ueda, K., Higashi, K., Yamamoto, K. & Moribe, K. The effect of HPMCAS functional groups on drug crystallization from the supersaturated state and dissolution improvement. *Int. J. Pharm.* **464**, 205–213 (2014).
52. Taylor, L. S. & Zografi, G. Spectroscopic Characterization of Interactions Between PVP and Indomethacin in Amorphous Molecular Dispersions. *Pharm. Res.* **14**, 1691–1698 (1997).
53. Solanki, N. G. *et al.* Effects of Surfactants on Itraconazole-HPMCAS Solid Dispersion Prepared by Hot-Melt Extrusion I: Miscibility and Drug Release. *J. Pharm. Sci.* **108**, 1453–1465 (2019).
54. Curatolo, W., Nightingale, J. A. & Herbig, S. M. Utility of Hydroxypropylmethylcellulose Acetate Succinate (HPMCAS) for Initiation and Maintenance of Drug Supersaturation in the GI Milieu. *Pharm. Res.* **26**, 1419–1431 (2009).
55. Zhang, Q. *et al.* Effect of HPMCAS on recrystallization inhibition of nimodipine solid

dispersions prepared by hot-melt extrusion and dissolution enhancement of nimodipine tablets. *Colloids Surfaces B Biointerfaces* **172**, 118–126 (2018).
56. Guyot, M., Fawaz, F., Bildet, J., Bonini, F. & Lagueny, A.-M. Physicochemical characterization and dissolution of norfloxacin/cyclodextrin inclusion compounds and PEG solid dispersions. *Int. J. Pharm.* **123**, 53–63 (1995).
57. Meng, F., Ferreira, R. & Zhang, F. Effect of surfactant level on properties of celecoxib amorphous solid dispersions. *J. Drug Deliv. Sci. Technol.* **49**, 301–307 (2019).
58. Han, R. *et al.* Insight into the Dissolution Molecular Mechanism of Ternary Solid Dispersions by Combined Experiments and Molecular Simulations. *AAPS PharmSciTech* **20**, 10–20 (2019).
59. Chaudhari, S. P. & Dugar, R. P. Application of surfactants in solid dispersion technology for improving solubility of poorly water soluble drugs. *J. Drug Deliv. Sci. Technol.* **41**, 68–77 (2017).
60. Siepmann, J. *et al.* Lipids and polymers in pharmaceutical technology: Lifelong companions. *Int. J. Pharm.* **558**, 128–142 (2019).
61. Jannin, V. & Cuppok, Y. Hot-melt coating with lipid excipients. *Int. J. Pharm.* **457**, 480–487 (2013).
62. Damian, F. *et al.* Physicochemical characterization of solid dispersions of the antiviral agent UC-781 with polyethylene glycol 6000 and Gelucire 44/14. *Eur. J. Pharm. Sci.* **10**, 311–322 (2000).
63. Lee, K. H., Park, C., Oh, G., Park, J. B. & Lee, B. J. New blends of hydroxypropylmethylcellulose and Gelucire 44/14: physical property and controlled release of drugs with different solubility. *J. Pharm. Investig.* **48**, 313–321 (2018).
64. Kawakami, K., Miyoshi, K. & Ida, Y. Solubilization behavior of poorly soluble drugs with combined use of Gelucire 44/14 and cosolvent. *J. Pharm. Sci.* **93**, 1471–1479 (2004).
65. Potluri, R. H. K., Bandari, S., Jukanti, R. & Veerareddy, P. R. Solubility enhancement and physicochemical characterization of carvedilol solid dispersion with Gelucire 50/13. *Arch. Pharm. Res.* **34**, 51–57 (2011).
66. Cortes-Rojas, D. F., Souza, C. R. F. F., Chen, M. J., Hochhaus, G. & Oliveira, W. P. Effects of lipid formulations on clove extract spray dried powders: comparison of physicochemical properties, storage stability and in vitro intestinal permeation. *Pharm. Dev. Technol.* **23**, 1047–1056 (2018).
67. Khan, N. & Craig, D. Q. M. M. The influence of drug incorporation on the structure and release properties of solid dispersions in lipid matrices. *J. Control. Release* **93**, 355–368 (2003).
68. Kasten, G., Löbmann, K., Grohganz, H. & Rades, T. Co-former selection for co-amorphous drug-amino acid formulations. *Int. J. Pharm.* **557**, 366–373 (2019).
69. Sosnik, A. & Seremeta, K. P. Advantages and challenges of the spray-drying technology for the production of pure drug particles and drug-loaded polymeric carriers. *Adv. Colloid Interface Sci.* **223**, 40–54 (2015).
70. Paudel, A., Worku, Z. A., Meeus, J., Guns, S. & Van Den Mooter, G. Manufacturing of solid dispersions of poorly water soluble drugs by spray drying: Formulation and process considerations. *Int. J. Pharm.* **453**, 253–284 (2013).
71. Baird, J. A., Santiago-Quinonez, D., Rinaldi, C. & Taylor, L. S. Role of viscosity in influencing the glass-forming ability of organic molecules from the undercooled melt state. *Pharm. Res.* **29**, 271–284 (2012).
72. Mahlin, D., Ponnambalam, S., Heidarian Höckerfelt, M. & Bergström, C. A. S. S. Toward in silico prediction of glass-forming ability from molecular structure alone: A screening tool in early drug development. *Mol. Pharm.* **8**, 498–506 (2011).

73. Mahlin, D. & Bergström, C. A. S. S. Early drug development predictions of glass-forming ability and physical stability of drugs. *Eur. J. Pharm. Sci.* **49**, 323–332 (2013).
74. Patil, H., Tiwari, R. V. & Repka, M. A. Hot-Melt Extrusion: from Theory to Application in Pharmaceutical Formulation. *AAPS PharmSciTech* **17**, 20–42 (2016).
75. Mendonsa, N. *et al.* Manufacturing strategies to develop amorphous solid dispersions: An overview. *J. Drug Deliv. Sci. Technol.* **55**, 101459 (2020).
76. De Brabander, C., Van Den Mooter, G., Vervaet, C. & Remon, J. P. Characterization of ibuprofen as a nontraditional plasticizer of ethyl cellulose. *J. Pharm. Sci.* **91**, 1678–1685 (2002).
77. Repka, M. A., Majumdar, S., Battu, S. K., Srirangam, R. & Upadhye, S. B. Applications of hot-melt extrusion for drug delivery. *Expert Opin. Drug Deliv.* **5**, 1357–1376 (2008).
78. Kelleher, J. F. *et al.* A comparative study between hot-melt extrusion and spray-drying for the manufacture of anti-hypertension compatible monolithic fixed-dose combination products. *Int. J. Pharm.* **545**, 183–196 (2018).
79. Dedroog, S., Huygens, C. & Van den Mooter, G. Chemically identical but physically different: A comparison of spray drying, hot melt extrusion and cryo-milling for the formulation of high drug loaded amorphous solid dispersions of naproxen. *Eur. J. Pharm. Biopharm.* **135**, 1–12 (2019).
80. Abreu-Villela, R., Schönenberger, M., Caraballo, I. & Kuentz, M. Early stages of drug crystallization from amorphous solid dispersion via fractal analysis based on chemical imaging. *Eur. J. Pharm. Biopharm.* **133**, 122–130 (2018).
81. Qian, F. *et al.* Is a distinctive single Tg a reliable indicator for the homogeneity of amorphous solid dispersion? *Int. J. Pharm.* **395**, 232–235 (2010).
82. Niederquell, A., Wyttenbach, N., Kuentz, M. & Panayiotou, C. Partial solvation parameters of drugs as a new thermodynamic tool for pharmaceutics. *Pharmaceutics* **11**, 1–17 (2019).
83. Kennedy, J. W. *Principles of Polymer Chemistry*. *Journal of the American Chemical Society* vol. 76 (Cornell University Press, 1954).
84. Jankovic, S. *et al.* Application of the solubility parameter concept to assist with oral delivery of poorly water-soluble drugs – a PEARRL review. *J. Pharm. Pharmacol.* **71**, 441–463 (2019).
85. Hansen, C. M. *The Three Dimensional Solubility Parameter and Solvent Diffusion Coefficient. Their Importance in Surface Coating Formulation*. (Danish Technical Press, 1967).
86. Kalam, M. A. *et al.* Solubility Measurement and Various Solubility Parameters of Glipizide in Different Neat Solvents. *ACS Omega* **5**, 1708–1716 (2020).
87. He, H. *et al.* Thermodynamic modelling and Hansen solubility parameter of N-hydroxy-5-norbornene-2,3-dicarboximide in twelve pure solvents at various temperatures. *J. Mol. Liq.* **300**, (2020).
88. Venkatram, S., Kim, C., Chandrasekaran, A. & Ramprasad, R. Critical Assessment of the Hildebrand and Hansen Solubility Parameters for Polymers. *J. Chem. Inf. Model.* **59**, 4188–4194 (2019).
89. Greenhalgh, D. J., Williams, A. C., Timmins, P. & York, P. Solubility parameters as predictors of miscibility in solid dispersions. *J. Pharm. Sci.* **88**, 1182–1190 (1999).
90. Marsac, P. J., Shamblin, S. L. & Taylor, L. S. Theoretical and Practical Approaches for Prediction of Drug–Polymer Miscibility and Solubility. *Pharm. Res.* **23**, 2417–2426 (2006).
91. Guan, J. *et al.* Synergetic effect of nucleation and crystal growth inhibitor on in vitro-in vivo performance of supersaturable lacidipine solid dispersion. *Int. J. Pharm.* **566**,

594–603 (2019).
92. Salem, A., Nagy, S., Pál, S. & Széchenyi, A. Reliability of the Hansen solubility parameters as co-crystal formation prediction tool. *Int. J. Pharm.* **558**, 319–327 (2019).
93. Turpin, E. R. *et al.* In Silico Screening for Solid Dispersions: The Trouble with Solubility Parameters and FH. *Mol. Pharm.* **15**, 4654–4667 (2018).
94. Niederquell, A., Wyttenbach N., Kuentz, M., Niederquell, A., Wyttenbach, N. & Kuentz, M. New prediction methods for solubility parameters based on molecular sigma profiles using pharmaceutical materials. *Int. J. Pharm.* **546**, 137–144 (2018).
95. Han, R. *et al.* Predicting physical stability of solid dispersions by machine learning techniques. *J. Control. Release* **311**–**312**, 16–25 (2019).
96. Gupta, P., Chawla, G. & Bansal, A. K. Physical Stability and Solubility Advantage from Amorphous Celecoxib: The Role of Thermodynamic Quantities and Molecular Mobility. *Mol. Pharm.* **1**, 406–413 (2004).
97. Price, D. J. *et al.* Approaches to increase mechanistic understanding and aid in the selection of precipitation inhibitors for supersaturating formulations – a PEARRL review. *J. Pharm. Pharmacol.* **71**, 483–509 (2019).
98. Frank, D. S. & Matzger, A. J. Effect of Polymer Hydrophobicity on the Stability of Amorphous Solid Dispersions and Supersaturated Solutions of a Hydrophobic Pharmaceutical. *Mol. Pharm.* **16**, 682–688 (2019).
99. Frank, K. J. *et al.* What is the mechanism behind increased permeation rate of a poorly soluble drug from aqueous dispersions of an amorphous solid dispersion? *J. Pharm. Sci.* **103**, 1779–1786 (2014).
100. Frank, K. J. *et al.* Amorphous solid dispersion enhances permeation of poorly soluble ABT-102: True supersaturation vs. apparent solubility enhancement. *Int. J. Pharm.* **437**, 288–293 (2012).
101. Harmon, P., Galipeau, K., Xu, W., Brown, C. & Wuelfing, W. P. Mechanism of Dissolution-Induced Nanoparticle Formation from a Copovidone-Based Amorphous Solid Dispersion. *Mol. Pharm.* **13**, 1467–1481 (2016).
102. Alhalaweh, A., Alzghoul, A. & Kaialy, W. Data mining of solubility parameters for computational prediction of drug–excipient miscibility. *Drug Dev. Ind. Pharm.* **40**, 904–909 (2014).
103. Kanzer, J. *et al.* In situ formation of nanoparticles upon dispersion of melt extrudate formulations in aqueous medium assessed by asymmetrical flow field-flow fractionation. *J. Pharm. Biomed. Anal.* **53**, 359–365 (2010).
104. Trasi, N. S. & Taylor, L. S. Thermodynamics of Highly Supersaturated Aqueous Solutions of Poorly Water-Soluble Drugs - Impact of a Second Drug on the Solution Phase Behavior and Implications for Combination Products. *J. Pharm. Sci.* **104**, 2583–2593 (2015).
105. Sun, D. D., Wen, H. & Taylor, L. S. Non-Sink Dissolution Conditions for Predicting Product Quality and In Vivo Performance of Supersaturating Drug Delivery Systems. *J. Pharm. Sci.* **105**, 2477–2488 (2016).
106. Hate, S. S., Reutzel-Edens, S. M. & Taylor, L. S. Insight into Amorphous Solid Dispersion Performance by Coupled Dissolution and Membrane Mass Transfer Measurements. *Mol. Pharm.* **16**, 448–461 (2019).
107. Saboo, S., Mugheirbi, N. A., Zemlyanov, D. Y., Kestur, U. S. & Taylor, L. S. Congruent release of drug and polymer: A "sweet spot" in the dissolution of amorphous solid dispersions. *J. Control. Release* **298**, 68–82 (2019).
108. Ma, X. & Williams, R. O. Characterization of amorphous solid dispersions: An update. *J. Drug Deliv. Sci. Technol.* **50**, 113–124 (2019).
109. Baghel, S., Cathcart, H. & O'Reilly, N. J. Polymeric Amorphous Solid Dispersions: A

Review of Amorphization, Crystallization, Stabilization, Solid-State Characterization, and Aqueous Solubilization of Biopharmaceutical Classification System Class II Drugs. *J. Pharm. Sci.* **105**, 2527–2544 (2016).
110. Medarević, D., Djuriš, J., Barmpalexis, P., Kachrimanis, K. & Ibrić, S. Analytical and computational methods for the estimation of drug-polymer solubility and miscibility in solid dispersions development. *Pharmaceutics* **11**, 1–33 (2019).
111. Ibrahim, M., Zhang, J., Repka, M. & Chen, R. Characterization of the Solid Physical State of API and Its Distribution in Pharmaceutical Hot Melt Extrudates Using Terahertz Raman Imaging. *AAPS PharmSciTech* **20**, 1–8 (2019).
112. Yang, F. *et al.* Rheology Guided Rational Selection of Processing Temperature to Prepare Copovidone-Nifedipine Amorphous Solid Dispersions via Hot Melt Extrusion (HME). *Mol. Pharm.* **13**, 3494–3505 (2016).
113. Ito, A. *et al.* Prediction of recrystallization behavior of troglitazone/polyvinylpyrrolidone solid dispersion by solid-state NMR. *Int. J. Pharm.* **383**, 18–23 (2010).
114. Yang, F. *et al.* Rheological and solid-state NMR assessments of copovidone/clotrimazole model solid dispersions. *Int. J. Pharm.* **500**, 20–31 (2016).
115. Purohit, H. S. *et al.* Insights into Nano- and Micron-Scale Phase Separation in Amorphous Solid Dispersions Using Fluorescence-Based Techniques in Combination with Solid State Nuclear Magnetic Resonance Spectroscopy. *Pharm. Res.* **34**, 1364–1377 (2017).
116. Saboo, S. & Taylor, L. S. Water-induced phase separation of miconazole-poly (vinylpyrrolidone-co-vinyl acetate) amorphous solid dispersions: Insights with confocal fluorescence microscopy. *Int. J. Pharm.* **529**, 654–666 (2017).
117. Wilson, V. *et al.* Relationship between amorphous solid dispersion In Vivo absorption and In Vitro dissolution: phase behavior during dissolution, speciation, and membrane mass transport. *J. Control. Release* **292**, 172–182 (2018).
118. Reufer, M. *et al.* Introducing diffusing wave spectroscopy as a process analytical tool for pharmaceutical emulsion manufacturing. *J. Pharm. Sci.* **103**, 3902–3913 (2014).
119. Lauer, M. E. *et al.* Atomic force microscopy-based screening of drug-excipient miscibility and stability of solid dispersions. *Pharm. Res.* **28**, 572–584 (2011).
120. Szente, V., Süvegh, K., Marek, T. & Zelkó, R. Prediction of the stability of polymeric matrix tablets containing famotidine from the positron annihilation lifetime distributions of their physical mixtures. *J. Pharm. Biomed. Anal.* **49**, 711–714 (2009).
121. Lakowicz, J. R. *Principles of Fluorescence Spectroscopy Principles of Fluorescence Spectroscopy*. *Principles of fluorescence spectroscopy, Springer, New York, USA, 3rd edn, 2006.* (Springer New York, 2006). doi:10.1007/978-0-387-46312-4.
122. Purohit, H. S. & Taylor, L. S. Phase separation kinetics in amorphous solid dispersions upon exposure to water. *Mol. Pharm.* **12**, 1623–1635 (2015).
123. Purohit, H. S. & Taylor, L. S. Miscibility of Itraconazole-Hydroxypropyl Methylcellulose Blends: Insights with High Resolution Analytical Methodologies. *Mol. Pharm.* **12**, 4542–4553 (2015).
124. Tian, B., Tang, X. & Taylor, L. S. Investigating the Correlation between Miscibility and Physical Stability of Amorphous Solid Dispersions Using Fluorescence-Based Techniques. *Mol. Pharm.* **13**, 3988–4000 (2016).
125. Tres, F., Hall, S. D., Mohutsky, M. A. & Taylor, L. S. *Monitoring the Phase Behavior of Supersaturated Solutions of Poorly Water-Soluble Drugs Using Fluorescence Techniques*. *Journal of Pharmaceutical Sciences* vol. 107 94–102 (Elsevier).
126. Ricarte, R. G. *et al.* Recent Advances in Understanding the Micro- and Nanoscale Phenomena of Amorphous Solid Dispersions. *Mol. Pharm.* **16**, 4089–4103 (2019).

127. Purohit, H. S. & Taylor, L. S. Phase Behavior of Ritonavir Amorphous Solid Dispersions during Hydration and Dissolution. *Pharm. Res.* **34**, 2842–2861 (2017).
128. Sivadasan, K. & Somasundaran, P. Polymer-surfactant interactions and the association behavior of hydrophobically modified hydroxyethylcellulose. *Colloids and Surfaces* **49**, 229–239 (1990).
129. Furst, E. M. & Squires, T. M. *Microrheology*. (OUP Oxford, 2017).
130. Pine, D. J., Weitz, D. A., Chaikin, P. M. & Herbolzheimer, E. Diffusing wave spectroscopy. *Phys. Rev. Lett.* **60**, 1134–1137 (1988).
131. Pine, D. J., Weitz, D. A., Zhu, J. X. & Herbolzheimer, E. Diffusing-wave spectroscopy: dynamic light scattering in the multiple scattering limit. *J. Phys.* **51**, 2101–2127 (1990).
132. Mason, T. G. & Weitz, D. A. Optical Measurements of Frequency-Dependent Linear Viscoelastic Moduli of Complex Fluids. *Phys. Rev. Lett.* **74**, 1250–1253 (1995).
133. Maret, G. Diffusing-wave spectroscopy. *Curr. Opin. Colloid Interface Sci.* **2**, 251–257.
134. Fluctuations, D. *et al.* Diffusing-wave spectroscopy : The technique and some applications Diffusing-Wave Spectroscopy : The Technique and Some Applications. (1993).
135. Dasgupta, B. R., Tee, S.-Y., Crocker, J. C., Frisken, B. J. & Weitz, D. A. Microrheology of polyethylene oxide using diffusing wave spectroscopy and single scattering. *Phys. Rev. E* **65**, 051505 (2002).
136. Constantin, D., Knaebel, A., Bellour, M., Padding, J. T. & Boek, E. S. Microrheology of giant-micelle solutions. (2002).
137. Narita, T. & Indei, T. Microrheological study of physical gelation in living polymeric networks. *Macromolecules* **49**, 4634–4646 (2016).
138. Veerman, C. *et al.* Gelation kinetics of β-hairpin peptide hydrogel networks. *Macromolecules* **39**, 6608–6614 (2006).
139. Schultz, K. M., Baldwin, A. D., Kiick, K. L. & Furst, E. M. Gelation of covalently cross-linked PEG-heparin hydrogels. *Macromolecules* **42**, 5310–5315 (2009).
140. Palmer, A., Xu, J. & Wirtz, D. High-frequency viscoelasticity of crosslinked actin filament networks measured by diffusing wave spectroscopy. *Rheol. Acta* **37**, 97–106 (1998).
141. Xu, J., Viasnoff, V. & Wirtz, D. Compliance of actin filament networks measured by particle-tracking microrheology and diffusing wave spectroscopy. *Rheol. Acta* **37**, 387–398 (1998).
142. Palmer, A., Mason, T. G., Xu, J., Kuo, S. C. & Wirtz, D. Diffusing wave spectroscopy microrheology of actin filament networks. *Biophys. J.* **76**, 1063–1071 (1999).
143. Rigato, A., Miyagi, A., Scheuring, S. & Rico, F. High-frequency microrheology reveals cytoskeleton dynamics in living cells. *Nat. Phys.* **13**, 771–775 (2017).
144. Moschakis, T., Murray, B. S. & Biliaderis, C. G. Modifications in stability and structure of whey protein-coated o/w emulsions by interacting chitosan and gum arabic mixed dispersions. *Food Hydrocoll.* **24**, 8–17 (2010).
145. Moschakis, T., Murray, B. S. & Dickinson, E. Particle tracking using confocal microscopy to probe the microrheology in a phase-separating emulsion containing nonadsorbing polysaccharide. *Langmuir* **22**, 4710–4719 (2006).
146. Blijdenstein, T. B. J., Hendriks, W. P. G., Van der Linden, E., Van Vliet, T. & Van Aken, G. A. Control of strength and stability of emulsion gels by a combination of long- and short-range interactions. *Langmuir* **19**, 6657–6663 (2003).
147. Blijdenstein, T. B. J., Veerman, C. & Van Der Linden, E. Depletion - Flocculation in oil-in-water emulsions using fibrillar protein assemblies. *Langmuir* **20**, 4881–4884 (2004).
148. Xu, D., Aihemaiti, Z., Cao, Y., Teng, C. & Li, X. Physicochemical stability,

microrheological properties and microstructure of lutein emulsions stabilized by multilayer membranes consisting of whey protein isolate, flaxseed gum and chitosan. *Food Chem.* **202**, 156–164 (2016).
149. Xu, D., Zhang, J., Cao, Y., Wang, J. & Xiao, J. Influence of microcrystalline cellulose on the microrheological property and freeze-thaw stability of soybean protein hydrolysate stabilized curcumin emulsion. *LWT - Food Sci. Technol.* **66**, 590–597 (2016).
150. Eliot, C., Horne, D. S. & Dickinson, E. Understanding temperature-sensitive caseinate emulsions: New information from diffusing wave spectroscopy. *Food Hydrocoll.* **19**, 279–287 (2005).
151. Liu, J., Verespej, E., Alexander, M. & Corredig, M. Comparison on the effect of high-methoxyl pectin or soybean-soluble polysaccharide on the stability of sodium casemate-stabilized oil/water emulsions. *J. Agric. Food Chem.* **55**, 6270–6278 (2007).
152. Kim, H. S., Şenbil, N., Zhang, C., Scheffold, F. & Mason, T. G. Diffusing wave microrheology of highly scattering concentrated monodisperse emulsions. *Proc. Natl. Acad. Sci. U. S. A.* **116**, 7766–7771 (2019).
153. Niederquell, A., Völker, A. C. & Kuentz, M. Introduction of diffusing wave spectroscopy to study self-emulsifying drug delivery systems with respect to liquid filling of capsules. *Int. J. Pharm.* **426**, 144–152 (2012).
154. Hörter, D. & Dressman, J. B. Influence of physicochemical properties on dissolution of drugs in the gastrointestinal tract. *Adv. Drug Deliv. Rev.* **25**, 3–14 (1997).
155. Zaheer, K. & Langguth, P. Formulation strategy towards minimizing viscosity mediated negative food effect on disintegration and dissolution of immediate release tablets. *Drug Dev. Ind. Pharm.* **44**, 444–451 (2018).
156. Silchenko, S. *et al.* In vitro dissolution absorption system (IDAS2): Use for the prediction of food viscosity effects on drug dissolution and absorption from oral solid dosage forms. *Eur. J. Pharm. Sci.* **143**, 105164 (2020).
157. D'Arcy, D. M. & Persoons, T. Understanding the Potential for Dissolution Simulation to Explore the Effects of Medium Viscosity on Particulate Dissolution. *AAPS PharmSciTech* **20**, 1–13 (2019).
158. Van Renterghem, J., Vervaet, C. & De Beer, T. Rheological Characterization of Molten Polymer-Drug Dispersions as a Predictive Tool for Pharmaceutical Hot-Melt Extrusion Processability. *Pharm. Res.* **34**, 2312–2321 (2017).
159. Sarabu, S. *et al.* Hypromellose acetate succinate based amorphous solid dispersions via hot melt extrusion: Effect of drug physicochemical properties. *Carbohydr. Polym.* **233**, 115828 (2020).
160. Hansen, C. M. *Hansen solubility parameter a user's handbook*. (CRC Press, 2007).
161. Hancock, B., York, P. & Rowe, R. The use of solubility parameters in pharmaceutical dosage form design. *Int. J. Pharm.* **148**, 1–21 (1997).
162. Kuentz, M., Holm, R. & Elder, D. P. Methodology of oral formulation selection in the pharmaceutical industry. *Eur. J. Pharm. Sci.* **87**, 136–163 (2016).
163. Hildebrand, J. H. & Scott, R. L. *Solubility of nonelectrolytes*. (Dover, 1964).
164. Stefanis, E. & Panayiotou, C. Prediction of Hansen Solubility Parameters with a New Group-Contribution Method. *Int. J. Thermophys.* **29**, 568–585 (2008).
165. Just, S., Sievert, F., Thommes, M. & Breitkreutz, J. J. Improved group contribution parameter set for the application of solubility parameters to melt extrusion. *Eur. J. Pharm. Biopharm.* **85**, 1191–1199 (2013).
166. Díaz, I., Díez, E., Camacho, J., León, S. & Ovejero, G. Comparison between three predictive methods for the calculation of polymer solubility parameters. *Fluid Phase Equilib.* **337**, 6–10 (2013).

167. Panayiotou, C., Mastrogeorgopoulos, S., Aslanidou, D., Avgidou, M. & Hatzimanikatis, V. Redefining solubility parameters: Bulk and surface properties from unified molecular descriptors. *J. Chem. Thermodyn.* **111**, 207–220 (2017).
168. Louwerse, M. J. *et al.* Revisiting Hansen Solubility Parameters by Including Thermodynamics. *ChemPhysChem* **18**, 2999–3006 (2017).
169. Bustamante, P., Peña, M. A. & Barra, J. The modified extended Hansen method to determine partial solubility parameters of drugs containing a single hydrogen bonding group and their sodium derivatives: benzoic acid/Na and ibuprofen/Na. *Int. J. Pharm.* **194**, 117–124 (2000).
170. Bashimam, M. Hansen solubility parameters : A quick review in pharmaceutical aspect. *J. Chem. Pharm. Res.* **7**, 597–599 (2015).
171. Scatchard, G. Equilibria in Non-electrolyte Solutions in Relation to the Vapor Pressures and Densities of the Components. *Chem. Rev.* **8**, 321–333 (1931).
172. Hildebrand, J. H. & Wood, S. E. The Derivation of Equations for Regular Solutions. *J. Chem. Phys.* **1**, 817 (1933).
173. Biroa, J., Zeman, L. & Patterson, D. Prediction of the x Parameter by the Solubility Parameter and Corresponding States Theories. *Macromolecules* **4**, 30–35 (1971).
174. Barton, A. *Handbook of solubility parameters and other cohesion parameters*. (CRC Press, 1991).
175. Brown, H. C. & Grayson, M. Homomorphs of 2,6-Dimethyl-t-butylbenzene [1,2]. *J. Am. Chem. Soc.* **75**, 20–24 (1953).
176. Brown, H. C. *et al.* Strained Homomorphs. [1] 14. General Summary. *J. Am. Chem. Soc.* **75**, 1–6 (1953).
177. Blanks, R. F. & Prausnitz, J. M. Thermodynamics of Polymer Solubility in Polar and Nonpolar Systems. *Ind. Eng. Chem. Fundam.* **3**, 1–8 (1964).
178. Hansen, C.M., Skaarup, K. Independent calculation of the parameter components. *J. Paint. Technol.* **37**, 511–515 (1967).
179. Hansen, C.M., Beerbower, C. H. *Solubility parameters*. *Kirk-Othmer Encyclopedia of Chemical Technology* (1971).
180. Hansen, C. M. 50 Years with solubility parameters—past and future. *Prog. Org. Coatings* **51**, 77–84 (2004).
181. Small, P. A. Some factors affecting the solubility of polymers. *J. Appl. Chem.* **3**, 71–80 (2007).
182. Sorenson, P. Application of the acid/base concept describing the interaction between pigments, binders, and solvents. *J. Paint Technol.* **47**, 31 (1975).
183. Beerbower, A., Wu, P. L. & Martin, A. Expanded Solubility Parameter Approach I: Naphthalene and Benzoic Acid in Individual Solvents. *J. Pharm. Sci.* **73**, 179–188 (1984).
184. Barra, J., Peña, M.-A. & Bustamante, P. Proposition of group molar constants for sodium to calculate the partial solubility parameters of sodium salts using the van Krevelen group contribution method. *Eur. J. Pharm. Sci.* **10**, 153–161 (2000).
185. Verheyen, S., Augustijns, P., Kinget, R. & Van den Mooter, G. Determination of partial solubility parameters of five benzodiazepines in individual solvents. *Int. J. Pharm.* **228**, 199–207 (2001).
186. Bustamante, P., Escalera, B., Martin, A. & Selles, E. A Modification of the Extended Hildebrand Approach to Predict the Solubility of Structurally Related Drugs in Solvent Mixtures. *J. Pharm. Pharmacol.* **45**, 253–257 (1993).
187. Jouyban, A. & Acree, W. E. Comments on "Prediction of Drug Solubility in Lipid Mixtures from the Individual Ingredients". *AAPS PharmSciTech* **15**, 83–85 (2014).
188. Vay, K., Scheler, S. & Frieß, W. Application of Hansen solubility parameters for

understanding and prediction of drug distribution in microspheres. *Int. J. Pharm.* **416**, 202–209 (2011).
189. Muela, S., Escalera, B., Peña, M. Á. & Bustamante, P. Influence of temperature on the solubilization of thiabendazole by combined action of solid dispersions and co-solvents. *Int. J. Pharm.* **384**, 93–99 (2010).
190. Kitak, T. *et al.* Determination of solubility parameters of ibuprofen and ibuprofen lysinate. *Molecules* **20**, 21549–21568 (2015).
191. Howell, J., Roesing, M. & Boucher, D. A Functional Approach to Solubility Parameter Computations. *J. Phys. Chem. B* **121**, 4191–4201 (2017).
192. Archer, W. L. Determination of Hansen solubility parameters for selected cellulose ether derivatives. *Ind. Eng. Chem. Res.* **30**, 2292–2298 (1991).
193. Janssen. *Development of a semi-automated system for the determination of the Hansen solubility parameters of pharmaceutical excipients*. *Unpublished Data* (2015).
194. Abbott, S., Hansen, C., & Yamamoto, H. (2017). Hansen Solubility Parameters in Practice, HSPiP, a package of software, datasets and eBook. (2017).
195. Klar, F. & Urbanetz, N. A. Solubility parameters of hypromellose acetate succinate and plasticization in dry coating procedures. *Drug Dev. Ind. Pharm.* **42**, 1621–1635 (2016).
196. Bustamante, P., Peña, M. A. & Barra, J. Partial solubility parameters of piroxicam and niflumic acid. *Int. J. Pharm.* **174**, 141–150 (1998).
197. Martin, A., Wu, P. L., Adjei, A., Beerbower, A. & Prausnitz, J. M. Extended Hansen Solubility Approach: Naphthalene in Individual Solvents. *J. Pharm. Sci.* **70**, 1260–1264 (1981).
198. Van Dyk, J. W., Frisch, H. L. & Wu, D. T. Solubility, solvency, and solubility parameters. *Ind. Eng. Chem. Prod. Res. Dev.* **24**, 473–478 (1985).
199. Segarceanu, O. & Leca, M. Improved method to calculate Hansen solubility parameters of a polymer. *Prog. Org. Coatings* **31**, 307–310 (1997).
200. Kent, D. J. & Rowe, R. C. Solubility studies on ethyl cellulose used in film coating. *J. Pharm. Pharmacol.* **30**, 808–810 (1978).
201. Han, K. H., Jeon, G. S., Hong, I. K. & Lee, S. B. Prediction of solubility parameter from intrinsic viscosity. *J. Ind. Eng. Chem.* **19**, 1130–1136 (2013).
202. Bustamante, P., Navarro-Lupión, J. & Escalera, B. A new method to determine the partial solubility parameters of polymers from intrinsic viscosity. *Eur. J. Pharm. Sci.* **24**, 229–237 (2005).
203. Madsen, C. G. *et al.* Simple measurements for prediction of drug release from polymer matrices – Solubility parameters and intrinsic viscosity. *Eur. J. Pharm. Biopharm.* **92**, 1–7 (2015).
204. Weerachanchai, P., Wong, Y., Lim, K. H., Tan, T. T. Y. & Lee, J.-M. Determination of Solubility Parameters of Ionic Liquids and Ionic Liquid/Solvent Mixtures from Intrinsic Viscosity. *ChemPhysChem* **15**, 3580–3591 (2014).
205. Mieczkowski, R. The determination of the solubility parameter components of polystyrene by partial specific volume measurements. *Eur. Polym. J.* **24**, 1185–1189 (1988).
206. Ravindra, R., Krovvidi, K. R. & Khan, A. A. Solubility parameter of chitin and chitosan. *Carbohydr. Polym.* **36**, 121–127 (1998).
207. Mieczkowski, R. The determination of the solubility parameter components of polystyrene. *Eur. Polym. J.* **25**, 1055–1057 (1989).
208. Mieczkowski, R. Solubility parameter components of some polyols. *Eur. Polym. J.* **27**, 377–379 (1991).
209. Huang, J.-C. Methods to determine solubility parameters of polymers at high temperature using inverse gas chromatography. *J. Appl. Polym. Sci.* **94**, 1547–1555

(2004).
210. DiPaola-Baranyi, G. & Guillet, J. E. Estimation of Polymer Solubility Parameters by Gas Chromatography. *Macromolecules* **11**, 228–235 (1978).
211. Ito, K. & Guillet, J. E. Estimation of Solubility Parameters for Some Olefin Polymers and Copolymers by Inverse Gas Chromatography. *Macromolecules* **12**, 1163–1167 (1979).
212. Adamska, K. & Voelkel, A. Hansen solubility parameters for polyethylene glycols by inverse gas chromatography. *J. Chromatogr. A* **1132**, 260–267 (2006).
213. Choi, P., Kavassalis, T. & Rudin, A. Measurement of Three-Dimensional Solubility Parameters of Nonyl Phenol Ethoxylates Using Inverse Gas Chromatography. *J. Colloid Interface Sci.* **180**, 1–8 (1996).
214. Adamska, K. & Voelkel, A. Inverse gas chromatographic determination of solubility parameters of excipients. *Int. J. Pharm.* **304**, 11–17 (2005).
215. Wang, Q., Chen, Y., Tang, J. & Zhang, Z. Determination of the Solubility Parameter of Epoxidized Soybean Oil by Inverse Gas Chromatography. *J. Macromol. Sci. Part B* **52**, 1405–1413 (2013).
216. Adamska, K., Bellinghausen, R. & Voelkel, A. New procedure for the determination of Hansen solubility parameters by means of inverse gas chromatography. *J. Chromatogr. A* **1195**, 146–149 (2008).
217. Price, G. J. & Shillcock, I. M. Inverse gas chromatographic measurement of solubility parameters in liquid crystalline systems. *J. Chromatogr. A* **964**, 199–204 (2002).
218. Cakar, F., Yazici, O., Bilgin-Eran, B., Cankurtaran, O. & Karaman, F. Physicochemical characterization of 5-Decyloxy-2-[[[4-Hexyloxyphenyl] Imino] Methyl] Phenol liquid crystal by inverse gas chromatography. *Optoelectron. Adv. Mater. Commun.* **2**, 871–875 (2008).
219. Liu, G. *et al.* Crystallization of Piroxicam Solid Forms and the Effects of Additives. *Chem. Eng. Technol.* **37**, 1297–1304 (2014).
220. Langer, S. H., Sheehan, R. J. & Huang, J. C. Gas-chromatographic study of the solution thermodynamics of hydroxylic derivatives and related compounds. *J. Phys. Chem.* **86**, 4605–4618 (1982).
221. Coca, J., Rodriguez, J. L., Medina, I. & Langer, S. H. Thermodynamic properties of some organic compounds with tetrachloroterephthaloyl oligomers by gas chromatography. *J. Chem. Eng. Data* **34**, 280–284 (1989).
222. Voelkel, A., Milczewska, K. & Jęczalik, J. Characterization of the interactions in polymer/silica systems by inverse gas chromatography. *Macromol. Symp.* **169**, 45–55 (2001).
223. Voelkel, A. & Fall, J. Influence of prediction method of the second virial coefficient on inverse gas chromatographic parameters. *J. Chromatogr. A* **721**, 139–145 (1996).
224. Price, G. J., Guillet, J. E. & Purnell, J. H. Measurement of solubility parameters by gas-liquid chromatrography. *J. Chromatogr. A* **369**, 273–280 (1986).
225. Voelkel, A. & Grześkowiak, T. Properties of zirconate modificates of silica gel as examined by inverse gas chromatography. *Macromol. Symp.* **169**, 35–44 (2001).
226. Voelkel, A. & Janas, J. Solubility parameters of broad and narrow distributed oxyethylates of fatty alcohols. *J. Chromatogr. A* **645**, 141–151 (1993).
227. Panayiotou, C. G. Inverse gas chromatography and partial solvation parameters. *J. Chromatogr. A* **1251**, 194–207 (2012).
228. Çavus, S., Çakal, E. & Sevgili, L. M. Solvent dependent swelling behaviour of poly(N-vinylcaprolactam) and poly(N-vinylcaprolactam-co-itaconic acid) gels and determination of solubility parameters. *Chem. Pap.* **69**, 1367–1377 (2015).
229. Bristow, G. M. & Watson, W. F. Cohesive energy densities of polymers: Part 1. -

Cohesive energy densities of rubbers by swelling measurements. *Trans. Faraday Soc.* **54**, 1731–1741 (1958).
230. Bristow, G. M. & Watson, W. F. Cohesive energy densities of polymers. Part 2.—Cohesive energy densities from viscosity measurements. *Trans. Faraday Soc.* **54**, 1742–1747 (1958).
231. Aharoni, S. M. The solubility parameters of aromatic polyamides. *J. Appl. Polym. Sci.* **45**, 813–817 (1992).
232. Eroğlu, M. S., Baysal, B. M. & Güven, O. Determination of solubility parameters of poly(epichlorohydrin) and poly(glycidyl azide) networks. *Polymer (Guildf).* **38**, 1945–1947 (1997).
233. Schenderlein, S., Lück, M. & Müller, B. W. Partial solubility parameters of poly(d,l-lactide-co-glycolide). *Int. J. Pharm.* **286**, 19–26 (2004).
234. Suh, K. W. & Corbett, J. M. Solubility parameters of polymers from turbidimetric titrations. *J. Appl. Polym. Sci.* **12**, 2359–2370 (1968).
235. Suh, K. W. & Clarke, D. H. Cohesive energy densities of polymers from turbidimetric titrations. *J. Polym. Sci. Part A-1 Polym. Chem.* **5**, 1671–1681 (1967).
236. Lin, X., Jiang, G. & Wang, Y. Hansen Solubility Parameters of Coal Tar-Derived Typical PAHs Using Turbidimetric Titration and an Extended Hansen Approach. *J. Chem. Eng. Data* **62**, 954–960 (2017).
237. Carvalho, S. P., Lucas, E. F., González, G. & Spinelli, L. S. Determining Hildebrand Solubility Parameter by Ultraviolet Spectroscopy and Microcalorimetry. *J. Braz. Chem. Soc.* **24**, 1998–2007 (2013).
238. Gee, G. The interaction between rubber and liquids. II. The thermodynamical basis of the swelling and solution of rubber. *Trans. Faraday Soc.* **38**, 276–282 (1942).
239. Hoy, K. L. New values of the solubility parameters from vapor pressure data. *J. Paint Technol.* **42**, 76–118 (1970).
240. Fedors, R. F. A method for estimating both the solubility parameters and molar volumes of liquids. *Polym. Eng. Sci.* **14**, 147–154 (1974).
241. Krevelen, D. W. van (Dirk W. *et al. Properties of polymers: their correlation with chemical structure; their numerical estimation and prediction from additive group contributions*. (Elsevier, 2009).
242. Stefanis, E. & Panayiotou, C. A new expanded solubility parameter approach. *Int. J. Pharm.* **426**, 29–43 (2012).
243. Forster, A., Hempenstall, J., Tucker, I. & Rades, T. Selection of excipients for melt extrusion with two poorly water-soluble drugs by solubility parameter calculation and thermal analysis. *Int. J. Pharm.* **226**, 147–161 (2001).
244. Shah, M. & Agrawal, Y. High throughput screening: an *in silico* solubility parameter approach for lipids and solvents in SLN preparations. *Pharm. Dev. Technol.* **18**, 582–590 (2013).
245. Klamt, A. *COSMO-RS: from quantum chemistry to fluid phase thermodynamics and drug design*. (Elsevier, 2005).
246. Gupta, J., Nunes, C., Vyas, S. & Jonnalagadda, S. Prediction of Solubility Parameters and Miscibility of Pharmaceutical Compounds by Molecular Dynamics Simulations. *J. Phys. Chem. B* **115**, 2014–2023 (2011).
247. Ruether, F. & Sadowski, G. Modeling the solubility of pharmaceuticals in pure solvents and solvent mixtures for drug process design. *J. Pharm. Sci.* **98**, 4205–4215 (2009).
248. Jouyban, A., Fakhree, M. A. A. & Acree, W. E. Comment on "Measurement and Correlation of Solubilities of (*Z*)-2-(2-Aminothiazol-4-yl)-2-methoxyiminoacetic Acid in Different Pure Solvents and Binary Mixtures of Water + (Ethanol, Methanol, or

Glycol)". *J. Chem. Eng. Data* **57**, 1344–1346 (2012).
249. Rogers, M. A. & Marangoni, A. G. Kinetics of 12-Hydroxyoctadecanoic Acid SAFiN Crystallization Rationalized Using Hansen Solubility Parameters. *Langmuir* **32**, 12833–12841 (2016).
250. Zhu, Z., Snellings, G. M. B. F., Koebel, M. M. & Malfait, W. J. Superinsulating Polyisocyanate Based Aerogels: A Targeted Search for the Optimum Solvent System. *ACS Appl. Mater. Interfaces* **9**, 18222–18230 (2017).
251. Masurel, E., Authier, O., Castel, C. & Roizard, C. Screening method for solvent selection used in tar removal by the absorption process. *Environ. Technol.* **36**, 2556–2567 (2015).
252. Cascant, M. M. *et al.* A green analytical chemistry approach for lipid extraction: computation methods in the selection of green solvents as alternative to hexane. *Anal. Bioanal. Chem.* **409**, 3527–3539 (2017).
253. Laboukhi-Khorsi, S., Daoud, K. & Chemat, S. Efficient Solvent Selection Approach for High Solubility of Active Phytochemicals: Application for the Extraction of an Antimalarial Compound from Medicinal Plants. *ACS Sustain. Chem. Eng.* **5**, 4332–4339 (2017).
254. Sánchez-Camargo, A. P., Montero, L., Cifuentes, A., Herrero, M. & Ibáñez, E. Application of Hansen solubility approach for the subcritical and supercritical selective extraction of phlorotannins from Cystoseira abies-marina. *RSC Adv.* **6**, 94884–94895 (2016).
255. Fardi, T., Stefanis, E., Panayiotou, C., Abbott, S. & van Loon, S. Artwork conservation materials and Hansen solubility parameters: A novel methodology towards critical solvent selection. *J. Cult. Herit.* **15**, 583–594 (2014).
256. Pudipeddi, M. & Serajuddin, A. T. M. Trends in Solubility of Polymorphs. *J. Pharm. Sci.* **94**, 929–939 (2005).
257. Liu, R. *Water-Insoluble Drug Formulation*. *Water-Insoluble Drug Formulation* vol. 133 (Taylor & Francis Inc., 2008).
258. Bauer, J. *et al.* Ritonavir: An Extraordinary Case of Conformational Polymorphism. *Pharm. Res.* **18**, 859–866 (2001).
259. Dinnebier, R. E., Sieger, P., Nar, H., Shankland, K. & David, W. I. F. Structural characterization of three crystalline modifications of telmisartan by single crystal and high-resolution X-ray powder diffraction. *J. Pharm. Sci.* **89**, 1465–1479 (2000).
260. Cimarosti, Z. *et al.* Development of Drug Substances as Mixture of Polymorphs: Studies to Control Form 3 in Casopitant Mesylate. *Org. Process Res. Dev.* **14**, 1337–1346 (2010).
261. Stahl, P. . & Wermuth, C. G. *Handbook of pharmaceutical salts*. (Wiley-VCH, 2011).
262. S.H. Neau. Pharmaceutical salts. in *Water-insoluble drug formulation* (ed. R. Liu) (Taylor & Francis Inc., 2008).
263. Gould, P. L. Salt selection for basic drugs. *Int. J. Pharm.* **33**, 201–217 (1986).
264. Paulekuhn, G. S., Dressman, J. B. & Saal, C. Trends in Active Pharmaceutical Ingredient Salt Selection based on Analysis of the Orange Book Database. *J. Med. Chem.* **50**, 6665–6672 (2007).
265. Saal, C. & Becker, A. Pharmaceutical salts: A summary on doses of salt formers from the Orange Book. *Eur. J. Pharm. Sci.* **49**, 614–623 (2013).
266. Berge, S. M. *et al.* Pharmaceutical salts. *J. Pharm. Sci.* **66**, 1–19 (1977).
267. Haynes, D. A., Jones, W. & Motherwell, W. D. S. Occurrence of Pharmaceutically Acceptable Anions and Cations in the Cambridge Structural Database. *J. Pharm. Sci.* **94**, 2111–2120 (2005).
268. Paulekuhn, G. S., Dressman, J. B. & Saal, C. Salt screening and characterization for

poorly soluble, weak basic compounds: Case study albendazole. *Pharmazie* **68**, 555–564 (2013).
269. Nechipadappu, S. K. & R. Trivedi, D. Pharmaceutical salts of ethionamide with GRAS counter ion donors to enhance the solubility. *Eur. J. Pharm. Sci.* **96**, 578–589 (2017).
270. Fini, A., Cavallari, C., Bassini, G., Ospitali, F. & Morigi, R. Diclofenac Salts, Part 7: Are the Pharmaceutical Salts with Aliphatic Amines Stable? *J. Pharm. Sci.* **101**, 3157–3168 (2012).
271. Surov, A. O., Manin, A. N., Churakov, A. V. & Perlovich, G. L. New Solid Forms of the Antiviral Drug Arbidol: Crystal Structures, Thermodynamic Stability, and Solubility. *Mol. Pharm.* **12**, 4154–4165 (2015).
272. Elder, D. P. *et al.* The Utility of Sulfonate Salts in Drug Development. *J. Pharm. Sci.* **99**, 2948–2961 (2010).
273. Saal, C. Weber, K.-D. F. Compositions of Anions and Cations with Pharmacological Activity. (2016).
274. Balk, A. *et al.* Ionic liquid versus prodrug strategy to address formulation challenges. *Pharm. Res.* **32**, 2154–2167 (2015).
275. Frizzo, C. P. *et al.* Pharmaceutical Salts: Solids to Liquids by Using Ionic Liquid Design. in *Ionic Liquids: New Aspects for the Future* (ed. Kadokawa, J. B. T.-I. L.-N. A. for the F.) Ch. 21 (InTech, 2013). doi:10.5772/51655.
276. Kumar, V. & Malhotra, S. V. Ionic Liquids as Pharmaceutical Salts: A Historical Perspective. in *Ionic Liquid Applications: Pharmaceuticals, Therapeutics, and Biotechnology* 1–12 (2010). doi:10.1021/bk-2010-1038.ch001.
277. Hough, W. L. *et al.* The third evolution of ionic liquids: active pharmaceutical ingredients. *New J. Chem.* **31**, 1429–1436 (2007).
278. FDA. List of generally regarded as safe ingredients. http://www.fda.gov/Food/IngredientsPackagingLabeling/GRAS/.
279. Fernández Casares, A. *et al.* An evaluation of salt screening methodologies. *J. Pharm. Pharmacol.* **67**, 812–822 (2015).
280. Mohammad, M. A., Alhalaweh, A. & Velaga, S. P. Hansen solubility parameter as a tool to predict cocrystal formation. *Int. J. Pharm.* **407**, 63–71 (2011).
281. Shetea, A., Murthyb, S., Korpalea, S. Cocrystals of itraconazole with amino acids: Screening, synthesis, solid state characterization, in vitro drug release and antifungal activity. *J. Drug Deliv. Sci. Technol.* **28**, 46–55 (2015).
282. Yuriy A. Abramov. *Computational Pharmaceutical Solid State Chemistry*. (Wiley Online Library, 2016).
283. Rane, S. S. & Anderson, B. D. What determines drug solubility in lipid vehicles: Is it predictable? *Adv. Drug Deliv. Rev.* **60**, 638–656 (2008).
284. Persson, L. C., Porter, C. J. H., Charman, W. N. & Bergström, C. A. S. Computational prediction of drug solubility in lipid based formulation excipients. *Pharm. Res.* **30**, 3225–3237 (2013).
285. Patel, S. V. & Patel, S. Prediction of the solubility in lipidic solvent mixture: Investigation of the modeling approach and thermodynamic analysis of solubility. *Eur. J. Pharm. Sci.* **77**, 161–169 (2015).
286. Alskär, L. C. C., Porter, C. J. H. J. H. & Bergström, C. a S. A. S. Tools for Early Prediction of Drug Loading in Lipid-Based Formulations. *Mol. Pharm.* **13**, 251–261 (2016).
287. Dumanli, I. Mechanistic studies to elucidate the role of lipid vehicles on solubility,formulation and bioavailability of poorly soluble compounds. (University of Rhode Island, 2002).
288. Shah, N. H., Phuapradit, W., Zhang, Y.-E., Ahmed, H. & Malick, A. W. *Oral Lipid-*

Based Formulations - Enhancing the Bioavailability of Poorly Water-Soluble Drugs. (informa healthcare, 2007).
289. Vaughan, C. D. Solubility parameters for characterizing new raw materials. *Cosmet. Toilet.* **108**, 57–64 (1993).
290. Van Loon. Van Loon Chemical Innovations Brochure. *Van Loon Chemical Innovations Brochure.* http://www.in-cosmetics.com/__novadocuments/326978?v=636220595266800000.
291. Yamamoto, D. H. Hansen Solubility Parameter (HSP) and Allergens for Cosmetics. *Hansen Solubility Parameter (HSP) and Allergens for Cosmetics* https://www.pirika.com/NewHP/PirikaE/Allergens.html.
292. Vaughan, C. D. Using solubility parameters in cosmetics formulation. *J. Soc. Cosmet. Chem* **36**, 19–333 (1985).
293. De La Peña-Gil, A., Toro-Vazquez, J. F. & Rogers, M. A. Simplifying Hansen Solubility Parameters for Complex Edible Fats and Oils. *Food Biophys.* **11**, 283–291 (2016).
294. Shah, M. & Agrawal, Y. Ciprofloxacin hydrochloride-loaded glyceryl monostearate nanoparticle: factorial design of Lutrol F68 and Phospholipon 90G. *J. Microencapsul.* **29**, 331–343 (2012).
295. Li, Y., Taulier, N., Rauth, A. M. & Wu, X. Y. Screening of Lipid Carriers and Characterization of Drug-Polymer-Lipid Interactions for the Rational Design of Polymer-Lipid Hybrid Nanoparticles (PLN). *Pharm. Res.* **23**, 1877–1887 (2006).
296. Breitkreutz, J. Prediction of intestinal drug absorption properties by three-dimensional solubility parameters. (1997).
297. Abd, E. 2015. Targeted Skin Delivery of Topically Applied Drugs by Optimised Formulation Design. (The University of Queensland, 2015).
298. Hossin, B., Rizi, K. & Murdan, S. Application of Hansen Solubility Parameters to predict drug–nail interactions, which can assist the design of nail medicines. *Eur. J. Pharm. Biopharm.* **102**, 32–40 (2016).
299. Kawabata, Y., Wada, K., Nakatani, M., Yamada, S. & Onoue, S. Formulation design for poorly water-soluble drugs based on biopharmaceutics classification system: Basic approaches and practical applications. *Int. J. Pharm.* **420**, 1–10 (2011).
300. Einfalt, T., Planinšek, O. & Hrovat, K. Methods of amorphization and investigation of the amorphous state. *Acta Pharm.* **63**, 305–334 (2013).
301. Chiou, W. L. & Riegelman, S. Pharmaceutical applications of solid dispersion systems. *J. Pharm. Sci.* **60**, 1281–1302 (1971).
302. Zhang, J. & Ma, P. X. Cyclodextrin-based supramolecular systems for drug delivery: Recent progress and future perspective. *Adv. Drug Deliv. Rev.* **65**, 1215–1233 (2013).
303. Hoppu, P., Jouppila, K., Rantanen, J., Schantz, S. & Juppo, A. M. Characterisation of blends of paracetamol and citric acid. *J. Pharm. Pharmacol.* **59**, 373–381 (2007).
304. Simovic, S., Ghouchi-Eskandar, N., Moom Sinn, A., Losic, D. & A. Prestidge, C. Silica Materials in Drug Delivery Applications. *Curr. Drug Discov. Technol.* **8**, 250–268 (2011).
305. Xu, W., Riikonen, J. & Lehto, V.-P. Mesoporous systems for poorly soluble drugs. *Int. J. Pharm.* **453**, 181–197 (2013).
306. Huang, Y. & Dai, W.-G. Fundamental aspects of solid dispersion technology for poorly soluble drugs. *Acta Pharm. Sin. B* **4**, 18–25 (2014).
307. Karavas, E., Georgarakis, E., Sigalas, M. P., Avgoustakis, K. & Bikiaris, D. Investigation of the release mechanism of a sparingly water-soluble drug from solid dispersions in hydrophilic carriers based on physical state of drug, particle size distribution and drug–polymer interactions. *Eur. J. Pharm. Biopharm.* **66**, 334–347

(2007).
308. Sekiguchi, K. & Obi, N. Studies on Absorption of Eutectic Mixture. I. A Comparison of the Behavior of Eutectic Mixture of Sulfathiazole and that of Ordinary Sulfathiazole in Man. *Chem. Pharm. Bull.* **9**, 866–872 (1961).
309. Thakral, S. & Thakral, N. K. Prediction of Drug–Polymer Miscibility through the use of Solubility Parameter based Flory–Huggins Interaction Parameter and the Experimental Validation: PEG as Model Polymer. *J. Pharm. Sci.* **102**, 2254–2263 (2013).
310. DeBoyace, K. & Wildfong, P. L. D. The Application of Modeling and Prediction to the Formation and Stability of Amorphous Solid Dispersions. *J. Pharm. Sci.* **107**, 57–74 (2017).
311. Djuris, J., Nikolakakis, I., Ibric, S., Djuric, Z. & Kachrimanis, K. Preparation of carbamazepine–Soluplus® solid dispersions by hot-melt extrusion, and prediction of drug–polymer miscibility by thermodynamic model fitting. *Eur. J. Pharm. Biopharm.* **84**, 228–237 (2013).
312. Sarode, A. L., Sandhu, H., Shah, N., Malick, W. & Zia, H. Hot melt extrusion (HME) for amorphous solid dispersions: Predictive tools for processing and impact of drug–polymer interactions on supersaturation. *Eur. J. Pharm. Sci.* **48**, 371–384 (2013).
313. Meng, F., Trivino, A., Prasad, D. & Chauhan, H. Investigation and correlation of drug polymer miscibility and molecular interactions by various approaches for the preparation of amorphous solid dispersions. *Eur. J. Pharm. Sci.* **71**, 12–24 (2015).
314. Bagley, E. B., Nelson, T. P. & Scigliano, J. M. Three-dimensional solubility parameters and their relationship to internal pressure measurements in polar and hydrogen bonding solvents. *J. Paint Technol.* **43**, 35–42 (1971).
315. Meaurio, E. *et al.* Predicting miscibility in polymer blends using the Bagley plot: Blends with poly(ethylene oxide). *Polymer (Guildf).* **113**, 295–309 (2017).
316. Arrighi, V., Cabral, J., & Cowie, J. M. Miscibility. in *Encyclopedia of Polymer Science and Technology* (John Wiley & Sons, Inc., 2002). doi:10.1002/0471440264.
317. Paudel, A., Van Humbeeck, J. & Van den Mooter, G. Theoretical and Experimental Investigation on the Solid Solubility and Miscibility of Naproxen in Poly(vinylpyrrolidone). *Mol. Pharm.* **7**, 1133–1148 (2010).
318. Qian, F. *et al.* Solution Behavior of PVP-VA and HPMC-AS-Based Amorphous Solid Dispersions and Their Bioavailability Implications. *Pharm. Res.* **29**, 2766–2776 (2012).
319. Tian, Y. *et al.* Construction of Drug–Polymer Thermodynamic Phase Diagrams Using Flory–Huggins Interaction Theory: Identifying the Relevance of Temperature and Drug Weight Fraction to Phase Separation within Solid Dispersions. *Mol. Pharm.* **10**, 236–248 (2013).
320. Zhao, Y., Inbar, P., Chokshi, H. P., Malick, A. W. & Choi, D. S. Prediction of the Thermal Phase Diagram of Amorphous Solid Dispersions by Flory–Huggins Theory. *J. Pharm. Sci.* **100**, 3196–3207 (2011).
321. Koningsveld, R., Stockmayer, W. H. & Nies, E. *Polymer phase diagrams: a textbook.* (Oxford University Press, USA, 2001).
322. O'Shea, J. P. *et al.* Mesoporous silica-based dosage forms improve bioavailability of poorly soluble drugs in pigs: case example fenofibrate. *J. Pharm. Pharmacol.* **69**, 1284–1292 (2017).
323. Lainé, A.-L. *et al.* Enhanced oral delivery of celecoxib via the development of a supersaturable amorphous formulation utilising mesoporous silica and co-loaded HPMCAS. *Int. J. Pharm.* **512**, 118–125 (2016).
324. Van Speybroeck, M. *et al.* Enhanced absorption of the poorly soluble drug fenofibrate by tuning its release rate from ordered mesoporous silica. *Eur. J. Pharm. Sci.* **41**, 623–

630 (2010).
325. Dressman, J. B. *et al.* Mesoporous silica-based dosage forms improve release characteristics of poorly soluble drugs: case example fenofibrate. *J. Pharm. Pharmacol.* **68**, 634–645 (2016).
326. McCarthy, C. A., Ahern, R. J., Dontireddy, R., Ryan, K. B. & Crean, A. M. Mesoporous silica formulation strategies for drug dissolution enhancement: a review. *Expert Opin. Drug Deliv.* **13**, 93–108 (2016).
327. Hideo Hata, †, Shuuya Saeki, †, Tatsuo Kimura, †, Yoshiyuki Sugahara, † and & Kazuyuki Kuroda*, †. Adsorption of Taxol into Ordered Mesoporous Silicas with Various Pore Diameters. *Chem. Mater.* **11**, 1110–1119 (1999).
328. ICH Expert Working Group. Impurities: Guideline for residual solvents. https://www.ich.org/fileadmin/Public_Web_Site/ICH_Products/Guidelines/Quality/Q3C/Q3C_R6__Step_4.pdf (2016).
329. Piccinni, P. *et al.* Solubility parameter-based screening methods for early-stage formulation development of itraconazole amorphous solid dispersions. *J. Pharm. Pharmacol.* **68**, 705–720 (2016).
330. Sun, J. *et al.* Effect of particle size on solubility, dissolution rate, and oral bioavailability: evaluation using coenzyme Q_{10} as naked nanocrystals. *Int. J. Nanomedicine* **7**, 5733–44 (2012).
331. Williams, H. D. *et al.* Strategies to Address Low Drug Solubility in Discovery and Development. *Pharmacol. Rev.* **65**, 315–499 (2013).
332. Junghanns, J.-U. A. H. & Müller, R. H. Nanocrystal technology, drug delivery and clinical applications. *Int. J. Nanomedicine* **3**, 295–309 (2008).
333. Khadka, P. *et al.* Pharmaceutical particle technologies: An approach to improve drug solubility, dissolution and bioavailability. *Asian J. Pharm. Sci.* **9**, 304–316 (2014).
334. Rasenack, N. & Müller, B. W. Micron-Size Drug Particles: Common and Novel Micronization Techniques. *Pharm. Dev. Technol.* **9**, 1–13 (2004).
335. Kundu, S. *Silk biomaterials for tissue engineering and regenerative medicine*. (Woodhead Publishing, 2014).
336. Singh, A. K. *Engineered nanoparticles: structure, properties and mechanisms of toxicity*. (Academic Press, 2015).
337. Merisko-Liversidge, E. M. & Liversidge, G. G. Drug Nanoparticles: Formulating Poorly Water-Soluble Compounds. *Toxicol. Pathol.* **36**, 43–48 (2008).
338. Date, A. A. & Patravale, V. B. Current strategies for engineering drug nanoparticles. *Curr. Opin. Colloid Interface Sci.* **9**, 222–235 (2004).
339. Wu, L., Zhang, J. & Watanabe, W. Physical and chemical stability of drug nanoparticles. *Adv. Drug Deliv. Rev.* **63**, 456–469 (2011).
340. Latere Dwan'Isa, J. P., Rouxhet, L., Préat, V., Brewster, M. E. & Ariën, A. Prediction of drug solubility in amphiphilic di-block copolymer micelles: The role of polymer-drug compatibility. *Pharmazie* **62**, 499–504 (2007).
341. Mahmud, A. *et al.* Self-Associating Poly(ethylene oxide)- *b* -poly(α-cholesteryl carboxylate-ε-caprolactone) Block Copolymer for the Solubilization of STAT-3 Inhibitor Cucurbitacin I. *Biomacromolecules* **10**, 471–478 (2009).
342. Khougaz, K. & Clas, S. D. Crystallization inhibiton in solid dispersions of MK-0591 and poly(vinylpyrrolidone) polymers. *J. Pharm. Sci.* **89**, 1325–1334 (2000).
343. Tantishaiyakul, V., Kaewnopparat, N. & Ingkatawornwong, S. Properties of solid dispersions of piroxicam in polyvinylpyrrolidone K-30. *Int. J. Pharm.* **143**, 59–66 (1996).
344. Masuda, T. *et al.* Cocrystallization and amorphization induced by drug–excipient interaction improves the physical properties of acyclovir. *Int. J. Pharm.* **422**, 160–169

(2012).
345. Matsumoto, T. & Zografi, G. Physical Properties of Solid Molecular Dispersions of Indomethacin with Poly(vinylpyrrolidone) and Poly(vinylpyrrolidone-co-vinyl-acetate) in Relation to Indomethacin Crystallization. *Pharm. Res.* **16**, 1722–1728 (1999).
346. Deng, Z., Xu, S. & Li, S. Understanding a relaxation behavior in a nanoparticle suspension for drug delivery applications. *Int. J. Pharm.* **351**, 236–243 (2008).
347. Marsac, P. J. *et al.* Effect of temperature and moisture on the miscibility of amorphous dispersions of felodipine and poly(vinyl pyrrolidone). *J. Pharm. Sci.* **99**, 169–185 (2010).
348. Ricarte, R. G., Lodge, T. P. & Hillmyer, M. A. Detection of pharmaceutical drug crystallites in solid dispersions by transmission electron microscopy. *Mol. Pharm.* **12**, 983–990 (2015).
349. Ricarte, R. G. *et al.* Direct Observation of Nanostructures during Aqueous Dissolution of Polymer/Drug Particles. *Macromolecules* **50**, 3143–3152 (2017).
350. Frank, K. J., Locher, K., Zecevic, D. E., Fleth, J. & Wagner, K. G. In vivo predictive mini-scale dissolution for weak bases: Advantages of pH-shift in combination with an absorptive compartment. *Eur. J. Pharm. Sci.* **61**, 32–39 (2014).
351. Ilevbare, G. A. & Taylor, L. S. Liquid-liquid phase separation in highly supersaturated aqueous solutions of poorly water-soluble drugs: Implications for solubility enhancing formulations. *Cryst. Growth Des.* **13**, 1497–1509 (2013).
352. Indulkar, A. S., Lou, X., Zhang, G. G. Z. Z. & Taylor, L. S. Insights into the Dissolution Mechanism of Ritonavir-Copovidone Amorphous Solid Dispersions: Importance of Congruent Release for Enhanced Performance. *Mol. Pharm.* **16**, 1327–1339 (2019).
353. Mosquera-Giraldo, L. I. & Taylor, L. S. Glass–Liquid Phase Separation in Highly Supersaturated Aqueous Solutions of Telaprevir. *Mol. Pharm.* **12**, 496–503 (2015).
354. Raina, S. A., Alonzo, D. E., Zhang, G. G. Z. Z., Gao, Y. & Taylor, L. S. Using Environment-Sensitive Fluorescent Probes to Characterize Liquid-Liquid Phase Separation in Supersaturated Solutions of Poorly Water Soluble Compounds. *Pharm. Res.* **32**, 3660–3673 (2015).
355. Tho, I. *et al.* Formation of nano/micro-dispersions with improved dissolution properties upon dispersion of ritonavir melt extrudate in aqueous media. *Eur. J. Pharm. Sci.* **40**, 25–32 (2010).
356. Uchiyama, H., Tozuka, Y., Asamoto, F. & Takeuchi, H. Fluorescence investigation of a specific structure formed by aggregation of transglycosylated stevias: Solubilizing effect of poorly water-soluble drugs. *Eur. J. Pharm. Sci.* **43**, 71–77 (2011).
357. Van Drooge, D. J. *et al.* Characterization of the mode of incorporation of lipophilic compounds in solid dispersions at the nanoscale using Fluorescence Resonance Energy Transfer (FRET). *Macromol. Rapid Commun.* **27**, 1149–1155 (2006).
358. Negrini, R., Aleandri, S. & Kuentz, M. Study of Rheology and Polymer Adsorption Onto Drug Nanoparticles in Pharmaceutical Suspensions Produced by Nanomilling. *J. Pharm. Sci.* **106**, 3395–3401 (2017).
359. Chauhan, H., Hui-Gu, C. & Atef, E. Correlating the behavior of polymers in solution as precipitation inhibitor to its amorphous stabilization ability in solid dispersions. *J. Pharm. Sci.* **102**, 1924–1935 (2013).
360. Usui, F., Maeda, K., Kusai, A., Nishimura, K. & Yamamoto, K. Inhibitory effects of water-soluble polymers on precipitation of RS-8359. *Int. J. Pharm.* **154**, 59–66 (1997).
361. Raghavan, S. L., Trividic, A., Davis, A. F. & Hadgraft, J. Crystallization of hydrocortisone acetate: Influence of polymers. *Int. J. Pharm.* **212**, 213–221 (2001).
362. Alonzo, D. E. *et al.* Dissolution and precipitation behavior of amorphous solid

dispersions. *J. Pharm. Sci.* **100**, 3316–3331 (2011).
363. Kanaujia, P. *et al.* Nanoparticle formation and growth during in vitro dissolution of ketoconazole solid dispersion. *J. Pharm. Sci.* **100**, 2876–2885 (2011).
364. Guo, Y., Shalaev, E. & Smith, S. Physical stability of pharmaceutical formulations: Solid-state characterization of amorphous dispersions. *TrAC - Trends Anal. Chem.* **49**, 137–144 (2013).
365. Bodratti, A. & Alexandridis, P. Formulation of Poloxamers for Drug Delivery. *J. Funct. Biomater.* **9**, 11 (2018).
366. Tsinman, O., Tsinman, K. & Ali, S. Excipient update - soluplus®: An understanding of supersaturation from amorphous solid dispersions. *Drug Dev. Deliv.* **15**, (2015).
367. Shamma, R. N. & Basha, M. Soluplus®: A novel polymeric solubilizer for optimization of Carvedilol solid dispersions: Formulation design and effect of method of preparation. *Powder Technol.* **237**, 406–414 (2013).
368. Alberty, R. A. & Hammes, G. G. Application of the theory of diffusion-controlled reactions to enzyme kinetics. *J. Phys. Chem.* **62**, 154–159 (1958).
369. Eftink, M. R. & Ghiron, C. A. Temperature and viscosity dependence of fluorescence quenching by oxygen in model systems. *Photochem. Photobiol.* **45**, 745–748 (1987).
370. Zinger, D. & Geacintoov, N. E. Acrylamide and molecular oxygen fluoirescence quenching as a probe of solvent-accessibility of aromatic fluorophores complexed with DNA in relation to their conformation: coronene-DNA and other complexes. *Photochem. Photobiol.* **47**, 181–188 (1988).
371. Ando, T. & Asai, H. Charge effects on the dynamic quenching of fluorescence of 1,N6-ethenoadenosine oligophosphates by iodide, thallium (I) and acrylamide. *J. Biochem.* **88**, 255–264 (1980).
372. Bombelli, C. *et al.* Efficiency of liposomes in the delivery of a photosensitizer controlled by the stereochemistry of a gemini surfactant component. *Mol. Pharm.* **7**, 130–137 (2010).
373. Gupta, P., Thilagavathi, R., Chakraborti, A. K. & Bansal, A. K. Role of molecular interaction in stability of celecoxib-PVP amorphous systems. *Mol. Pharm.* **2**, 384–391 (2005).
374. Sun, D. D. & Lee, P. I. Evolution of supersaturation of amorphous pharmaceuticals: The effect of rate of supersaturation generation. *Mol. Pharm.* **10**, 4330–4346 (2013).
375. Obaidat, R. M., AlTaani, B. & Ailabouni, A. Effect of different polymeric dispersions on In-vitro dissolution rate and stability of celecoxib class II drug. *J. Polym. Res.* **24**, (2017).
376. Juenemann, D. *et al.* Online monitoring of dissolution tests using dedicated potentiometric sensors in biorelevant media. *Eur. J. Pharm. Biopharm.* **78**, 158–165 (2011).
377. Leo, E., Cameroni, R. & Forni, F. Dynamic dialysis for the drug release evaluation from doxorubicin–gelatin nanoparticle conjugates. *Int. J. Pharm.* **180**, 23–30 (1999).
378. Marasini, N. *et al.* Fabrication and evaluation of pH-modulated solid dispersion for telmisartan by spray-drying technique. *Int. J. Pharm.* **441**, 424–432 (2013).
379. Buckley, S. T., Frank, K. J., Fricker, G. & Brandl, M. Biopharmaceutical classification of poorly soluble drugs with respect to 'enabling formulations'. *Eur. J. Pharm. Sci.* **50**, 8–16 (2013).
380. Buckley, S. T. *et al.* In vitro models to evaluate the permeability of poorly soluble drug entities: Challenges and perspectives. *Eur. J. Pharm. Sci.* **45**, 235–250 (2012).
381. Ruff A, Fiolka T, K. E. Prediction of Ketoconazole absorption using an updated in vitro transfer model coupled to physiologically based pharmacokinetic modelling. *Eur. J. Pharm. Sci.* **100**, 42–55 (2017).

382. O'Dwyer, P. J. *et al. In vitro* methods to assess drug precipitation in the fasted small intestine - a PEARRL review. *J. Pharm. Pharmacol.* (2018) doi:10.1111/jphp.12951.
383. Heigoldt, U. *et al.* Predicting in vivo absorption behavior of oral modified release dosage forms containing pH-dependent poorly soluble drugs using a novel pH-adjusted biphasic in vitro dissolution test. *Eur. J. Pharm. Biopharm.* **76**, 105–111 (2010).
384. Sironi, D., Rosenberg, J., Bauer-Brandl, A. & Brandl, M. PermeaLoop^{TM} a novel in vitro tool for small-scale drug-dissolution/permeation studies. *J. Pharm. Biomed. Anal.* **156**, 247–251 (2018).
385. Shi, Y., Gao, P., Gong, Y. & Ping, H. Application of a Biphasic Test for Characterization of In Vitro Drug Release of Immediate Release Formulations of Celecoxib and Its Relevance to In Vivo Absorption. *Mol. Pharm.* **7**, 1458–1465 (2010).
386. Xu, H., Vela, S., Shi, Y., Marroum, P. & Gao, P. In Vitro Characterization of Ritonavir Drug Products and Correlation to Human in Vivo Performance. *Mol. Pharm.* **14**, 3801–3814 (2017).
387. Tsume, Y. *et al.* The in vivo predictive dissolution for immediate release dosage of donepezil and danazol, BCS class IIc drugs, with the GIS and the USP II with biphasic dissolution apparatus. *J. Drug Deliv. Sci. Technol.* 0–1 (2019) doi:10.1016/j.jddst.2019.01.035.
388. Psachoulias, D. *et al.* Precipitation in and Supersaturation of Contents of the Upper Small Intestine After Administration of Two Weak Bases to Fasted Adults. *Pharm. Res.* **28**, 3145–3158 (2011).
389. Sarode A. , Obara S., T. F. Stability assessment of hypromellose acetate succinate (HPMCAS) NF for application in hot melt extrusion (HME). *Carbohydr. Polym.* **101**, 146–153 (2014).
390. Maniruzzaman, M., Islam, M. T., Halsey, S., Amin, D. & Douroumis, D. Novel Controlled Release Polymer-Lipid Formulations Processed by Hot Melt Extrusion. *AAPS PharmSciTech* **17**, 191–199 (2016).
391. Alexander M, Piska I, D. D. Investigation of particle dynamics in gels involving casein micelles: A diffusing wave spectroscopy and rheology approach. *Food Hydrocoll.* **22**, 1124–1134 (2008).
392. Vasbinder A, D. K. C. Casein–whey protein interactions in heated milk: the influence of pH. *Int. Dairy J.* **13**, 669–677 (2003).
393. Eloy, J. D. O., Saraiva, J., Albuquerque, S. De & Marchetti, J. M. Solid Dispersion of Ursolic Acid in Gelucire 50 / 13 : a Strategy to Enhance Drug Release and Trypanocidal Activity. *AAPS PharmSciTech* **13**, 1436–1445 (2012).
394. Barnes, H. A. *Rheology: Principles, Measurements and Applications*. *Powder Technology* vol. 86 (1996).
395. Blaabjerg, L. *et al.* The Influence of Polymers on the Supersaturation Potential of Poor and Good Glass Formers. *Pharmaceutics* **10**, 164 (2018).
396. Aleandri, S., Jankovic, S. & Kuentz, M. Towards a better understanding of solid dispersions in aqueous environment by a fluorescence quenching approach. *Int. J. Pharm.* **550**, 130–139 (2018).
397. Konno H, T. L. Influence of Different Polymers on the Crystallization Tendency of Molecularly Dispersed Amorphous Felodipine. *J. Pharm. Sci.* **95**, 2692–2705 (2006).
398. Matsen, M. W. Soft Matter, Volume 1: Polymer Melts and Mixtures. (2006).
399. Singh, Y. Martin's physical pharmacy and pharmaceutical sciences. *Rutgers, State Univ. New Jersey* (2006).
400. Martin, A., Swarbrick, J. & Cammarata, A. Physical pharmacy. *Lea Febiger* (2006).
401. Van Duong, T. *et al.* Spectroscopic Investigation of the Formation and Disruption of Hydrogen Bonds in Pharmaceutical Semicrystalline Dispersions. *Mol. Pharm.* **14**,

1726–1741 (2017).
402. Broman, E., Khoo, C. & Taylor, L. S. A comparison of alternative polymer excipients and processing methods for making solid dispersions of a poorly water soluble drug. *Int. J. Pharm.* **222**, 139–151 (2001).
403. De Kee, D. & Wissbrun, K. F. Polymer Rheology. *Phys. Today* **51**, 24–29 (1998).
404. Räntzsch, V. *et al.* Polymer Crystallization Studied by Hyphenated Rheology Techniques: Rheo-NMR, Rheo-SAXS, and Rheo-Microscopy. *Macromol. Mater. Eng.* **304**, 1800586 (2019).
405. Del Giudice, F., Tassieri, M., Oelschlaeger, C. & Shen, A. Q. When Microrheology, Bulk Rheology, and Microfluidics Meet: Broadband Rheology of Hydroxyethyl Cellulose Water Solutions. *Macromolecules* **50**, 2951–2963 (2017).
406. MacKintosh, F. C. & John, S. Diffusing-wave spectroscopy and multiple scattering of light in correlated random media. *Phys. Rev. B* **40**, 2383–2406 (1989).
407. Jankovic, S. *et al.* Biphasic drug release testing coupled with diffusing wave spectroscopy for mechanistic understanding of solid dispersion performance. *Eur. J. Pharm. Sci.* **137**, 105001 (2019).
408. Lacoulonche, F., Chauvet, A. & Masse, J. An investigation of flurbiprofen polymorphism by thermoanalytical and spectroscopic methods and a study of its interactions with poly-(ethylene glycol) 6000 by differential scanning calorimetry and modelling. *Int. J. Pharm.* **153**, 167–179 (1997).
409. Cheng, L. *et al.* Design and evaluation of bilayer pump tablet of flurbiprofen solid dispersion for zero-order controlled delivery. *J. Pharm. Sci.* **107**, 1434–1442 (2018).
410. Ditzinger, F., Scherer, U., Schönenberger, M., Holm, R. & Kuentz, M. Modified polymer matrix in pharmaceutical hot melt extrusion by molecular interactions with a carboxylic coformer. *Mol. Pharm.* **16**, 141–150 (2018).
411. Bellour, M., Skouri, M., Munch, J.-P. & Hébraud, P. Brownian motion of particles embedded in a solution of giant micelles. *Eur. Phys. J. E* **8**, 431–436 (2002).
412. Niederquell, A., Machado, A. H. E. E. & Kuentz, M. A diffusing wave spectroscopy study of pharmaceutical emulsions for physical stability assessment. *Int. J. Pharm.* **530**, 213–223 (2017).
413. Niederquell, A., Dujovny, G., Probst, S. E. & Kuentz, M. A Relative Permittivity Approach for Fast Drug Solubility Screening of Solvents and Excipients in Lipid-Based Delivery. *J. Pharm. Sci.* **108**, 3457–3460 (2019).
414. Law, S. L., Lo, W. Y., Lin, F. M. & Chaing, C. H. Dissolution and absorption of nifedipine in polyethylene glycol solid dispersion containing phosphatidylcholine. *Int. J. Pharm.* **84**, 161–166 (1992).
415. Lacoulonche, F., Chauvet, A., Masse, J., Egea, M. A. & Garcia, M. L. An investigation of FB interactions with poly(ethylene glycol) 6000, poly(ethylene glycol) 4000, and poly-ε-caprolactone by thermoanalytical and spectroscopic methods and modeling. *J. Pharm. Sci.* **87**, 543–551 (1998).
416. Lauritzen, J. I. & Hoffman, J. D. Formation of polymer crystals with folded chains from dilute solution. *J. Chem. Phys.* **31**, 1680–1681 (1959).
417. Tang, X., Chen, W. & Li, L. The Tough Journey of Polymer Crystallization: Battling with Chain Flexibility and Connectivity. *Macromolecules* **52**, 3575–3591 (2019).
418. He, P., Yu, W. & Zhou, C. Agglomeration of Crystals during Crystallization of Semicrystalline Polymers: A Suspension-Based Rheological Study. *Macromolecules* **52**, 1042–1054 (2019).
419. Ballard, M. J., Buscall, R. & Waite, F. A. The theory of shear-thickening polymer solutions. *Polymer (Guildf).* **29**, 1287–1293 (1988).
420. MacMillan*, S. D. *et al.* In Situ Small Angle X-ray Scattering (SAXS) Studies of

Polymorphism with the Associated Crystallization of Cocoa Butter Fat Using Shearing Conditions. (2002) doi:10.1021/CG0155649.
421. Strobl, G. R. & IUCr. Determination of the lamellar structure of partially crystalline polymers by direct analysis of their small-angle X-ray scattering curves. *J. Appl. Crystallogr.* **6**, 365–370 (1973).